# MULTI-PHASED SCAFFOLDS DERIVED FROM DECELLULARIZED EXTRACELLULAR MATRICES FOR TENDON-TO-BONE INTERFACE TISSUE ENGINEERING

**Noura Alom** MSc

Thesis submitted to the University of Nottingham for the degree of Doctor of Philosophy

September 2016



# Abstract

The tendon-to-bone interface exhibits gradients in tissue organization, with variation in chemical, physical and biological properties for each. After injury, a mechanically weaker and structurally disorganized tissue is formed. Tissue engineering approaches have focused on developing and investigating tissue-engineered scaffolds to replicate the native biological, structural, and mechanical features of the tendon-to-bone interface site. The idealized technique for regenerating the interface is to design a multi-phased scaffold with multiple zones, and multiple cell types to functionally restore the structural, cellular, and mechanical properties of the tendon-to-bone interface.

Hydrogel scaffolds derived from the extracellular matrix (ECM) of mammalian tissues have been successfully used to promote tissue repair in vitro and in vivo. In this study, ECM hydrogels prepared from demineralized and decellularized bovine bone were investigated to evaluate the osteoinductive properties of these hydrogels in the presence and absence of osteogenic medium, and their ability to act as a carrier for local delivery of cells and growth factors. Decellularized bone matrix (bECM) hydrogels stimulated osteogenic differentiation in C2C12 mouse myoblast cells and mouse primary calvarial cells (mPCs) even in the absence of osteogenic medium. Moreover, these hydrogels demonstrated stable release of human serum albumin (HSA); the release

kinetics of proteins from hydrogels was dependent on bECM hydrogel concentration.

Hydrogels derived from decellularized equine tendon extracellular matrix were also prepared; decellularized tendon matrix (tECM) hydrogels had distinct structural and biological properties and it supported human mesenchymal stem cells (hMSCs) attachment and proliferation. tECM enhanced hMSCs tenogenic differentiation and suppressed osteogenic differentiation, while the presence of bECM greatly induced hMSCs osteogenic differentiation and suppressed tenogenic differentiation.

An electrospun scaffold was produced using decellularized bovine bone extracellular matrix (bECM), to contribute to multi-phased scaffold design, and to present this unique ECM material in a new advanced form. In the present research, we optimised a method to electrospin decellularized bovine bone extracellular matrix (bECM) without the addition of any other materials as a potential improvement for cell adhesion, proliferation and differentiation. bECM was dissolved in 50/50 1, 1, 1, 3, 3, 3-Hexafluoro-2-propanol/ Trifluoroacetic acid. A high voltage was applied to the bECM solution and fibers were collected as a uniform mesh, the solutions were electrospun for 3 hours at 20°C in 40% relative humidity. We assessed the biological activity and osteogenic capability in vitro of electrospun bECM scaffolds in comparison to electrospun gelatin scaffolds using mouse primary calvarial cells (mPCs) and human mesenchymal stem cells (hMSCs).

Overall, the results of the three experimental chapters suggest the utility of these bone ECM and tendon ECM hydrogels, with the electrospun ECM in designing a gradient hydrogel scaffold for tendon-to-bone interface tissue engineering.

# Acknowledgments

There are many people whom I owe gratitude, first and foremost I would like to thank my husband Maher, my parents Hasan and Hanaa, my son Ayman, and my future kids (just in case) for giving me all kind of support to complete my PhD during the good and bad times.

I would like to thank my supervisor Prof Kevin Shakesheff for the opportunity to undertake this project, and the freedom to work independently. Your supervision and guidance helped me to develop my scientific knowledge as well as my personality. I also would like to thank Dr Lisa White for her helpful and insightful input throughout my studies, and Dr Heather Peto for providing me with the essential training and help during my first year.

A huge thanks to all the members of tissue engineering group, I was lucky to be in such lovely group surrounded with very friendly and supportive friends, I am very grateful to the help and advice you guys gave me on the top of the entertainment and fun.

I would like to acknowledge Dr Rachel Oldershaw (Institute of ageing and chronic disease, University of Liverpool), Dr Marco Tatullo and Dr Francesco Paduano (TECNOLOGICA Research Institute, Crotone, Italy), and Dr Heidi Janicke (Vet School, University of Nottingham) for their input and help with this project.

Finally, I would like to dedicate this work to my beloved Syria. As Albert Camus Says: "*where there is no hope, it is incumbent on us to invent it*" So I am full of hope that, by the time you are reading this, I will be busy in Syria rebuilding what the war has destroyed.

## Publications

- Noura Alom, Heather Peto, Glen R. Kirkham, Kevin M. Shakesheff, and Lisa J. White “Decellularized Bone Matrix Hydrogel Enhances Osteogenic Differentiation of C2C12 Myoblasts and Mouse Primary Calvarial Cells” Journal of Biomedical Materials Research part B: Applied Biomaterials (2017).

- Francesco Paduano, Massimo Marrelli, Noura Alom, Mahetab Amer, Lisa J. White, Kevin M. Shakesheff, and Marco Tatullo “Decellularized bone extracellular matrix and human dental pulp stem cells as a construct for bone regeneration” Journal of Biomaterials Science, Polymer Edition (2017) P: 1-19.

- N. Alom, K. M. Shakesheff, L. J. White “Osteoinductive Activity of Decellularized Bone Matrix Hydrogel with Controlled Protein Release for Bone Regeneration” journal of TISSUE ENGINEERING: Part A, Volume 21, Supplement 1, 4th TERMIS World Congress Boston, Massachusetts, USA. (poster presentation)

- N. Alom, K. M. Shakesheff, L. J. White “Hydrogel Scaffold derived from decellularized extracellular matrices for tendon-to-bone tissue engineering” Journal of Tissue Science and Engineering, Vol: 6, issue: 02. Rome, Italy. (poster presentation)

- N. Alom, K.M. Shakesheff, L.J. White “Hydrogel Scaffold derived from decellularized bone matrix with osteogenesis-inducing activity and protein carrier ability for bone regeneration” Journal of European cells and Materials, Vol: 29, issue: 03, Page 26. Southampton, UK. (poster presentation)

# Table of Contents

Abstract.....II

Acknowledgments ..... V

Publications..... VII

List of figures.....XIII

List of abbreviations ..... XVII

Chapter 1. General introduction .....1

1.1 Tissue engineering and regenerative medicine.....1

1.1.1 Background and overview .....1

1.2 Overview of the enthesis: tissue interface at the tendon-to-bone insertion.....4

1.3 Structure and function of fibrocartilaginous enthesis.....7

1.3.1 Tendon/ligament .....7

1.3.2 Non-mineralized fibrocartilage.....7

1.3.3 Mineralized fibrocartilage .....9

1.3.4 Bone.....9

1.4 Healing process of tendon to bone insertion .....9

1.5 Strategies for interface tissue engineering.....12

1.5.1 Scaffold Design for Tendon-to-Bone Interface Tissue Engineering.....13

1.6 Aims and Objectives....29

Chapter 2. General Materials and Methods....32

2.1 Gel production....32

2.1.1 ECM hydrogel....32

2.1.2 Collagen type I hydrogel....32

2.2 General cell culture....33

2.2.1 C2C12 mouse myoblast cell line....33

2.2.2 Mouse primary calvarial cells....33

2.2.3 Primary human bone-marrow mesenchymal stem cells....34

2.2.4 Cryopreservation....35

2.2.5 Thawing cells after cryopreservation....35

2.2.6 Cell viability assessment....36

2.2.7 Immunohistochemical staining for osteogenic proteins....36

2.3 Statistical analysis....37

Chapter 3. Hydrogel scaffold derived from decellularized bone matrix with osteogenesis-inducing activity and protein carrier ability....38

3.1 Introduction....38

3.2 Materials and methods....41

3.2.1 Preparation of DBM and bECM hydrogels....41

3.2.2 SDS-PAGE and BCA assay....44

3.2.3 C2C12 osteogenic differentiation....44

3.2.4 Alkaline phosphatase activity assay .....45

3.2.5 mPCs osteogenic differentiation .....46

3.2.6 Immunohistochemical staining for mouse osteopontin and osteocalcin .....46

3.2.7 Real time qPCR analysis .....47

3.2.8 Controlled release of proteins from bECM hydrogel .....48

3.3 Results .....50

3.3.1 Protein content of demineralized & decellularized bone matrix 50

3.3.2 C2C12 osteoblastic differentiation in different culture conditions.....52

3.3.3 Expression of osteogenic proteins in mouse primary calvarial cells.....55

3.3.4 mRNA expression of osteogenic markers.....58

3.3.5 HSA release from bECM hydrogels.....60

3.4 Discussion.....63

Chapter 4. Hydrogel scaffolds derived from decellularized tendon and bone extracellular matrices selectivity enhance MSC tenogenic and osteogenic differentiation for tendon-to-bone interface tissue engineering .....67

4.1 Introduction .....67

4.2 Materials and methods.....70

4.2.1 Preparation of tendon extracellular matrix hydrogel .....70

4.2.2 Assessment of Cellular content ..... 73

4.2.3 Assessment of collagen content ..... 73

4.2.4 Scanning electron microscopy (SEM) ..... 74

4.2.5 Turbidimetric gelation kinetics ..... 74

4.2.6 *In vitro* hMSCs culture and viability ..... 75

4.2.7 hMSCs multipotent differentiation and cellular morphology on bECM and tECM ..... 75

4.2.8 Quantitative PCR analysis ..... 76

4.3 Results ..... 77

4.3.1 Cellular and collagen content of decellularized tendon extracellular matrix ..... 77

4.3.2 Hydrogel morphology ..... 79

4.3.3 Turbidimetric gelation kinetics ..... 81

4.3.4 *In vitro* hMSCs culture and viability ..... 84

4.3.5 hMSCs multipotent differentiation and cellular morphology on bECM and tECM ..... 86

4.3.6 Gene expression ..... 89

4.4 Discussion ..... 95

Chapter 5. Novel electrospun decellularized bone extracellular matrix for bone tissue engineering ..... 100

5.1 Introduction ..... 100

5.2 Materials and methods ..... 103

5.2.1 Solvent selection for bECM and gelatin materials ..... 103

5.2.2 Electrospinning ..... 103

5.2.3 Crosslinking of the electrospun fibres ..... 105

5.2.4 Morphology ..... 105

5.2.5 mPCs and hMSCs seeding onto electrospun scaffolds ..... 106

5.2.6 Assessment of mineralisation ..... 106

5.2.7 Immunohistochemical staining for osteopontin and osteocalcin ..... 107

5.2.8 Quantitative PCR analysis ..... 107

5.3 Results ..... 107

5.3.1 Selection of an appropriate solvent ..... 107

5.3.2 Electrospinning and crosslinking of bECM and gelatin fibers ..... 110

5.3.3 mPCs and hMSCs seeding onto electrospun scaffolds ..... 117

5.3.4 Von Kossa staining ..... 120

5.3.5 Expression of osteogenic proteins in mPCs and hMSCs ..... 122

5.3.6 mRNA expression of osteogenic markers ..... 125

5.4 Discussion ..... 127

Chapter 6. Summary and future direction ..... 132

6.1 Future direction ..... 135

References ..... 137

## List of Figures

**Figure 1:** Concept of tissue engineering.....3

**Figure 2:** The anatomy of fibrocartilaginous enthesis.....6

**Figure 3:** Histological section of a normal rat supraspinatus tendon-to-bone fibrocartilaginous enthesis .....8

**Figure 4:** Structure and composition of fibrocartilaginous entheses. The four different zones of the fibrocartilaginous enthesis .....10

**Figure 5:** Rotator cuff anatomy. .....14

**Figure 6:** Schematic shows the fibroblast (FB) and osteoblast (OB) seeding on poly-l-lactic acid (PLA) scaffolds are co-cultured to make a tendon region and a bone region on the scaffold.....18

**Figure 7**: Structure of extracellular matrix and its composition .....23

**Figure 8**: Schematic overview of skeletal muscle reconstruction using an ECM scaffold.....26

**Figure 9:** Production of ECM hydrogel from bone .....43

**Figure 10:** Controlled release of proteins form bECM hydrogels .....49

**Figure 11:** Quantification of bECM and DBM proteins.....51

**Figure 12:** C2C12 differentiation on bECM and on collagen type.....53

F**igure 13:** Alkaline phosphatase activity in C2C12.....54

**Figure 14:** Expression of osteopontin and osteocalcin in mouse primary calvarial cells cultured on bECM and DBM hydrogels.....56

**Figure 15:** Expression of osteopontin and osteocalcin in mouse primary calvarial cells cultured on Coll I hydrogel and TCP .....57

**Figure 16:** RT-qPCR of osteogenic markers ALP (A), OPN (B), RUNX2 (C), and OCN (D) .....59

**Figure 17:** Release profiles of HSA from bECM hydrogels .....61

**Figure 18:** The cumulative mass release of HSA .....62

**Figure 19:** Production of ECM hydrogel from tendon.....72

**Figure 20:** Decellularization of tendon ECM sections, was assessed by imaging and analysis of DAPI staining and (H&E) staining.....78

**Figure 21:** Scanning electron micrographs.....80

**Figure 22:** Turbidimetric gelation kinetics of tECM and Coll I hydrogels.....82

**Figure 23:** Proliferation of hMSCs on Coll I and tECM hydrogels.....85

**Figure 24:** Multi-lineage differentiation of hMSCs.....87

F**igure 25:** Morphology of hMSCs cultured on tECM hydrogel and bECM hydrogels .....88

**Figure 26:** RT-qPCR of tenogenic gene markers SCX (A), TNMD (B), and TNC (C) expression in human mesenchymal stem cells (hMSCs) seeded on tECM, coll I hydrogels and TCP .....91

**Figure 27:** RT-qPCR of osteogenic gene markers: ALP (A), OCN (B), OPN (C), and RUNX2 (D) expression in human mesenchymal stem cells (hMSCs) seeded on tECM, coll I hydrogels and TCP .....92

**Figure 28:** RT-qPCR of osteogenic gene markers: ALP (A), OCN (B), OPN (C), and RUNX2 (D) expression in human mesenchymal stem cells (hMSCs) seeded on bECM, coll I hydrogels and TCP .....93

**Figure 29:** RT-qPCR of tenogenic gene markers SCX (A), TNMD (B), and TNC (C) expression in human mesenchymal stem cells (hMSCs) seeded on bECM, coll I hydrogels and TCP .....94

**Figure 30:** A schematic of the electrospinning apparatus.....104

**Figure 31:** Selection of an appropriate solvent for bECM electrospinning....109

**Figure 32:** Electrospinning of bECM .....111

**Figure 33:** SEM image of bECM electrospun fibers after crosslinking .....112

**Figure 34:** Distribution of fibre diameters of electrospun bECM before and after crosslinking. .....113

**Figure 35:** Electrospinning of gelatin type A .....114

**Figure 36:** SEM image of gelatin electrospun fibers after crosslinking. .....115

**Figure 37:** Distribution of fibre diameters of electrospun gelatin before and after crosslinking.....116

**Figure 38:** Proliferation of mPCs on electrospun bECM after 2 and 4 days....118

**Figure 39:** Proliferation of hMSCs on electrospun gelatin and electrospun bECM after 3 and 7 days. .....119

**Figure 40:** Von Kossa staining of mPCs cultured on tissue culture plate (TCP) and electrospun bECM .....121

**Figure 41:** Expression of osteopontin (A & E) and osteocalcin (C & G) in mPCs cultured on electrospun bECM.....123

**Figure 42:** Expression of osteocalcin in hMSCs cultured on electrospun bECM (A & E) and electrospun gelatin (C & G) .....124

**Figure 43:** RT-qPCR of osteogenic markers OPN (A), OCN (B), RUNX2 (C), and ALP (D) expression in hMSCs seeded onto electrospun gelatin and electrospun bECM.....126

# List of Abbreviations

| | |
|---|---|
| ACL | anterior cruciate ligament |
| ALP | alkaline phosphatase |
| ASCs | adipose derived stem cells |
| bECM | decellularized bone extracellular matrix |
| bFGF | basic fibroblast growth factor |
| BMPs | bone morphogenetic proteins |
| BSA | Bovine serum albumin |
| Coll I | collagen type I |
| DBM | demineralized bone extracellular matrix |
| DCM | Dichloromethane |
| DMEM | Dulbecco's Modified Eagle Medium |
| DMSO | Dimethyl Sulfoxide |
| ECM | extracellular matrix |
| FCS | fetal calf serum |
| FGF2 | fibroblast growth factor-2 |
| GAGs | glycosaminoglycans |
| G-CSF | granulocyte colony-stimulating factor |
| HBSS | Hank's Balanced Salt Solution |
| HFP | 1, 1, 1, 3, 3, 3-Hexafluoro-2-propanol |
| hMSCs | human mesenchymal stem cells |
| HSA | human serum albumin |
| IGF-2 | insulin like growth factor-2 |
| MCL | medial collateral ligament |
| mPCs | mouse primary calvarial cells |
| MSCs | mesenchymal stem cells |
| OCN | osteocalcin |
| OPN | osteopontin |

PDGF-BB dual platelet derived growth factorβ

PFA paraformaldehyde

PLGA polylactid-co-glycolid acid

PLLA poly-L-lactic acid

*p*NPP *p*-Nitrophenyl Phosphate

RCTs Rotator cuff tears

RUNX2 related transcription factor 2

SCX scleraxis

SDS Sodium dodecyl sulfate

SEM scanning electron microscopy

SIS small intestine submucosa

TCP tissue culture plastic

tECM decellularized tendon extracellular matrix

TFA Trifluoroacetic acid

TGF- β transforming growth factor-β

TNC tenascin-C

TNMD tenomodulin

VEGF vascular endothelial growth factor

# Chapter 1. General Introduction

## 1.1 Tissue engineering and regenerative medicine

### 1.1.1 Background and overview

Tissue engineering was first defined by the National Science Foundation workshop in 1988 as 'the application of principles and methods of engineering and life sciences toward the fundamental understanding of structure-function relationships in normal and pathological mammalian tissues and the development of biological substitutes to restore, maintain or improve tissue function'[4]. However, while the tissue engineering field was emerging as a new approach, the principle of replacing damaged tissue with another was used in the 16$^{th}$ century by an Italian Gasparo Tagliacozzi (1546–99), Professor of Surgery and Anatomy at the Bologna University, in 1597 he published his work 'De Custorum Chirurigia per Insitionem' (The Surgery of Defects by Implantation), which described in details the nose replacement procedure he performed using forearm flap.

Tissue engineering is a discipline that aims to relate principles from both engineering and life sciences to produce biological substitutes that are fully functional from the start, or that develop *in vivo* into the required functionality to restore, maintain, or improve damaged tissues or whole organs [5]. In

general, tissue engineering strategies has three common principles: utilization of isolated cells, deliver bioactive molecules such as growth factors, and scaffold matrices with or without the incorporation of cells [6] (Figure 1).

Regenerative medicine is a wide field that share the same aims with tissue engineering of replacing and regenerating human cells and rebuilding tissues and organs in order to restore or establish normal function. However, regenerative medicine focuses on biological principles of self-healing and the use of stem cells [7].

In the early twentieth century, transplant surgeries gained pace with successful organ transplants including: pancreas, liver, heart and lung. However, the high doses of immunosuppressants used to prevent graft rejection meant that the risk of infection was high [8]. The goal of regenerative medicine is to be able to maintain the body function after a destructive disease when the traditional medicine can only cure them by replacing the patient whole organ [9]. Despite this, the terms “tissue engineering” and “regenerative medicine” have become mostly interchangeable with the focus of both fields being cures instead of treatments.

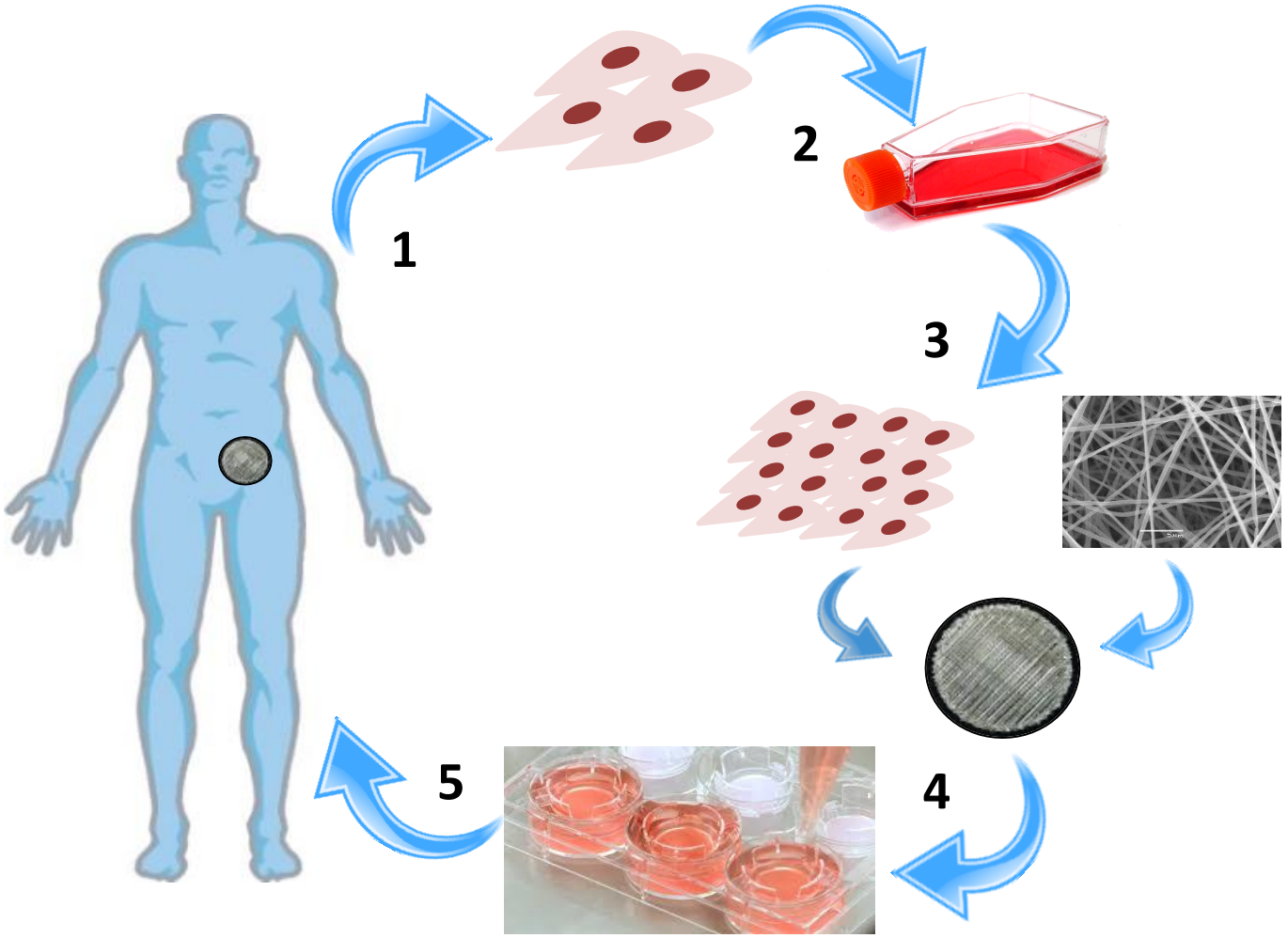



**Figure 1:** Concept of tissue engineering, cell harvest from biopsy or stem cells (1), cell isolation and expansion (2), cell seeding into scaffold (3), *in vitro* culturing (4), scaffold implantation (5).

## 1.2 Overview of the enthesis: tissue interface at the tendon-to-bone insertion

The musculoskeletal system consists of bone, cartilage, muscle, tendon, ligament and other connective tissues that provides support and stability for the human body and facilitates its movement. The attachment of soft material of ligaments and tendons to the hard bone should present high level of stress because of the difference in stiffness between the connective tissues and bone, but the presence of special transitional tissue known as enthesis has solved this problem. The enthesis connects tendons and ligaments to bone with an interface region, which can transfer the stress between the soft tissue and hard tissue and consequently eases joints motion [10-12].

There are two types of entheses based on the type of tissue present at the attachment site: fibrous enthesis are usually present where tendon or ligament is connected directly to the bone with dense fibrous tissue, e.g. the tibial attachment of the medial collateral ligament (MCL) of the knee. Fibrous entheses are further classified as either 'bony' or 'periosteal' to indicate whether the tendon inserts directly into the bone or indirectly to it via the periosteum respectively [13, 14].

The second type is fibrocartilaginous enthesis; this type of enthesis is characterized by layer of fibrocartilage that connects fibrous tendon tissue to

bone [13, 15]. Fibrocartilaginous entheses are more common than fibrous entheses and received more attention in the literature, likely because injuries are more common in fibrocartilaginous tendon-to-bone insertions such as those of the anterior cruciate ligament (ACL), Achilles tendons and rotator cuff [10, 16, 17] (Figure 2).

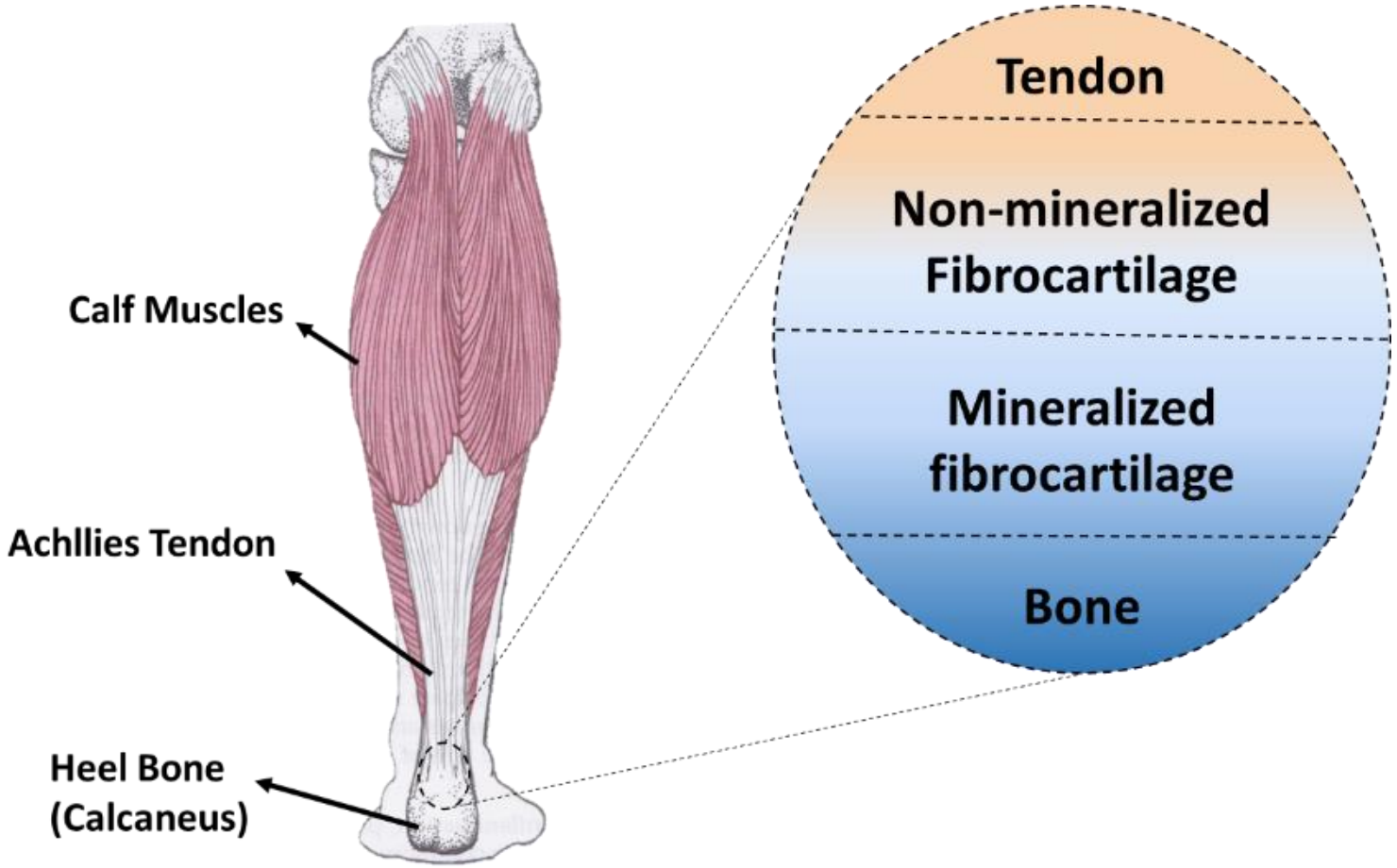



**Figure 2:** The anatomy of fibrocartilaginous enthesis.

## 1.3 Structure and function of fibrocartilaginous enthesis

The enthesis exhibits gradients in tissue organization that are classified into four distinct zones of tissue: tendon/ligament, fibrocartilage, mineralized fibrocartilage, and bone (Figure 3) .These four zones have different mechanical properties that are essential for the enthesis function [10, 11].

### 1.3.1 Tendon/ligament

Tendon/ligament is the first part of the insertion site, it consists of pure dense fibrous connective tissue, where linearly aligned collagen type I is the main component of the extracellular matrix (ECM), with small amount of collagen type III, elastin, and proteoglycans [17, 18]. Elongated fibroblasts are the dominant cells in the tendon/ligament tissue zone [19] (Figure 4).

### 1.3.2 Non-mineralized fibrocartilage

Non-mineralized fibrocartilage is the next zone, heavily populated by fibrochondrocytes. The ECM consists of collagen type II and III and small amounts of collagen type I and X, as well as proteoglycan aggrecan [19-21] (Figure 4). This zone has an important role in reducing the stress generated from the bending collagen fibers in the ligament/tendon zone during joint movement[22].

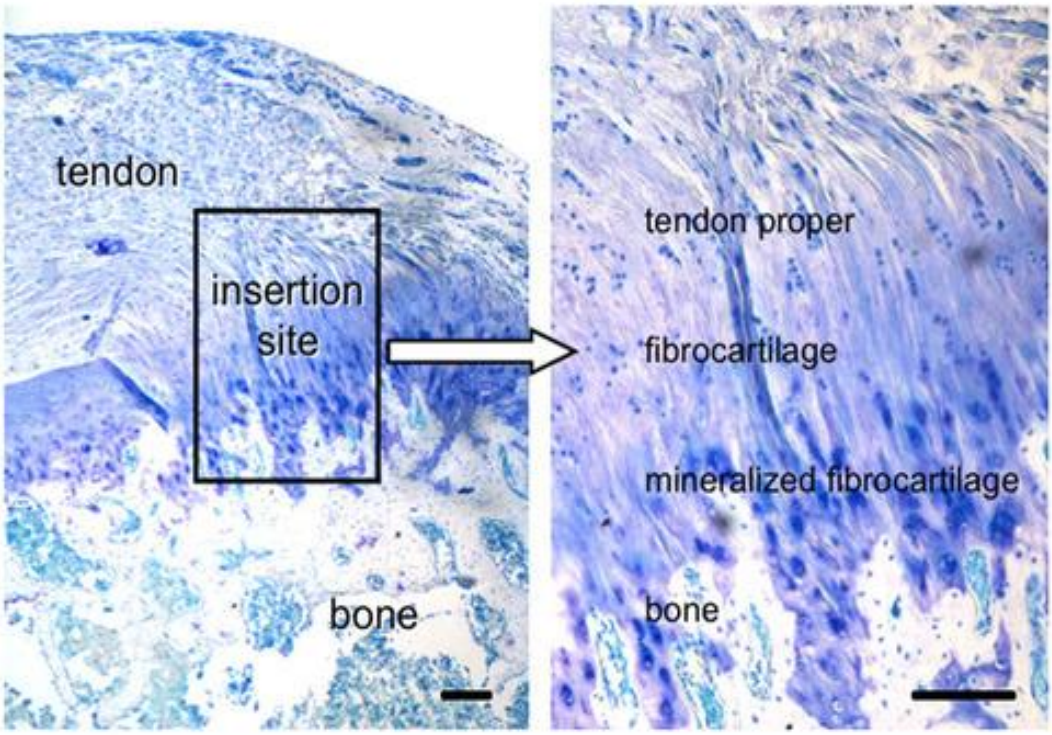



**Figure 3:** Histological section of a normal rat supraspinatus tendon-to-bone fibrocartilaginous enthesis, toluidine blue-stained section from a rat supraspinatus tendon-to-bone insertion is shown; scale bar = 200mm. The four different zones of the fibrocartilaginous enthesis are indicated. *Source* : figure reprinted with permission from reference [1].

### 1.3.3 Mineralized fibrocartilage

The third zone is mineralized fibrocartilage. Hypertrophic fibrochondrocytes are the dominant cells in this zone, which are round and bigger than fibrochondrocytes found in the non-mineralized fibrocartilage zone. ECM consists of predominantly collagen type II, with some amounts of aggrecan and collagen type I and X [10, 19, 20, 22] (Figure 4).

The actual junction of the tendon to bone insertion site is characterized in this zone, which creates irregular boundary with the subchondral bone, this irregularity provides the mechanical integrity of the insertion site [22, 23].

### 1.3.4 Bone

The final zone is bone, which contains osteoclasts, osteocytes, and osteoblasts, as well as collagen type I and carbonated apatite mineral [12, 19] (Figure 4).

## 1.4 Healing process of tendon to bone insertion

Understanding the mechanism of tendon to bone insertion healing is essential for developing new scaffolds for soft tendon to hard bone interface tissue engineering. The construction of a tissue with cellular and component gradient such as entheses are poorly understood. Moreover, it has been reported that

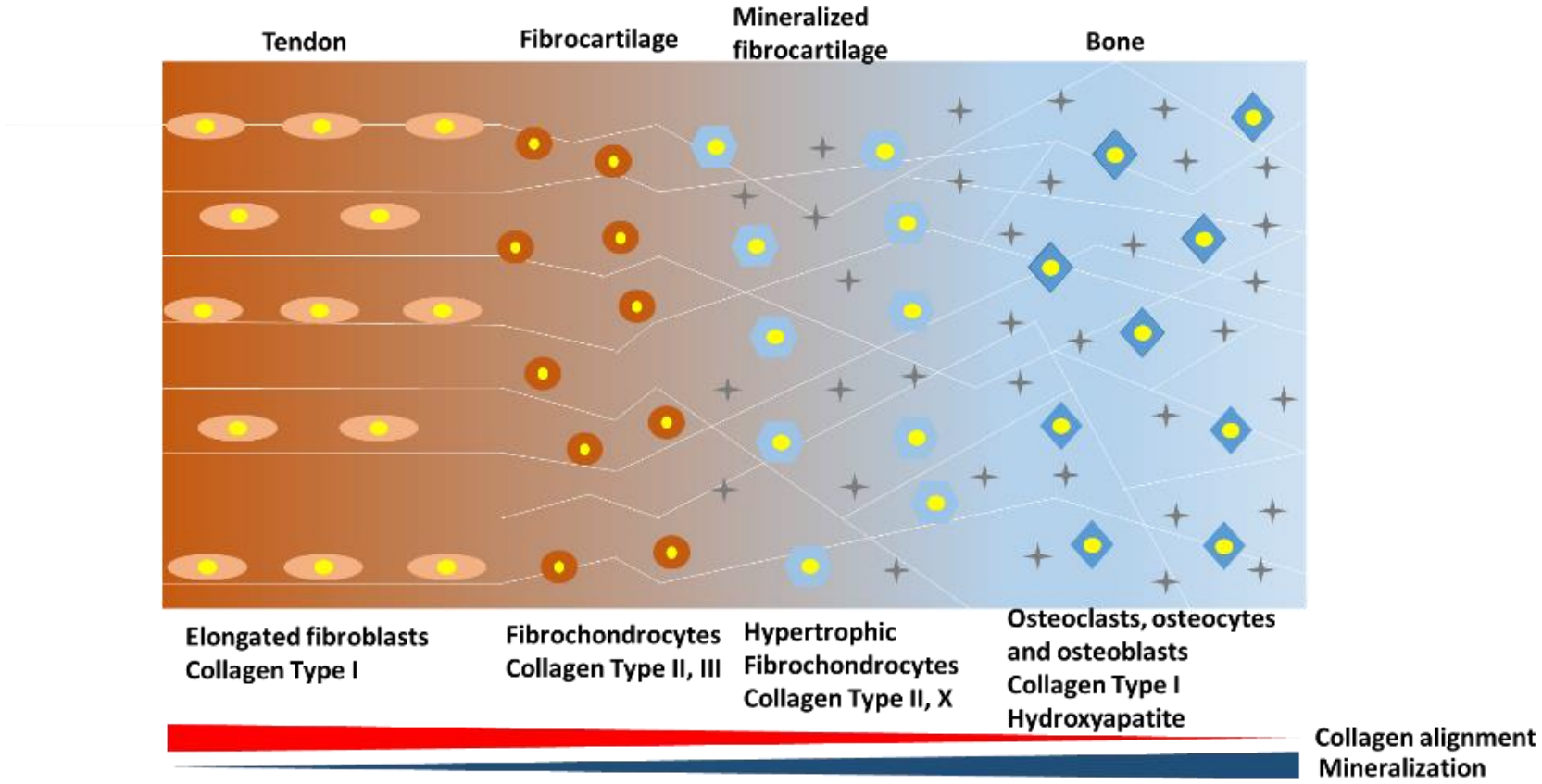



**Figure 4:** Structure and composition of fibrocartilaginous entheses. The four different zones of the fibrocartilaginous enthesis; tendon, fibrocartilage, mineralized fibrocartilage, and bone are indicated with their main extracellular matrix components and cellular types. Collagen fibres become less organised and mineral content increases as the tendon tissue reaches the bone.

the healing process occurs through the formation of fibrovascular scar tissue and does not restore the native tendon to bone insertion formed during embryological development [10, 18, 24, 25]. The development process of interface tissue involves a combination of biomolecular and biophysical cues. However, the specific cues involved in this process are still unknown [26-28].

Thomopoulos and colleagues previously reported it is likely that the gradation of the biological factors present in the tendon bone insertion site stimulate gradation in cell differentiation and subsequent tissue formation [26, 29, 30]. However, this gradation has not shown to be regenerated during tendon to bone insertion healing. Therefore, the resultant fibrovascular scar tissue has shown to be mechanically weaker and ineffective in recreating the original insertion site [26, 31, 32]. Thomopoulos *et al.* reported an excessive scar tissue formation with absence of any fibrocartilage tissue in a rat rotator cuff model [33].

The healing process takes place in four stages: the first stage is inflammation, followed by proliferation, then matrix synthesis, and the last stage is remodeling. During the first stage, inflammatory and marrow derived cells are recruited at the enthesis site, cytokines and growth factors such as TGF-beta and PDGF are released at this stage, with ingrowth of blood vessels and nerves caused by the growth factors stimulation and hypoxia [31, 34, 35]. At the proliferative and matrix synthesis stages stem cell proliferation and differentiation take place, as well as degradation in the provisional matrix by

matrix metalloproteinases and serine proteases. New extracellular matrix is synthesized by the healing cells at matrix synthesis stage. Remodeling of newly formed bone, interfacial tissue and graft occur during the remodeling stage with the formation of collagen fibers between tendon and bone [18, 36-39].

Mineralization, establishment of collagen fibers and fibrocartilage formation are essential factors for the regeneration of enthesis. Development of an insertion site requires number of elements such as: biological cues, mechanical properties, and specific composition and function of the four zones of the fibrocartilaginous enthesis [26]. Thus, it is very difficult and challenging to regenerate the native tendon to bone interface site with the specific properties of each zone.

## 1.5 Strategies for interface tissue engineering

There has been much interest in regenerating entheses due to their functional importance, and the fact that these critical tissue transitions lack their normal structure after healing. Fibrocartilaginous enthesis healing usually results in the formation of fibrovascular scar with poor mechanical properties [40, 41]. Therefore, enthesis injures do not heal effectively without surgical intervention. Tissue engineering strategies have been applied in the field of interface tissue engineering in order to develop a scaffold system capable of retaining the consistent integration between tendon and bone tissues, as well

as replicating the complex gradation cellular and biochemical composition [42]. To develop a scaffold for tendon to bone insertion site fixation, a number of factors must be taken in consideration including structural and mechanical properties of the enthesis, scaffold composition and cell populations [10, 43].

### 1.5.1 Scaffold Design for Tendon-to-Bone Interface Tissue Engineering

The rotator cuff is a group of four muscles (supraspinatus, infraspinatus, teres minor and subscapularis) and their associated tendons inserted into bone [44, 45]. The Rotator cuff is an example of a complex tendon to bone insertion site, consisting of four zones: tendon, fibrocartilage, mineralized fibrocartilage, and bone [46]. The zonal distribution of extracellular matrix allows sustainable tensile and compressive stresses and enables gradual transition in strain across the interface site [47].

Rotator cuff tears are very common; they can be managed surgically or conservatively. However, tendon to bone insertion healing is poor and associated with high failure rate [18]. The most commonly used techniques for rotator cuff repair are: the traditional open repair; it evolves an incision with detachment of one of the shoulder muscles to gain access to the torn tendon. The second technique is arthroscopic repair; an arthroscope is inserted through small incision. The third technique is mini-open repair; an arthroscope is used to remove any damaged tissue or bone spurs, then a small incision is made to repair the rotator cuff [48].

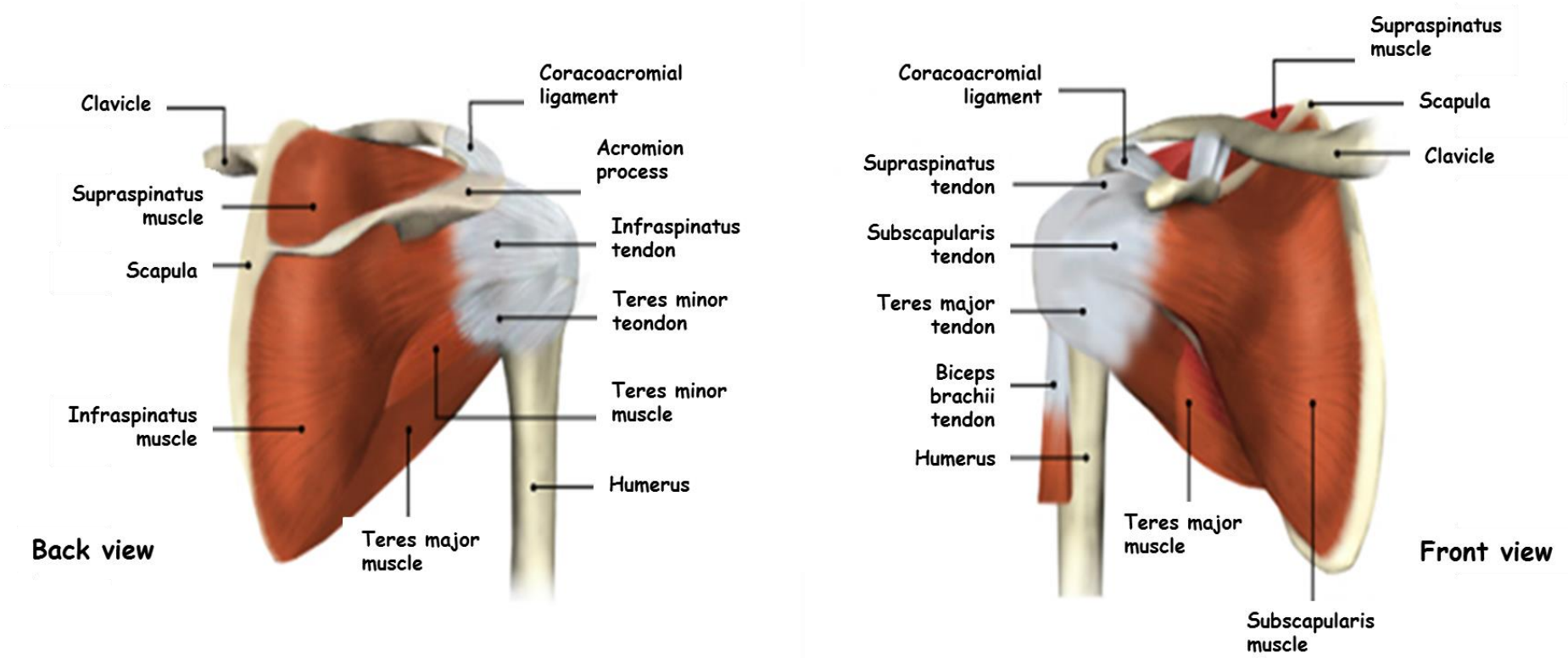



**Figure 5:** Rotator cuff anatomy.

#### 1.5.1.1 Growth factors

Although the specific signals and cues responsible for stem cell differentiation in tendon to bone interface tissues are still unknown, previous studies have shown enhancement in tendon to bone cell proliferation and differentiation with the aid of some growth and differentiation factors. It was hypothesised that growth factors used to promote chondrogenic differentiation would provide the required stimulus for enthesis formation given the similarity between the fibrocartilage and the hyaline cartilage [49]. Transforming growth factor-β1 (TGF-β1) [50, 51], transforming growth factor-β3 (TGF-β3) [52], bone morphogenetic protein-2 (BMP2) [52, 53], and bone morphogenetic protein-7 (BMP7) [50, 52] have been shown to promote chondrogenesis of mesenchymal stem cells (MSCs). Among these growth factors BMP2 is especially interesting for interface regeneration purposes, since is it has been reported that BMP2 at low doses (50 ng/ml) could induce chondrogenic differentiation of MSCs and upregulate the expression of collagen type II. In addition, the administration of BMP2 at high doses (100 to 400 ng/ml) could induce chondrocyte hypertrophy and promote the expression of collagen type X, alkaline phosphatase and osteocalcin [54].

Based on that Hashimoto *et al.* used BMP2 to induce ectopic ossicle formation in flexor digitorum communis tendon in a rabbit model to provide a starting point for enthesis formation. The tendon-ossicle complex was transferred onto the surface of rabbit tibia, and the insertion of the complex in the proximal tibia was confirmed with histomorphological examination. These results suggest

that using BMP2 can assist the regeneration of tendon to bone interface [55]. Moreover, BMP12 administered in several carriers has been shown to accelerate enthesis healing in sheep models [56].

Other growth factors used in the literature to enhance enthesis repair include granulocyte colony-stimulating factor (G-CSF) [57], transforming growth factor beta-3 (TGF-β3) [58], and fibroblast growth factor-2 (FGF2) [59].

#### 1.5.1.2 Cell based scaffolds

Seeding therapeutic cells in biodegradable scaffolds has become the most commonly used and well-established scaffolding approach in tissue engineering [60]. In addition, stem cells have emerged as a promising cell source because of their ability to differentiate into several cell types and consequently regenerate different tissues [5].

Several cell types can be identified in the tendon to bone insertion site including elongated fibroblasts, chondrocytes, hypertrophic chondrocytes, osteoblasts, osteoclasts, and osteocytes. Several cell culture strategies have been developed to mimic the complex cellular composition of the enthesis. Wang *et al.* reported that the addition of human ligament fibroblasts and osteoblasts to a hydrogel scaffold initiated fibrocartilage formation. However, the fibrocartilage-like interface was not formed *in vitro* during the culture period examined and there was not any evidence of interface tissue regeneration [61]. In a similar approach, Cooper *et al*. (2014) cultured NIH 3T3

mouse fibroblasts and 3T3-E1 mouse calvarial osteoblasts on poly-l-lactic acid (PLA) woven fabric; a transition zone was created between the two regions to allow fibroblasts and osteoblasts interaction (Figure 6). Unfortunately, the glycosaminoglycan and collagen content measured by Alcian Blue staining and Hydroxyproline did not show any significant differences between scaffold regions [3].

Mesenchymal stem cells (MSCs) have the potential to differentiate into various musculoskeletal tissue types; including fibroblasts chondrocytes and osteoblasts [62]. Soon *et al*. (2007) coated tendon allograft with bone marrow derived mesenchymal stem cells (BMSCs) in fibrin gel to reconstruct anterior cruciate ligament (ACL) in a rabbit model, the results suggested that fibrocartilage zone was formed with an enhancement in the mechanical properties of the repaired enthesis [63]. Comparable results were obtained by Nourissat *et al*. when injected BMSCs in fibrin glue into an enthesis in a rat model [64]. Furthermore, the transduction of BMSCs with scleraxis (a transcription factor that is thought to direct tendon development during embryogenesis) or with matrix metalloproteinase (MMP) gene improved the healing of tendon to bone insertion site [41, 65].

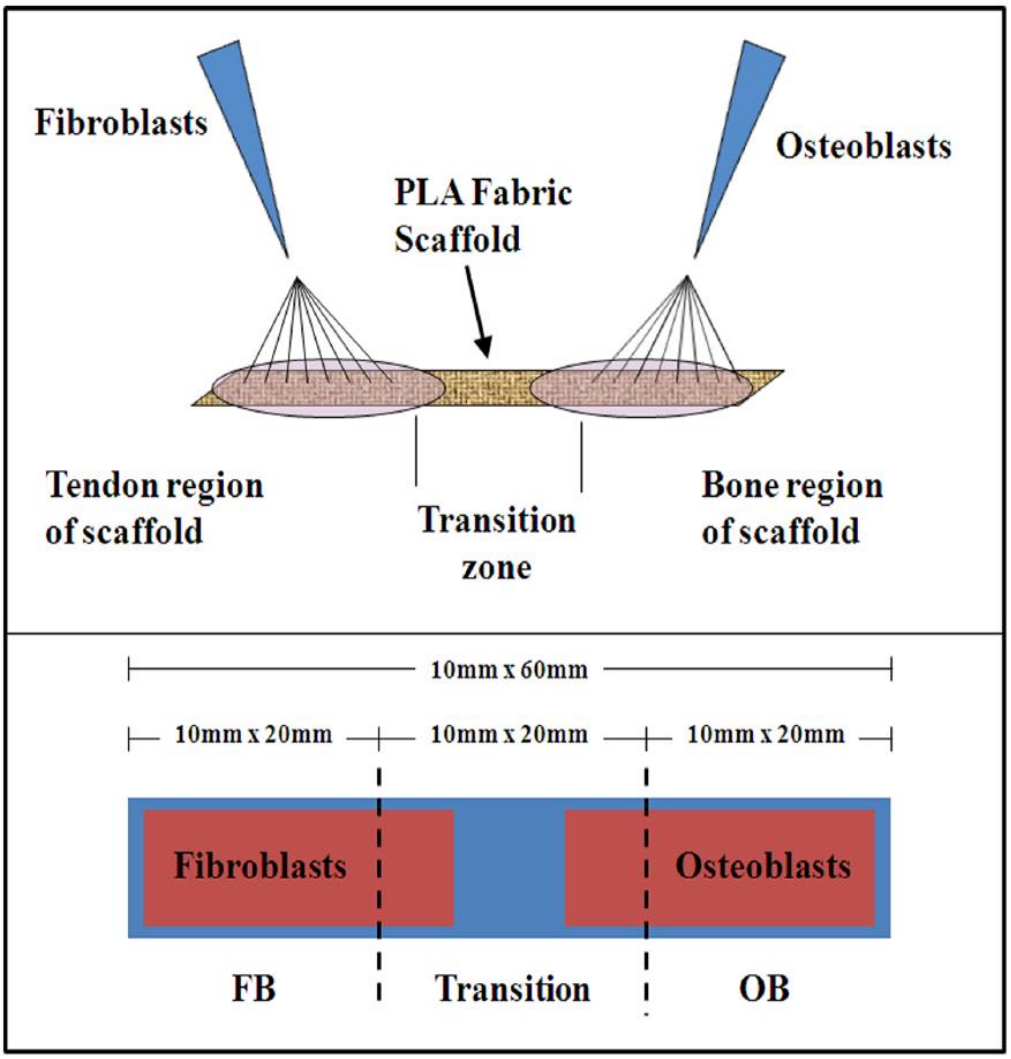



**Figure 6:** Schematic shows the fibroblast (FB) and osteoblast (OB) seeding on poly-l-lactic acid (PLA) scaffolds are co-cultured to make a tendon region and a bone region on the scaffold. The seeding area is shown as the red area in the bottom schematic. There is a transition zone between the two regions where both cells interact. For analysis, the scaffold is sectioned into equal thirds to measure the FB, OB, and transition regions. *Source:* figure reprinted with permission from reference [3].

There are very few studies published in the literature exploring the use of adipose derived stem cells (ASCs) in tendon to bone interface tissue engineering, even though many studies have reported the capacity of these cells to regenerate tendon [66, 67], ligament [68], cartilage [69, 70], bone [71, 72], and osteochondral [73, 74] tissues. Min *et al*. (2014) investigated the effect of reverse gradients of dual platelet derived growth factorβ (PDGF-BB) and bone morphogenetic protein-2 (BMP2) concentrations on ASCs differentiation to regenerate tendon to bone interface. The results illustrated that ASC differentiation was mediated by gradients of biological molecules stimulated by gradient growth factor concentrations [75].

#### 1.5.1.3 Biomaterials

Synthetic and natural biomaterials have been widely used for regeneration of tendon and bone tissues; these biomaterials have reported success *in vitro* and *in vivo.* However, these studies mostly described the regeneration of either bone or tendon tissue, and did not describe the regeneration of the insertion site.

Biomaterials used in bone tissue engineering include calcium phosphate ceramics [76], collagen [77-79], alginate[80], decellularized bone matrices [81] and polylactic-co-glycolic acid (PLGA) [82, 83]. Additionally, collagen [84, 85], poly-L-lactic acid (PLLA) [86], and decellularized tendon matrices [87, 88] have been used for tendon tissue engineering.

Technological advancements in tissue-engineered biomaterials have contributed to improving the enthesis repair outcomes. For example, scaffolds that connect the tendon to bone may provide reinforcement during the healing process; on the other hand, it must be strong to endure the physiological and pathophysiological loading of the joint [89, 90]. A number of preclinical devices have failed to repair entheses because of the insufficient mechanical and structural properties of the graft material used [91, 92].

Electrospinning technique is a distinctive technique that uses electrostatic forces to produce spatially aligned or randomly oriented, thin nanofiber sheets; electrospun polymers have also been used in preclinical augmentation of the tendon-bone interface [93, 94]. The advantages of an electrospun scaffold are wide range of materials, pore size and surface area control, density, fibril alignment, and mechanical properties [95]. Moreover, the functional properties can be modified during or after the electrospinning process, for example Kolluru *et al.* modified the micromechanical properties of electrospun PLGA fibers using crystalline coating of hydroxyapatite [96].

The use of electrospinning techniques to fabricate biomaterials for tendon-to-bone tissue engineering holds promises for mimicking the micro-pattern of the native enthesis and spatial deposition of biomolecules to help guide regeneration of the enthesis.

The multi-tissue structure of the tendon to bone insertion site represents a significant challenge in the field of interface tissue engineering, initial attempts to design scaffold for enthesis repair focused on hybrid biomaterial scaffolds to mimic the graded structure of the native enthesis. Soo Kim *et al*. constructed collagen based multilayer scaffold consists of four different layers: (a) a tendon layer composed of collagen; (b) an uncalcified fibrocartilage layer composed of collagen and chondroitin sulfate; (c) a calcified fibrocartilage layer composed of collagen and less apatite and (d) a bone layer composed of collagen and apatite [97]. The results showed gradual transition in the mechanical properties across the scaffold, with proliferation of human fibroblasts, chondrocytes, and osteoblasts in each corresponding layer [97]. In a similar approach, Sahoo *et al*. developed a hybrid scaffold made of knitted microfibers coated with: (a) poly (ε-caprolactone), (b) poly (D, L-lactide-co-glycolide) nanofibers, (c) collagen type I. This work demonstrated that the coating techniques could modulate the mechanical properties of each layer of the hybrid scaffold and consequently enhance different cell type proliferation in the hybrid scaffold [98]. Similar results were obtained by Li *et al*. and Erisken *et al*. when developed a scaffold of electrospun nanofibers with a gradient in mineral composition, the gradient in mineral content resulted in spatial gradient in the stiffness of the scaffold and the behaviour of the seeded cells [99, 100].

The stratified scaffolds described above were designed to mimic the multi-tissue structure of the tendon-to-bone insertion site. As such, given the complexity of the interface site and the need to support the related tissue-specific cell phenotypes, there is emerging interest in designing scaffolds with gradations in properties.

#### 1.5.1.4 Extracellular matrix bioscaffolds

Extracellular matrix (ECM) is a 3D network made of the secreted components of the tissue resident cells; it is composed of functional and structural proteins including collagen, growth factors, fibronectin and proteoglycans (Figure 7). ECM provides appropriate microenvironment for the cellular constituents and direct cell behaviour such as proliferation and differentiation via biochemical and biomechanical cues [101, 102].

Decellularization of tissues is a common strategy for creating biologic scaffold materials composed of extracellular matrix; the advantages of using extracellular-derived scaffolds are the 3D ultrastructure and ECM composition. ECM integrity, ultrastructure, as well as the vascular, lymphatic and nervous networks, can be preserved with an appropriate decellularization process [103, 104]. Moreover, the extent of decellularization has also been shown to impact host response, with ineffective decellularization of small intestinal ECM (SIS-ECM) stimulating a pro-inflammatory response [105].

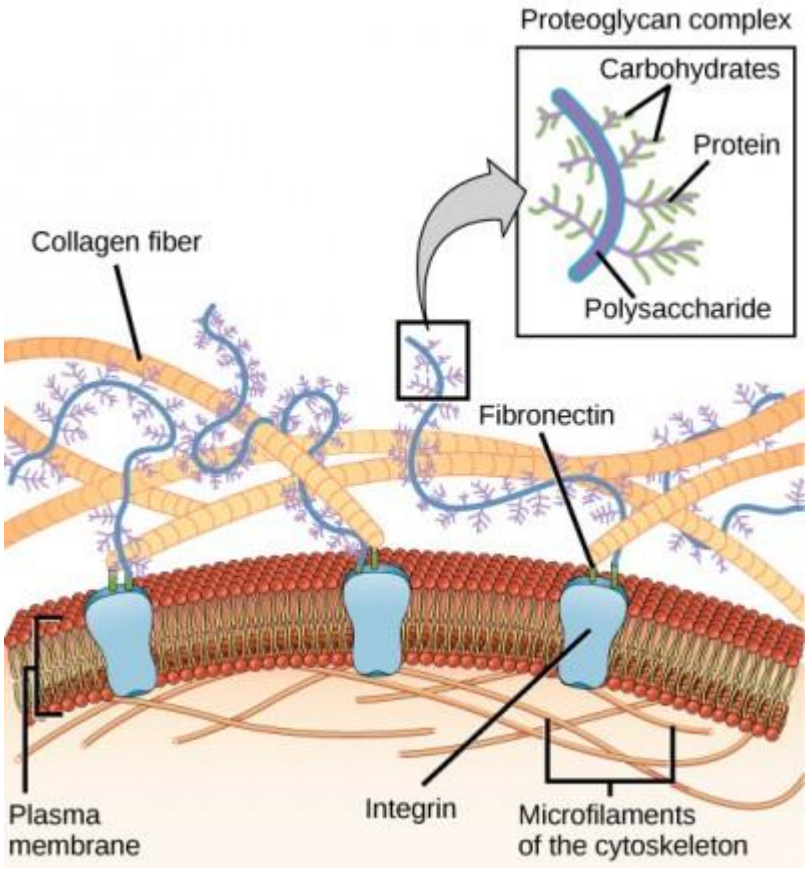



**Figure 7**: Structure of extracellular matrix and its composition. *Source:* available online: [https://opentextbc.ca/biology/chapter/3-3-eukaryotic-cells/](https://opentextbc.ca/biology/chapter/3-3-eukaryotic-cells/)

In the past decade, bioscaffold materials composed of ECM derived from human or animal tissues and organs have become available as regenerative medicines for the repair and regeneration of musculoskeletal tissues with examples of available clinical products are; dCELL® (Tissue Regenix Ltd, Leeds, UK), Permacol (Tissue Science Laboratories, Covington, Georgia), and Restore (DePuy Orthopaedics, Warsaw, Indiana).

In addition to the above, ECM scaffolds are biodegradable and can play critical roles in cell signalling and tissue homeostasis by providing necessary biological stimulus for appropriate tissue development [103, 104, 106]. Tissue development depends on the recruitment and differentiation of stem/progenitor cells [106, 107], as well as the elicitation of an immune response from the host (Figure 8) [108, 109]. Proper decellularization of the source tissue to produce ECM scaffolds is crucial as cell remnant may be retained with ineffective decellularization processing and these have been shown to be associated with an extreme inflammatory response that can interfere with constructive remodeling outcomes [105].

Previous studies have demonstrated some growth factors that been released upon the degradation of ECM scaffold, these GFs provide bioactive cues required for cell viability, motility, and differentiation and they consequently induce tissue regeneration (Figure 8) [110, 111]. Examples of these GFs are: basic fibroblast growth factor (bFGF), vascular endothelial growth factor (VEGF), insulin-like growth factor and hepatocyte growth factor in addition to cryptic peptides [112-114]. Based on that many studies have reported that ECM

scaffolds differ in initiating host response through the release of different growth factors and cryptic peptides, because each tissue has its specific biochemical composition. Thus, it has been suggested that biological scaffolds derived from homologous tissues had superior function and were more suitable for tissue repair compared to scaffolds derived from non-homologous tissues [113-115].

ECM scaffolds have been used successfully to support constructive remodeling of various tissues, these scaffolds have been introduced in different forms including sheets [116], powder [117], tubular [118], whole organ [104], and hydrogels [81]. The sheet and powder ECM are very popular for topical wound dressings, while tubular ECM devices have been used in many studies for regeneration of cardiovascular and gastrointestinal tissues [119, 120].

Moreover, whole organs were decellularized to generate a 3D scaffold with the native tissue architecture, such methods were used for several lung, heart and liver applications [121-123].

In recent years, methods have been available to enzymatically digest ECM materials to form a liquid dispersion that can be injected and induced to form a hydrogel under physiologic conditions *in situ* [124]. ECM hydrogels have been used to promote the constructive remodeling for different tissues including ischemic myocardium and central nervous system [125, 126]. Such scaffolds

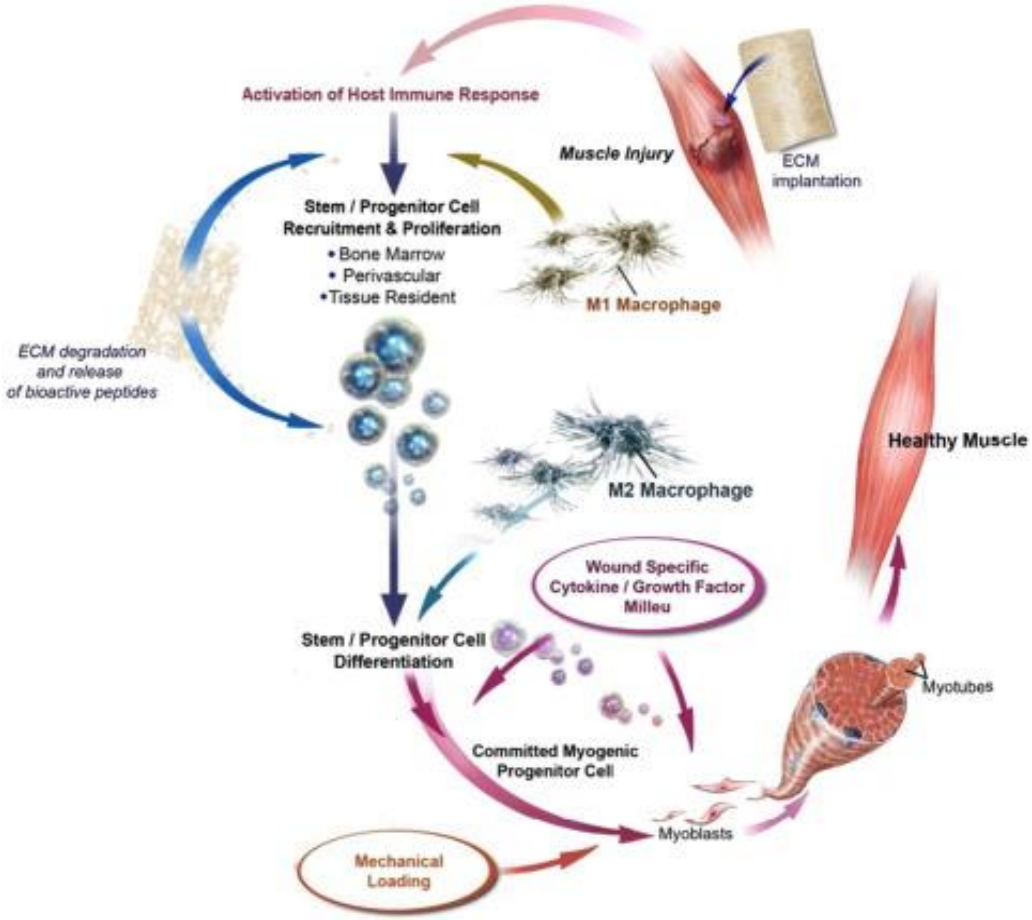



**Figure 8**: Schematic overview of skeletal muscle reconstruction using an ECM scaffold. Implantation followed by degradation of an ECM scaffold releases GFs and bioactive peptides responsible for eliciting immune response and consequently the recruitment, proliferation, and differentiation of multi-potent stem/progenitor cells. Wound-specific factors determine cell fate resulting in site specific-tissue remodeling. *Source:* reprinted with permission from reference [2].

have the advantage of being delivered in a minimally invasive manner, fill an irregular shaped space, and as a carrier for drugs, growth factors and cells [127, 128].

Furthermore, ECM bioscaffolds have been introduced to the tendon and bone regeneration field; several studies have used scaffolds derived from decellularized bone extracellular matrix and have shown to successfully promote bone formation *in vivo* [129-131]. Also scaffolds derived from decellularized tendon extracellular matrix were explored; Yang *et al.* reported that tendon ECM extracted proteins enhance tenogenic differentiation of human adipose stem cells [88].

The clinical use of scaffolds for enthesis repair has reported some few successful attempts in human patients. Scaffold devices derived from extracellular matrix have had limited number of follow-up studies on human patient [132]. Example of ECM derived scaffold is GraftJacket; acellular human decellularized dermal allograft, has shown some promising results after implantation clinically in small cohorts of patients, the magnetic resonance imaging scans confirmed the attachment of the scaffold to the native tissue. Moreover, patients with GraftJacket showed improvement in external rotation strength compared to preoperative metrics [133, 134]. However, GraftJacket expressed some potential failure mechanisms upon further cadaveric and laboratory studies related to suture pull-through and breakage [135, 136].

These data suggest that several criteria play a role in the success of scaffold-based repair of an enthesis such as the structural and mechanical properties of the scaffold as well as the suture techniques used in the procedure. Fisher *et al.* have used extracellular matrix bioscaffold derived from porcine small intestine submucosa (SIS) in conjunction with a sheet form of ECM-SIS to heal a surgically transacted anterior cruciate ligament (ACL) in a goat model. The application of ECM-SIS hydrogel and sheet was found to accelerate the healing process [137]. However, clinical studies have reported less favourable outcomes with the use of Restore, an ECM scaffold derived from small intestine submucosa, whereby magnetic resonance imaging scans revealed that 10 out of 11 Restore-augmented repairs failed [138]. A further controlled trial of 30 patients with rotator cuff tears showed that unaugmented patients were 7% more likely to heal than Restore-augmented patients [139].

The use of ECM derived scaffolds is increasing in the orthopaedic field, their utilization for enthesis repair represents a different and better strategy compared to the previous orthopaedic approaches. However, the ideal mechanical, structural, and biological properties of ECM scaffolds for enthesis repair have not been fully defined yet.

## 1.6 Aims and Objectives

Despite the advancement and innovative approaches to many aspects of tissue engineering, the generation of a functional tendon to bone interface tissue has not yet been achieved. There is a pressing need to create a functional tendon to bone construct that can mimic the graded structural and cellular heterogeneity of the native tissue.

The aim of this thesis was to design a gradient bECM/tECM bioscaffold with different conditions to induce mesenchymal stem cells (MSCs) differentiation into multiple interface-specific lineages.

The aims of the following results chapters are as follows:

Chapter 3:

- To assess the osteogenic inducing capability of hydrogels derived from bovine bone ECM *in vitro*
- To demonstrate the ability of these hydrogels to promote bone regeneration
- To assess bone ECM ability as a carrier for local delivery of cells and growth factor

Chapter 4:

- To develop a protocol to produce a hydrogel from decellularized equine tendon extracellular matrix
- To determine the structure and mechanical properties of tendon ECM
- To assess the ability of tendon ECM to induce tenogenic differentiation in hMSCs
- To analyse the potential of bone ECM to induce osteogenic differentiation in hMSCs

Chapter 5:

The aim of this chapter is to produce an electrospun scaffold using decellularized bovine bone extracellular matrix (bECM) to serve in the long term as a base for the gradient scaffold with bone ECM and tendon ECM hydrogels

- To optimise a method to electrospin decellularized bovine bone extracellular matrix (bECM)
- To assess the biocompatibility of electrospun bECM and compare it to electrospun gelatin
- To assess the osteogenic capability *in vitro* of electrospun bECM scaffolds in comparison to electrospun gelatin

# Chapter 2. General Materials and Methods

## 2.1 Gel production

### 2.1.1 ECM hydrogel

ECM gel was produced as previously described [81, 124, 128]; decellularized ECM from bone or tendon in a powdered form were added to a solution made up of 1mg/ml porcine pepsin (Sigma–Aldrich) in 0.01N HCl and stirred for up to 96h at room temperature to create ECM digest solutions. Gels were formed by mixing them with 0.1 N NaOH (sigma-Aldrich, UK) (1/10 of the volume of digest solution) and 10× PBS (Thermo Fisher Scientific, UK) (1/9 of the volume of digest solution) on ice. The solution was made up to the final volume with 1× PBS then placed at 37°C for gelation to occur.

### 2.1.2 Collagen type I hydrogel

Gels from rat tail collagen type I (Corning™, Fisher Scientific, UK) were made following the manufacturer's instructions; the volume of the pre-gel collagen to be used was calculated as following: ((final volume × final collagen concentration in mg/ml)/ concentration of pre-gel collagen). Then 10× PBS (final volume /10) was mixed with 1 N NaOH (volume of pre-gel collagen to be added × 0.023) and added to pre-gel collagen on ice, the final volume was made up with $dH_2O$ then placed at 37°C for gelation to occur.

## 2.2 General cell culture

### 2.2.1 C2C12 mouse myoblast cell line

The C2C12 mouse myoblast cell line was purchased from Sigma-Aldrich (UK), Lot: BN23942. Cells were cultured in Dulbecco's Modified Eagle Medium (DMEM, Sigma-Aldrich) supplemented with 10% fetal calf serum (FCS) and 1% penicillin/streptomycin, 1mM L-Glutamine. Cultures were maintained at 37°C and 5% (v/v) $CO_2$ as monolayers on tissue culture treated polystyrene. When cells were confluent (80%) they were passaged by trypsinisation and reseeded at $1/10^{th}$ of this density. Passage procedure for a T75 flask was as follows: culture medium was aspirated from the flask and the cell monolayer washed with 10 ml in phosphate buffer saline (PBS). After aspiration of the PBS, 5 ml of trypsin/EDTA (Sigma-Aldrich) was added to the flask, and incubated at 37°C for up to 5 min. The trypsin was deactivated by the addition of 10 ml of culture medium and the resulting suspension was centrifuged at 200xg for 5 minutes. The supernatant was aspirated and the cell pellet resuspended in fresh culture medium for further seeding.

### 2.2.2 Mouse primary calvarial cells

Mouse primary calvarial cells (mPCs) were extracted in house from skulls of neonatal mice 1-3 day old as previously described [140]. mPCs were cultured

in Alpha MEM (αMEM, Lonza), supplemented with 10% fetal bovine serum (FBS), 1% penicillin/streptomycin, and 1mM L-Glutamine. Cultures were maintained at 37°C and 5% (v/v) $CO_2$ as monolayers on tissue culture treated polystyrene. When cells were confluent (80%) they were passaged by trypsinisation and reseeded 1/3$^{rd}$ and 1/5$^{th}$ of this density. Passage procedure for a T75 flask was as follows: culture medium was aspirated from the flask and the cell monolayer washed with 10 ml in phosphate buffer saline (PBS). After aspiration of the PBS, 4 ml of trypsin/EDTA (Sigma-Aldrich) was added to the flask, and incubated at 37°C for up to 5 min. The trypsin was deactivated by the addition of 11 ml of culture medium and the resulting suspension was centrifuged at 200xg for 5 minutes. The supernatant was aspirated and the cell pellet resuspended in fresh culture medium for further seeding.

### 2.2.3 Primary human bone-marrow mesenchymal stem cells

Primary human bone-marrow mesenchymal stem cells (hMSCs) were purchased from Lonza (Cologne, Germany). hMSCs were cultured in mesenchymal stem cell growth medium (MSCGM) (PT-3001, Lonza) supplemented with mesenchymal cell growth supplement (MCGS), L-glutamine and GA-1000 (SingleQuots™, Lonza). Cultures were maintained at 37°C and 5% (v/v) $CO_2$ as monolayers on tissue culture treated polystyrene. When cells were confluent (80%) they were passaged by trypsinisation and reseeded at seeding density: 5,000-6,000 cells per cm$^2$. Passage procedure for a T175 flask was as follows: culture medium was aspirated from the flask and the cell monolayer

washed with 20 ml in HEPES buffered saline solution (CC-5024, Lonza). After aspiration of the HEPES, sufficient volume of Clonetics™ trypsin/EDTA (CC-3232, Lonza) solution was added (approx. 0.05 ml/$cm^2$), and incubated at 37°C for up to 6 min. The trypsin was deactivated by the addition of equal volume of MSCGM™ culture medium and the resulting suspension was centrifuged at 600xg for 5 minutes. The supernatant was aspirated and the cell pellet resuspended in fresh culture medium for further seeding.

### 2.2.4 Cryopreservation

Cells were preserved and saved for later use in liquid nitrogen, the cryopreservation medium was made of: fetal bovine serum (FBS) supplemented with 10% (v/v) dimethyl sulphoxide (DMSO) (Sigma-Aldrich,UK), for hMSCs cryopreservation medium was made of: 85% MSCBM ,10% DMSO and 5% Human serum albumin (HSA) (w/v). Cells were trypsinised and centrifuged as appropriate to the cell type.

Cells were then resuspended in cryopreservation media at 500,000 to 2,000,000 cells per ml in cryovials, and stored at -80°C overnight then placed in liquid nitrogen until required.

### 2.2.5 Thawing cells after cryopreservation

Cryovials were warmed in water bath (37°C) for no longer than 1 min, the thawed cell suspension were then added to 5 ml culture medium and

centrifuged as appropriate for each cell type. Finally, cell pellets were resuspended in pre-warmed culture medium and seeded into desired flasks.

### 2.2.6 Cell viability assessment

The proliferation of cells was assessed with PrestoBlue (ThermoFisher) over several days; a solution of 10% PrestoBlue and 90% culture medium was added to each well and incubated for 1h and 30 min at 5% $CO_2$ and 37°C. Triplicate 100µl were transferred to 96 well plate to measure fluorescence (Ex 560 nm/ Em 590 nm) on a Tecan Infinite M200 plate reader.

### 2.2.7 Immunohistochemical staining for osteogenic proteins

The osteogenic differentiation of cells was assessed by immunohistochemical staining for osteogenic marker proteins. Briefly, cells were fixed with 3.7% paraformaldehyde (PFA) for 2h, washed with PBS and permeabilized with 0.1% Triton X-100 (Sigma, UK) in PBS for 45 mins, cells were washed 3 x 5 min then blocked. The blocking solution was made up of PBS containing 1% (w/v) BSA (Sigma, UK) and 3% (v/v) serum from the animal in which the secondary antibody was raised. Donkey serum (sigma, UK) for Anti-osteopontin primary antibody, goat polyclonal (R&D Systems) and goat serum (sigma, UK) for Anti-osteocalcin primary antibody, rabbit polyclonal (Millipore, UK). The blocking solution was removed then 1:200 dilution of primary antibody in 1% BSA in PBS was added and incubated at 4°C overnight. Samples were washed 3x5 min with

PBS then 1:200 dilution of secondary antibody; Alexa Fluor 546 (red) donkey anti-goat IgG. (Invitrogen, UK) and Alexa Fluor 488 (green) goat anti-rabbit IgG (Invitrogen) in 1% BSA in PBS was added and left for 1 h at room temperature, followed by final wash 3x5 min with PBS. Staining was then imaged on an inverted fluorescent microscope. Control wells of no primary and only secondary antibody were imaged to determine background fluorescence.

## 2.3 Statistical analysis

All data are presented as mean ± standard deviation, and experiments were run separately at least three times, one-way or two-way analysis of variance (ANOVA) determined statistical significance of two-group comparisons and multiple-group comparisons. Statistical analyses were performed using GraphPad Prism 6 software, significance was defined as **** indicates $p<0.0001$; *** indicates $p<0.001$; ** indicates $p<0.01$ and * indicates $p<0.05$ for all statistical analyses.

# Chapter 3. Hydrogel Scaffold Derived from Decellularized Bone Matrix with Osteogenesis-Inducing Activity and Protein Carrier Ability

## 3.1 Introduction

Clinically, replacement of damaged bone tissue due to trauma, tumours, or other diseases is still a major challenge. To date, autologous bone grafts are considered the gold standard for fracture repair and bone restoration. However, autografts and allografts have a number of limitations including donor site morbidity, limited availability of graft material, and potential of disease transmission with allografts [141-143].

The increasing clinical demand for bone substitutes has driven attention towards biological scaffold materials composed of extracellular matrix (ECM) of decellularized tissues, as they have been shown to facilitate the reconstruction of many different tissues [88, 104, 144, 145]. This property arises from the retention of ECM molecular components such as growth factors, proteoglycans and glycosaminoglycans [88, 146]. A number of decellularized ECM scaffolds have been used to repair tissues; design requirements for these scaffolds differ depending on the tissue of interests and type of application. ECM hydrogels have previously been derived from native

tissues including bone [81] , small intestinal submucosa [125], skin [128], and urinary bladder [124].

ECM is tissue-specific and its components differ based on the source of tissue [101, 146]. Previous reports have suggested that biological scaffolds derived from site-specific tissues are more suitable for tissue repair than non-site specific scaffolds such as the liver [123, 147, 148], skin tissue [148], and cardiovascular [149].

Hydrogel scaffolds derived from decellularized and demineralized bovine bone extracellular matrix, have been previously investigated as a biologic scaffold with distinct structural, mechanical and biological properties [81]. Further studies of the bone ECM hydrogel have shown that the incorporation of growth factors within ECM/alginate hydrogels enhanced skeletal tissue repair within *ex vivo* chick femur defects [130, 131] and increased *in vivo* tissue mineralization and bone formation [129]. However, in these applications it was not clear whether the osteoinductive properties arose from the addition of osteogenic growth factors or from the bone derived ECM hydrogels. Moreover, previous studies have reported that high BMP doses in clinical use may contribute to numerous adverse effects in humans not seen in rodent animal models [150-152]. The osteogenic potential of decellularized and demineralized bone matrices in the absence of osteogenic inducers (growth factors or osteogenic medium) is still an under-researched area, and a quantitative, sensitive and reliable assessment is needed to evaluate the

osteoinductive activity of these biomaterials without the incorporation of osteogenic inducers.

The aim of this chapter is: (1) to assess the osteogenic inducing capability of hydrogels derived from bovine bone ECM *in vitro* using the pluripotent myoblast C2C12 cell line and mouse primary calvarial cells (mPCs), in the presence and absence of osteogenic inducers (osteogenic medium). For this objective, we prepared bECM and DBM hydrogels and examined their biological activity and osteogenic capability in comparison to collagen type I hydrogels; the expression levels of osteogenesis-specific genes and proteins were analysed, (2): to demonstrate the ability of these hydrogels to promote bone regeneration and act as a carrier for local delivery of cells and growth factor.

## 3.2 Materials and methods

### 3.2.1 Preparation of DBM and bECM hydrogels

Demineralized bone matrix (DBM) and decellularized bone matrix (bECM) were prepared as previously described [81]. Briefly, cancellous bone segments were selected from fresh bovine tibias harvested from 12–24 month old animals from an EU certified butcher (J. Broomhall Ltd, Eastington, UK) (Figure 9A). Cancellous bone segments were washed with 0.1% w/v Gentamicin in phosphate-buffered saline (PBS). Segments were immersed in liquid nitrogen and ground in coffee mill (Tefal, 200W).

Bone granules were demineralised using an adaptation of previously reported methods [153] and as previously reported by Sawkins *et al*. [81]. Briefly, the granules were demineralized in 0.5N HCL (25ml/g bone) for 24h at room temperature under agitation at 300 rpm. The demineralized granules were then washed with distilled water and the lipids extracted with a 1:1 mixture of chloroform and methanol (Fisher Scientific, Loughborough, UK) for 1h, followed by rinsing with methanol then distilled water. The DBM then was frozen with liquid nitrogen, lyophilized for 24h and stored at -20°C until required.

The demineralized bone granules were then decellularized by adaptation of a previous method [154]. DBM granules were washed with distilled water and decellularized with 0.05% trypsin (Sigma–Aldrich, Poole, UK) and 0.02% ethylenediamine tetraacetic acid (EDTA) (Sigma–Aldrich) at 37°C for 24h. The decellularized bone matrix (bECM) then was washed with PBS with 1% w/v penicillin/streptomycin for 24h at 4°C, followed by snap freezing, and lyophilization for 24h then stored at -20°C (Figure 9B).

A hydrogel was produced following the method of enzymic digestion, solubilization and neutralisation given in 2.1.1. (Figure 9C).

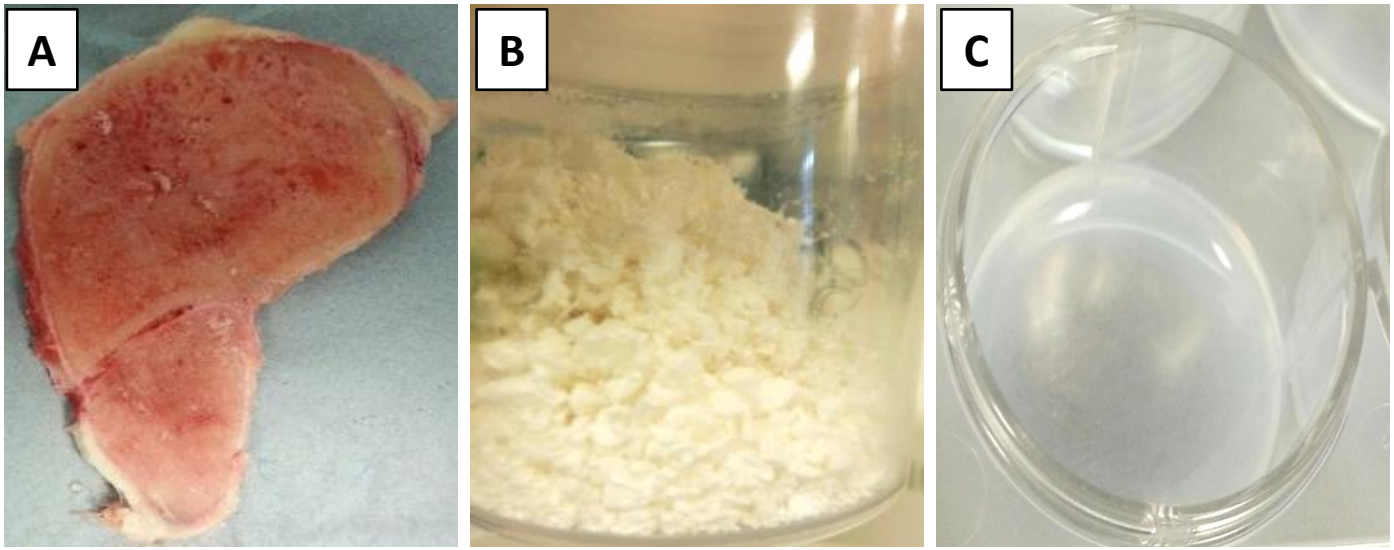



**Figure 9:** Production of ECM hydrogel from bone. (A) Bovine tibiae bone were subjected to mineral, lipid and cell removal procedures to produce (B) decellularized bone (bECM) prior to pepsin digestion and solubilization to form an ECM hydrogel (C).

### 3.2.2 SDS-PAGE and BCA assay

15µl pepsin digested ECM samples of the same concentration (10mg/ml) of DBM and bECM were treated with 1µl 50mM Dithiothreitol (DTT) reducing agent (Thermo Scientific), mixed with 5µl NuPage LDS sample buffer (Novex, life technologies, USA), and heated at 70°C for 10 min. Samples were then loaded into wells of pre-cast NuPAGE gels (NuPage 10% Bis-Tris Gel, life technologies, USA) and separated by electrophoresis in MES running buffer for 45 min at 200V. Gels were stained with Coomassie Blue for 20 min, and then washed with 10% acetic acid (Fisher Scientific).

BCA assay was performed to determine variations in total protein concentration between bECM and DBM hydrogels; pepsin digested bECM and DBM were assayed in triplicates following the manufacturer's instructions (Thermo Scientific).

### 3.2.3 C2C12 osteogenic differentiation

C2C12 were cultured on the surface of 8mg/ml bECM, DBM and collagen type I hydrogels. Briefly the digests were neutralized to the desired concentration and kept on ice at 4°C, 0.5ml of 8mg/ml gel was added to 12 well plate and incubated at 37°C for 1 h. Once the hydrogels were formed $4x10^4$ C2C12 cells were added to the surface of the gels and cultured for 7 days in medium.

Two different media were used: rich-serum medium consisted of Dulbecco's Modified Eagle Medium (DMEM, Sigma-Aldrich) supplemented with 10% fetal

calf serum (FCS) and 1% penicillin/streptomycin, 1mM L-Glutamine, and low-serum medium: Dulbecco's Modified Eagle Medium (DMEM, Sigma-Aldrich) supplemented with 2% horse serum and 1% penicillin/streptomycin, 1mM L-glutamine. Cells were maintained at 37°C and 5% $CO_2$. Osteogenic differentiation was determined by alkaline phosphatase activity assay.

### 3.2.4 Alkaline phosphatase activity assay

Intracellular alkaline phosphatase (ALP) is a marker for early differentiation of osteoblast-like cells [155], and was used here to measure differentiation stimulated by bECM hydrogels. ALP activity was evaluated with a commercial phosphatase substrate Colorimetric kit following the manufacturer's instructions (Abcam, UK).

A digestion solution was made of 0.5% collagenase from *Clostridium histolyticum* (Sigma, USA), 1% Bovine serum albumin (BSA, Sigma) in Hank's Balanced Salt Solution (HBSS, Gibco). bECM and collagen type I hydrogels were digested with the digestion solution and centrifuged at 300xg for 5 minutes then homogenized in the assay buffer and centrifuged to remove insoluble material at 13,000 x g for 3 mins following the manufacturer's instructions. Samples were incubated at room temperature for 60 minutes with 5mM *p*-Nitrophenyl Phosphate (pNPP). Absorbance was then read at 405 nm using Tecan Infinite M200 plate reader (Tecan UK, Reading, UK). Assaying of ALP standards was also performed to derive a standard curve that could be used to quantify ALP concentration within the samples. The live cell count was

determined on a haemocytometer by staining dead cells with Trypan blue (Sigma-Aldrich, UK).

### 3.2.5 mPCs osteogenic differentiation

Mouse primary calvarial cells were cultured on tissue culture plastic (TCP) and surface of 8mg/ml bECM, DBM, and collagen type I, at $4x10^4$ cells per well in 12-well plate, in basal media: Alpha MEM (αMEM, Lonza), supplemented with 10% fetal bovine serum (FBS), 1% penicillin/streptomycin, and 1mM L-Glutamine (basal media). Cells were also cultured with osteogenic media: basal media supplemented with 50 µg/ml L-ascorbic acid (Sigma-Aldrich), 50 mM β-glycerophosphate (Merck), and 10 µM dexamethasone (Sigma-Aldrich). mPCs used in the study were between third to fifth passages.

### 3.2.6 Immunohistochemical staining for mouse osteopontin and osteocalcin

The osteogenic differentiation of mPCs was assessed by immunohistochemical staining for the osteogenic marker proteins osteocalcin and osteopontin, these are widely used as indicators of pre-nodule protein structures [156-158].

Immunohistochemical staining for the osteogenic marker proteins osteocalcin (OCN) and osteopontin (OPN) in mPCs and hMSCs was performed as described previously in section (2.2.7).

### 3.2.7 Real time qPCR analysis

On Day 21 bECM, DBM, and collagen type I hydrogels were treated with the digestion solution described above in section (3.2.4), mPCs were collected and resuspended in TRIZOL reagent (Thermofisher). RNA was isolated using RNA extraction kit (Qiagen) according to the manufacturer's protocol. First standard cDNA was synthesized using First strand synthesis system (Invitrogen).

Taqman PCR primers (Applied Biosystems, Life Technologies) were used: ALP (Assay ID: Mm01187112_m1), RUNX2 (Assay ID: Mm00501584_m1), SPP1 (Assay ID: Mm00436767_m1), Bglap (Assay ID: Mm03413826_mH), β-actin (Assay ID: Mm01324804_m1). The real-time qPCR reactions were performed in 7500 fast real-time PCR system (Applied Biosystems). The method used: an initial denaturation step at 95°C for 10 min followed by 40 cycles of 15 s at 95°C and then 1 min at 60°C. The expression levels of the four genes were obtained from the threshold PCR cycle-values (Ct), and ΔΔCt method was used to calculate relative gene expression normalized to β-actin. Briefly, the threshold cycle (Ct) was obtained as the fractional cycle number at which the amount of amplified target reached a fix threshold. Data normalization was performed by subtracting Ct value of the β-actin from that of the target gene. The ΔΔCt was calculated as the difference of the normalized Ct value (ΔCt) of the target gene and control samples. ΔΔCt =ΔCt target gene -ΔCt control. The fold change in gene expression was calculated as $2^{-\Delta\Delta Ct}$.

### 3.2.8 Controlled release of proteins from bECM hydrogel

bECM hydrogels were prepared at 5 different concentrations (6, 8, 10, 12 and 14mg/ml bECM) in pipette tip. To study the release of protein from bECM hydrogel scaffold, 1ml of each hydrogel sample was prepared on ice and loaded with 1ug/ml fluorescent tag HSA before the gelation occur, then they were incubated at 37°C for 2h to form a hydrogel. The hydrogels were then placed in 12-well plate and covered with 2ml PBS incubated at 37°C on GyroTwister GX-1000 (Labnet) (Figure 10). Samples of the supernatant to measure HSA release were taken alternative days until day 11 and then on days 14, 18, 23, and 28, fluorescence measured at emission 518 nm, excitation 488 nm using Tecan Infinite M200 plate reader (Tecan UK, Reading, UK).

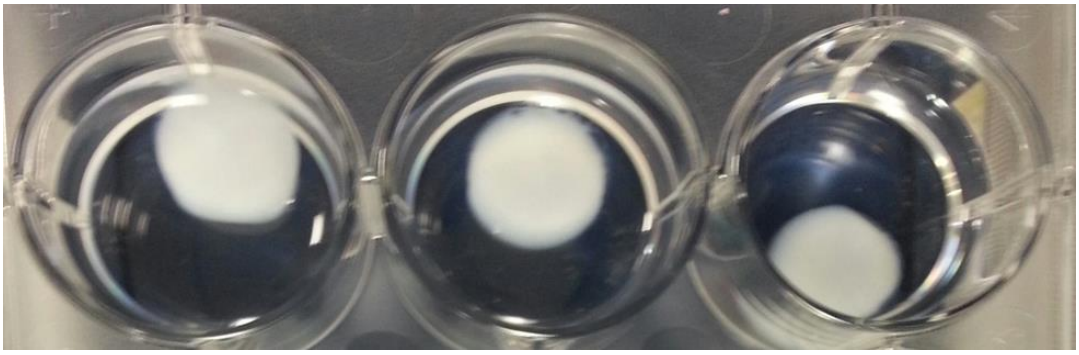


**Figure 10:** Controlled release of proteins form bECM hydrogels. bECM hydrogel at different concentrations loaded with 1µg/ml fluorescent tag HSA, placed in 12-well plate and covered with 2ml PBS.

## 3.3 Results

### 3.3.1 Protein content of demineralized and decellularized bone matrix

SDS-PAGE analysis showed that consistent protein patterns were seen in bECM and DBM. bECM contained a number of proteins that were also present in DBM. Proteins were separated according to their molecular weight and represented with bands on the gel, DBM exhibited darker bands which may be an indication of higher protein concentration (Figure 11A).

The total protein content, expressed as the final protein content divided by the weight of bECM and DBM in pre gel solutions, was 1.649% ± 0.030% for bECM and 1.925% ± 0.034% for DBM assessed by BCA (Figure 11B).

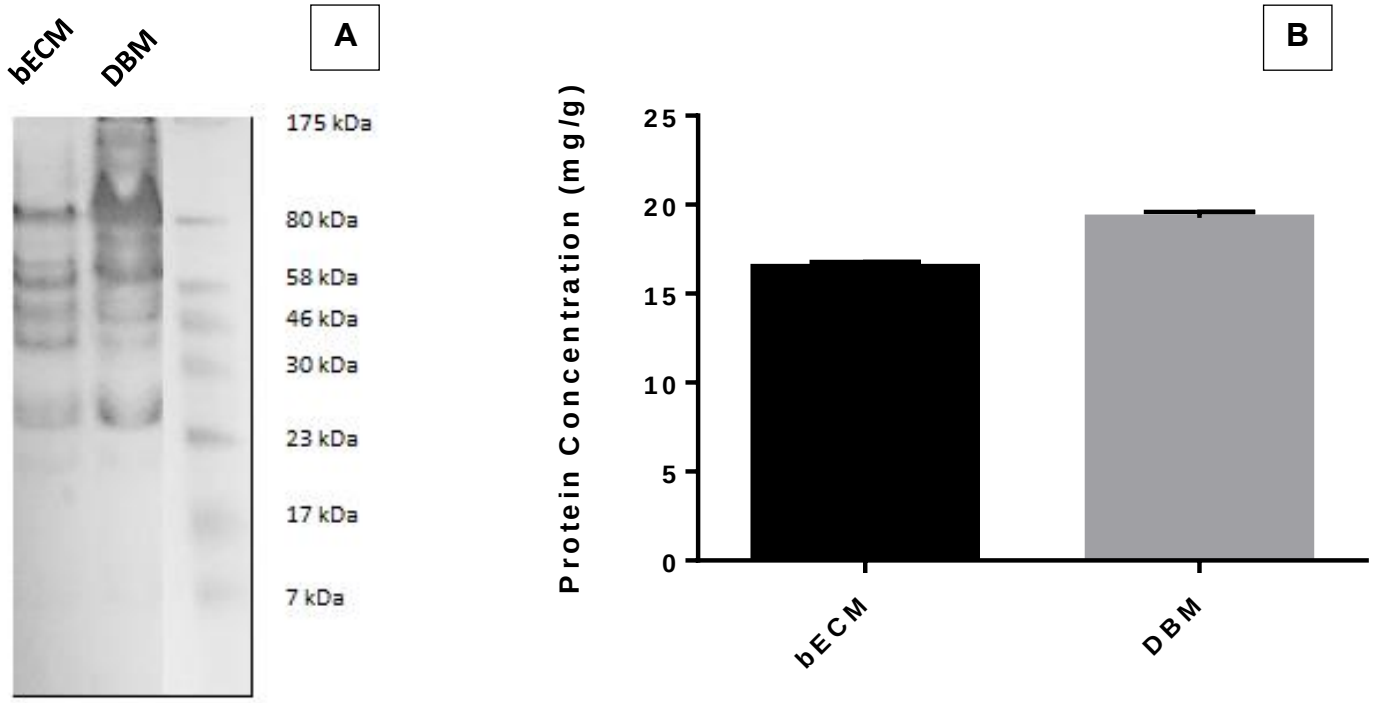



**Figure 11:** Quantification of bECM and DBM proteins was assessed by (A) SDS-PAGE and (B) the BCA assay; results are mean ± SD of triplicate measurements ($p < 0.01$).

### 3.3.2 C2C12 osteoblastic differentiation in different culture conditions

Since the components present in serum are not well characterized, two different media were used in this study; rich serum media (10% fetal calf serum) and low serum media (2% horse serum) to assess the osteogenic inducing capability of these hydrogels in different culture conditions. Moreover, it was reported previously that low serum media induces C2C12 myoblastic differentiation [159]. C2C12 cells cultured on bECM with both rich and low serum media were observed to have different morphologies (Figure 12A & B) and higher ALP levels compared to C2C12 cells cultured on collagen I (Figure 12C & D).

The osteogenic differentiation of C2C12 cells was assessed with ALP assay; the obtained values were converted to quantitative results through a standard curve created using standard alkaline phosphatase. C2C12 cells showed higher induction of ALP activity when grown on bECM hydrogels compared to cells grown on collagen in the presence of both media (Figure 13).

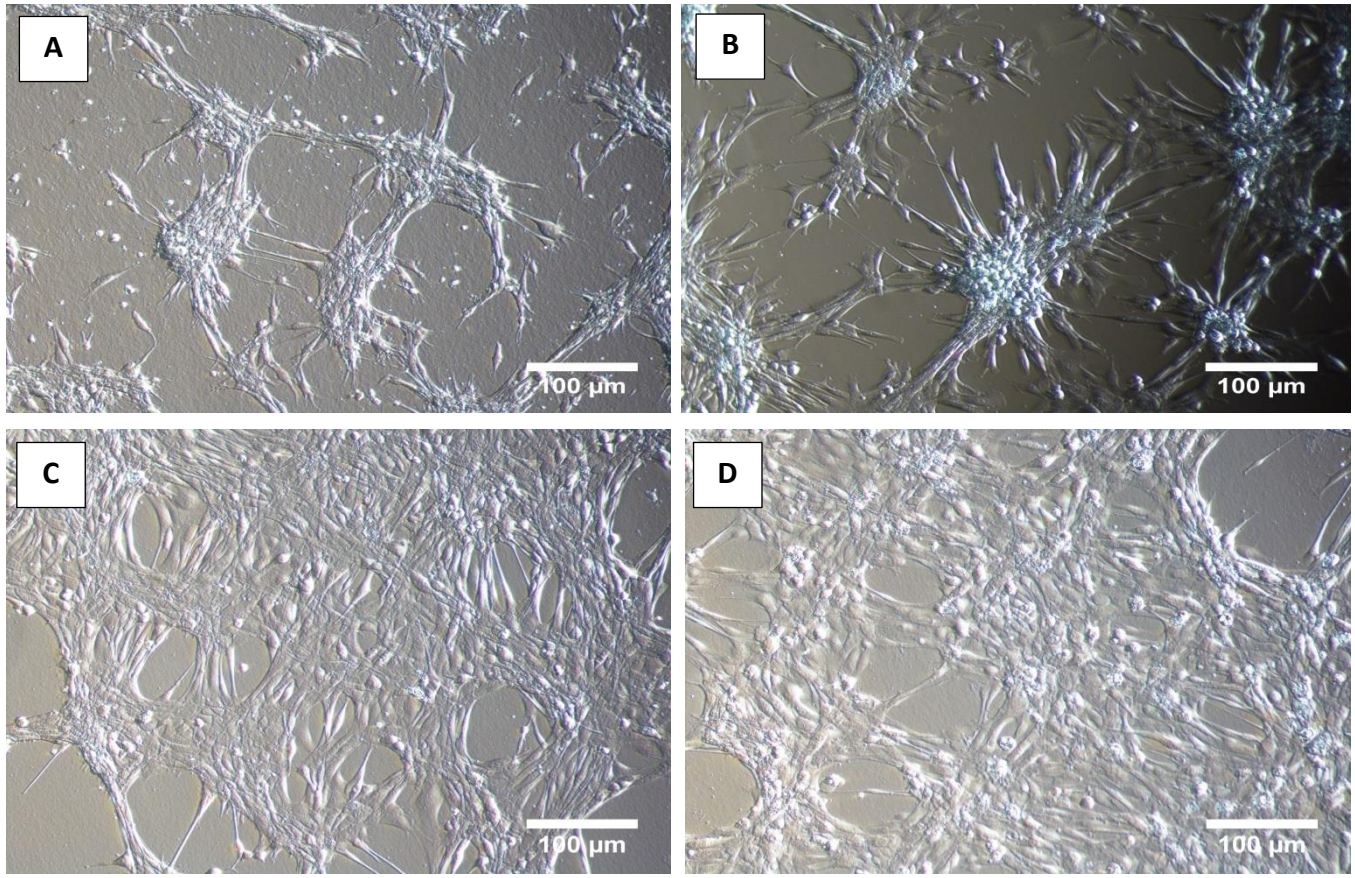



**Figure 12:** C2C12 differentiation on 8mg/ml bECM in rich-serum medium (A) low-serum medium (B) and on 8mg/ml collagen type I in rich-serum medium (C) low-serum medium (D).

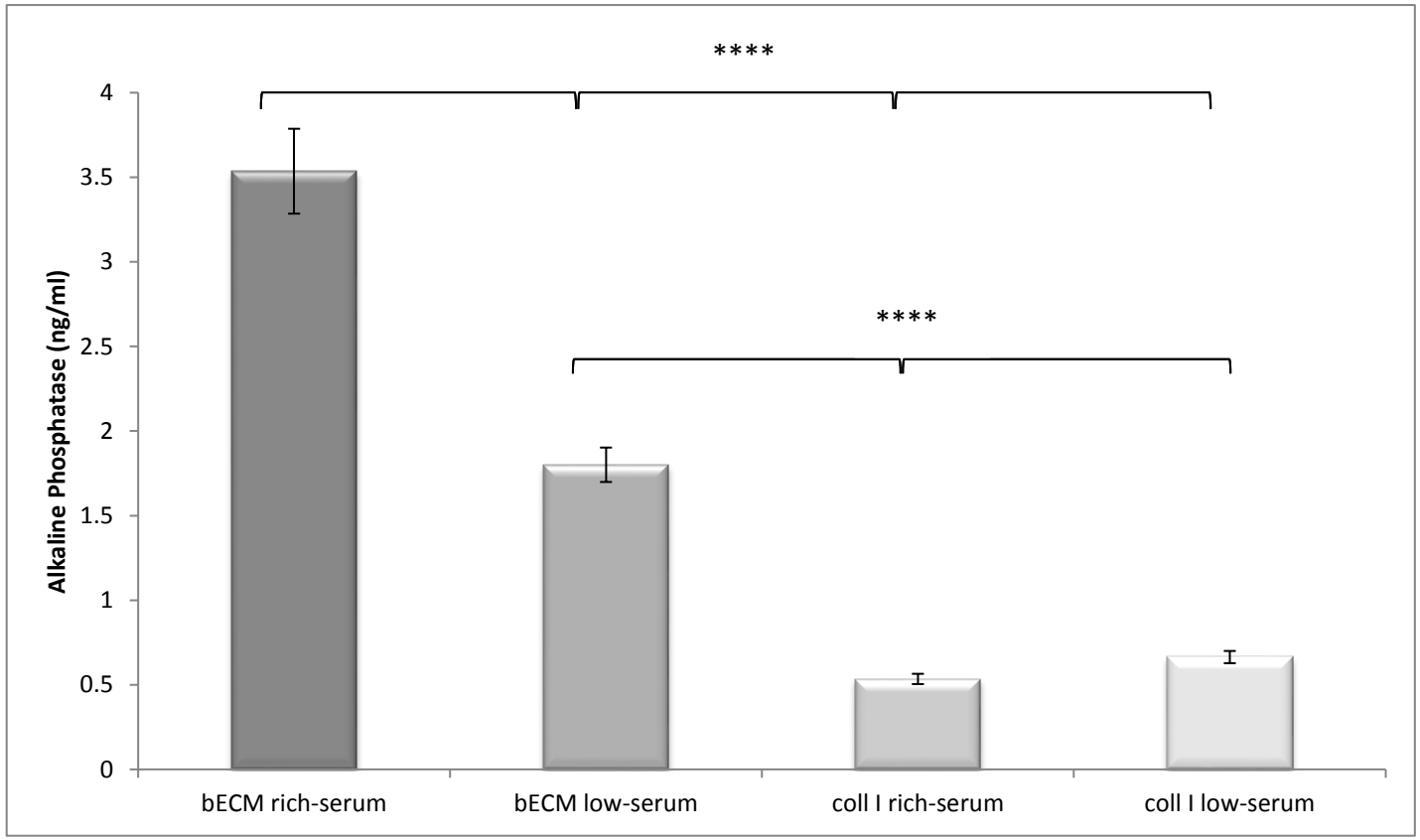



**Figure 13:** Alkaline phosphatase activity in C2C12 cultured on 8mg/ml bECM and collagen type I in both rich and low serum media, ALP activity was measured using *p*-nitrophenylphosphatase as a substrate, and normalized to active cell number. Statistical significance of expression **** indicates $p < 0.0001$

### 3.3.3 Expression of osteogenic proteins in mouse primary calvarial cells

The formation of pre-nodules was assessed after 21 days by immunocytochemistry staining for the osteogenic marker proteins osteocalcin and osteopontin. Staining of expressed ECM proteins OPN and OCN were observed in mPC cells cultured on bECM and DBM in osteogenic and basal medium (Figure 14); these proteins were only observed in osteogenic medium in cells cultured on coll I and TCP with negligible staining seen in mPCs cultured on coll I and TCP in basal medium (Figure 15).

Alizarin red and von Kossa staining were performed to assess the formation of calcified matrix or bone nodules, but all attempts were unsuccessful because the gels took up alizarin red and von Kossa stain (data not shown).

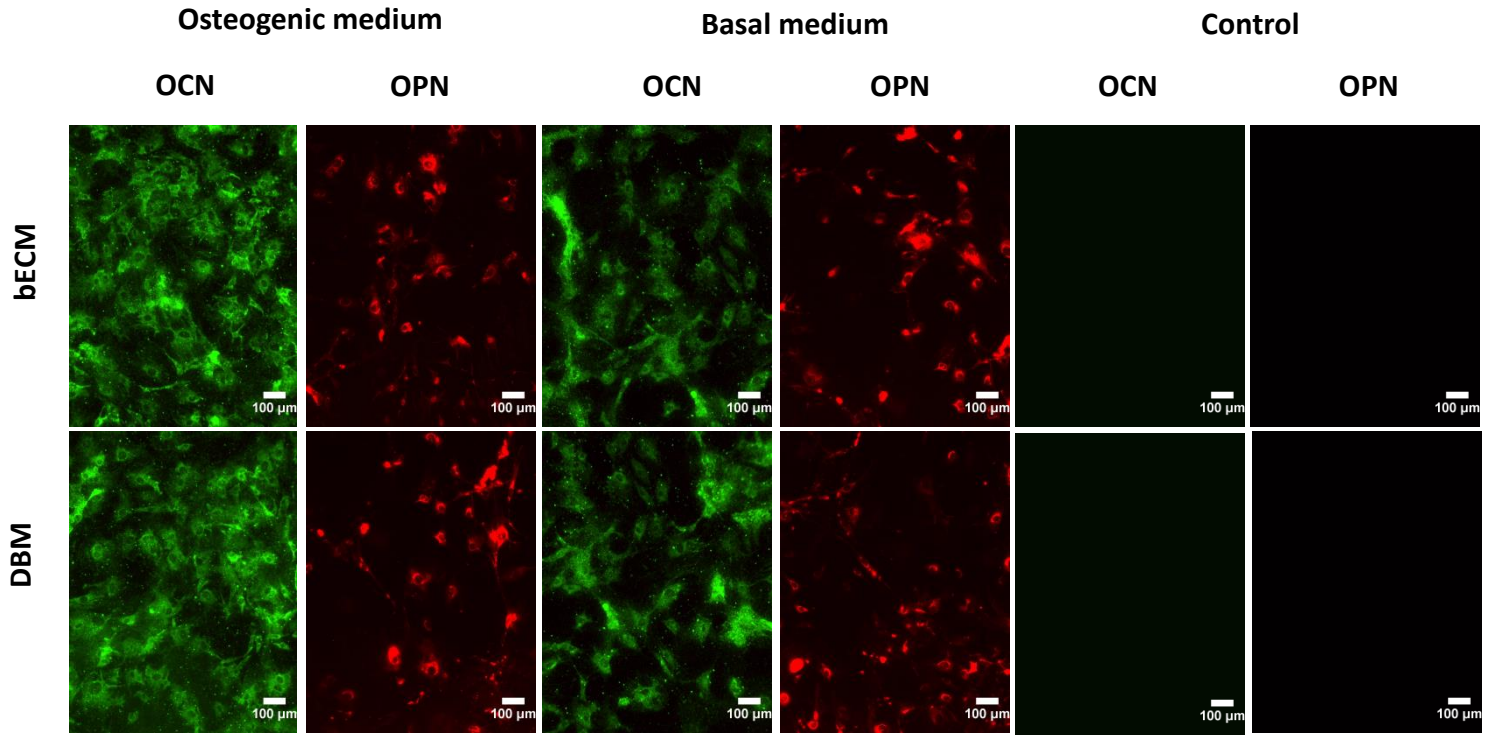



**Figure 14:** Expression of osteopontin and osteocalcin in mouse primary calvarial cells cultured on bECM and DBM hydrogels with osteogenic and basal medium. OPN and OCN expression was assessed by immunocytochemistry on day 21. Control samples were treated with secondary antibody only.

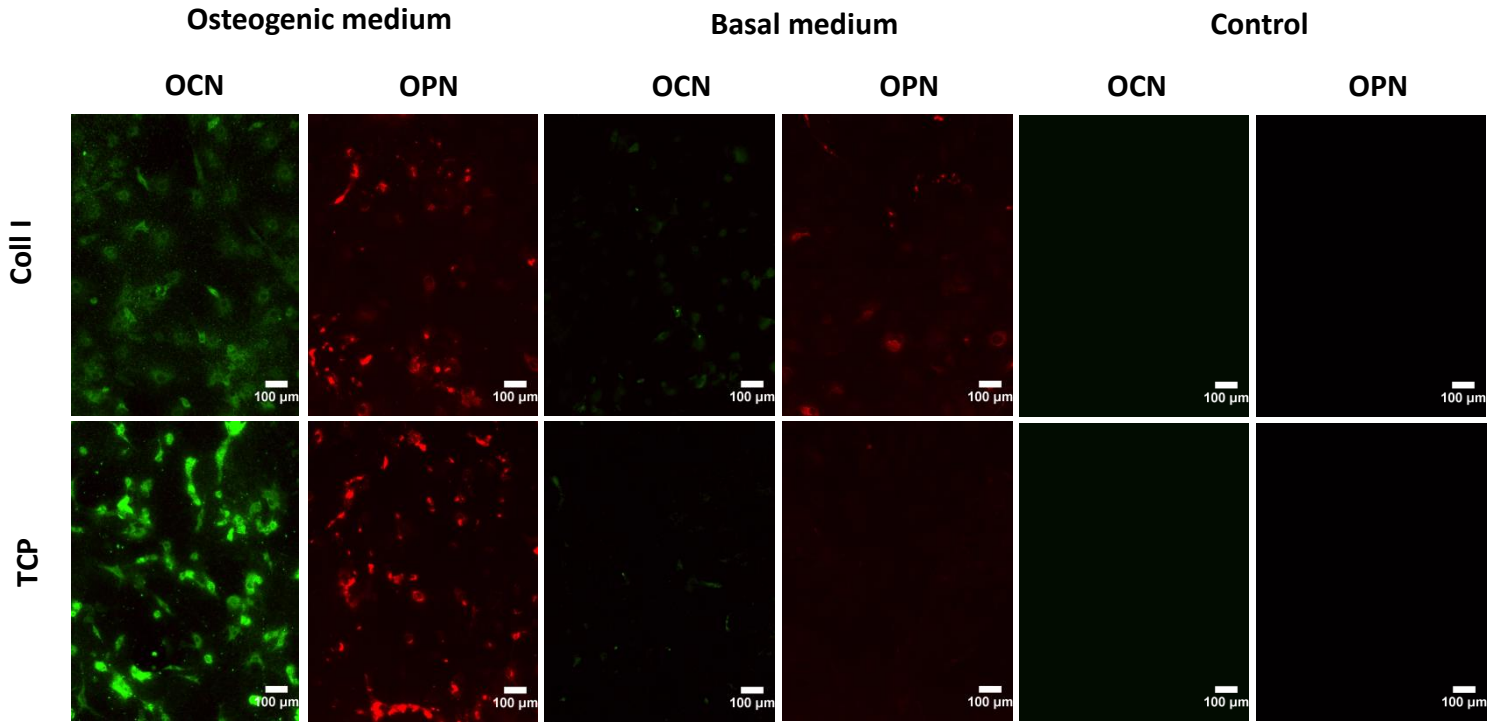



**Figure 15:** Expression of osteopontin and osteocalcin in mouse primary calvarial cells cultured on coll I hydrogel and TCP with osteogenic and basal medium. OPN and OCN expression was assessed by immunocytochemistry on day 21. Control samples were treated with secondary antibody only.

### 3.3.4 mRNA expression of osteogenic markers

Osteogenic differentiation of mPCs was further assessed by RT-qPCR analysis for expression of four genes: osteopontin (OPN), osteocalcin (OCN), runt related transcription factor 2 (RUNX-2) and alkaline phosphatase (ALP). mPCs were cultured at $4x10^4$ cells per well in 12-well plate for 21 days on 8mg/ml bECM, DBM, and coll I hydrogels in osteogenic and basal media, mPCs were cultured on TCP as well and used as a control.

Figure 16A shows the expression of ALP is upregulated in all cultures treated with osteogenic media, but this expression was highest in cells cultured on bECM with osteogenic media. With basal media ALP was only expressed in cells cultured on DBM and bECM. OPN (Figure 16B) showed similar expression, it was expressed in all cells cultured with osteogenic media, and in cells cultured on bECM and DBM with basal media. RUNX-2 and OCN (Figure 16C and D) were upregulated in all samples but the expression was maximised in bECM with osteogenic media.

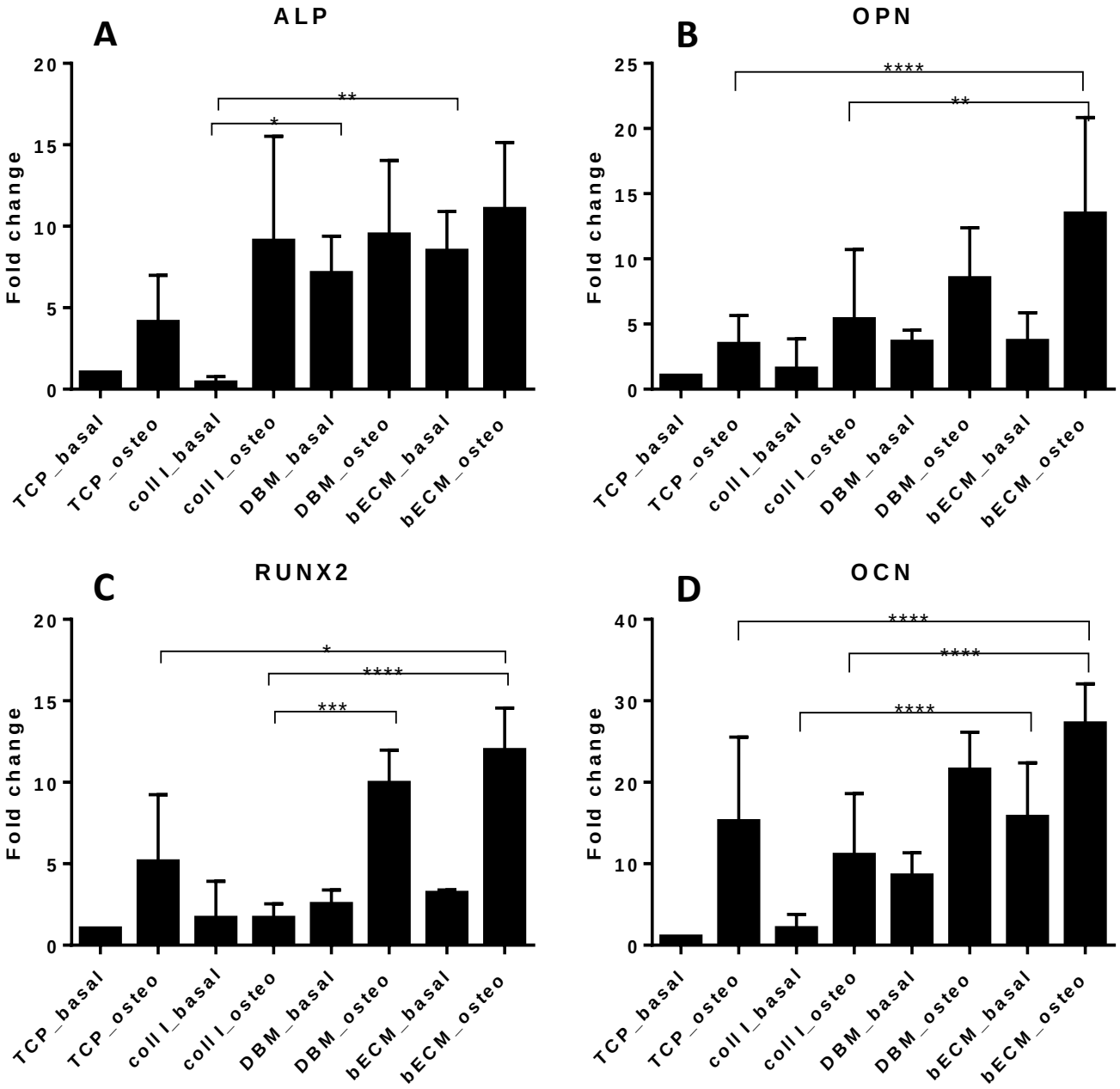



**Figure 16:** RT-qPCR of osteogenic markers ALP (A), OPN (B), RUNX2 (C), and OCN (D) expression in mouse primary calvarial cells (mPCs) seeded on bECM, DBM, coll I hydrogels and TCPS cultured in basal and osteogenic medium. Expression of each target gene normalized to β-actin. Data shown is mean ± SD of 3 independent experiments (n=3). Statistical significance of expression **** indicates $p<0.0001$; *** indicates $p<0.001$; and * indicates $p<0.05$.

### 3.3.5 HSA release from bECM hydrogels

HSA loaded bECM hydrogels were placed in phosphate buffer saline (PBS), and shaken at 37°C, samples of PBS were taken at different time points to measure HSA released. Figure 17 shows the release profile of HSA from bECM hydrogels.

Based on the results, we suggested that diffusion was the main driving force, the release kinetics were dependent on bECM concentration in each hydrogel. Approximately 75% of HSA was rapidly released in the first 2 hours from 6mg/ml bECM; the percentage of HSA released was decreased by increasing the bECM hydrogel concentration, to reach its minimal values 30% HSA released from 14mg/ml bECM (Figure 18).

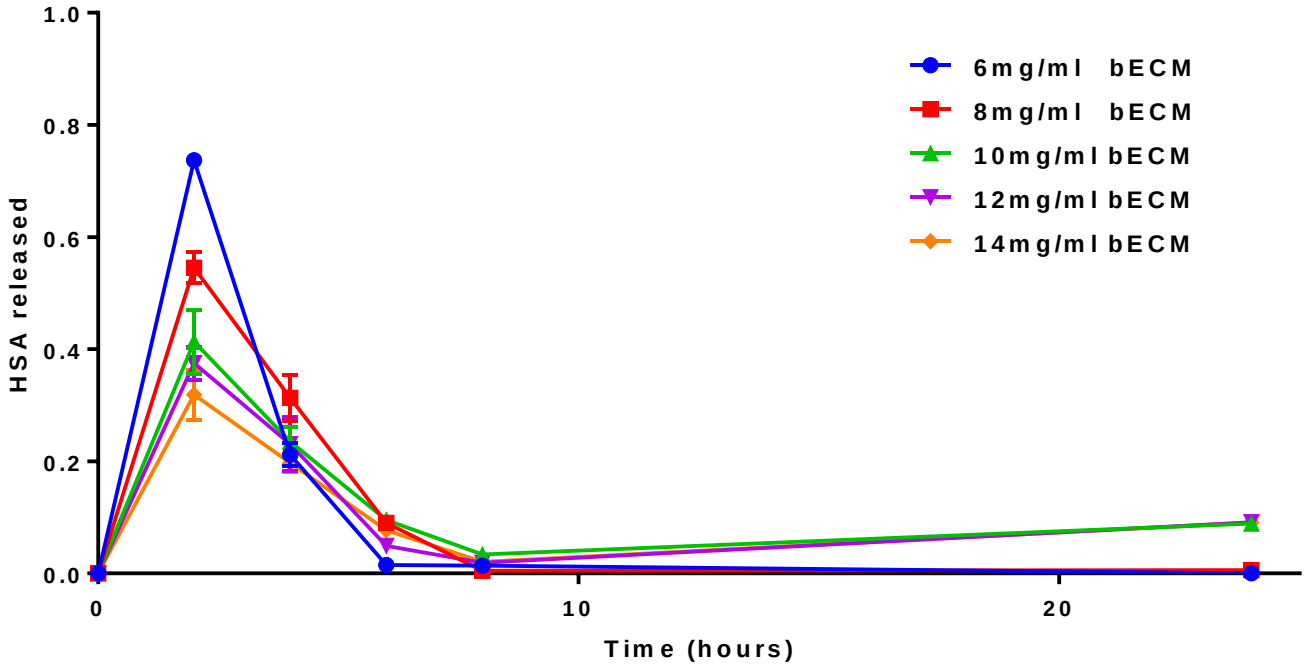



**Figure 17:** Release profiles of HSA from bECM hydrogels of different concentrations, release was assessed alternative days until day 11.

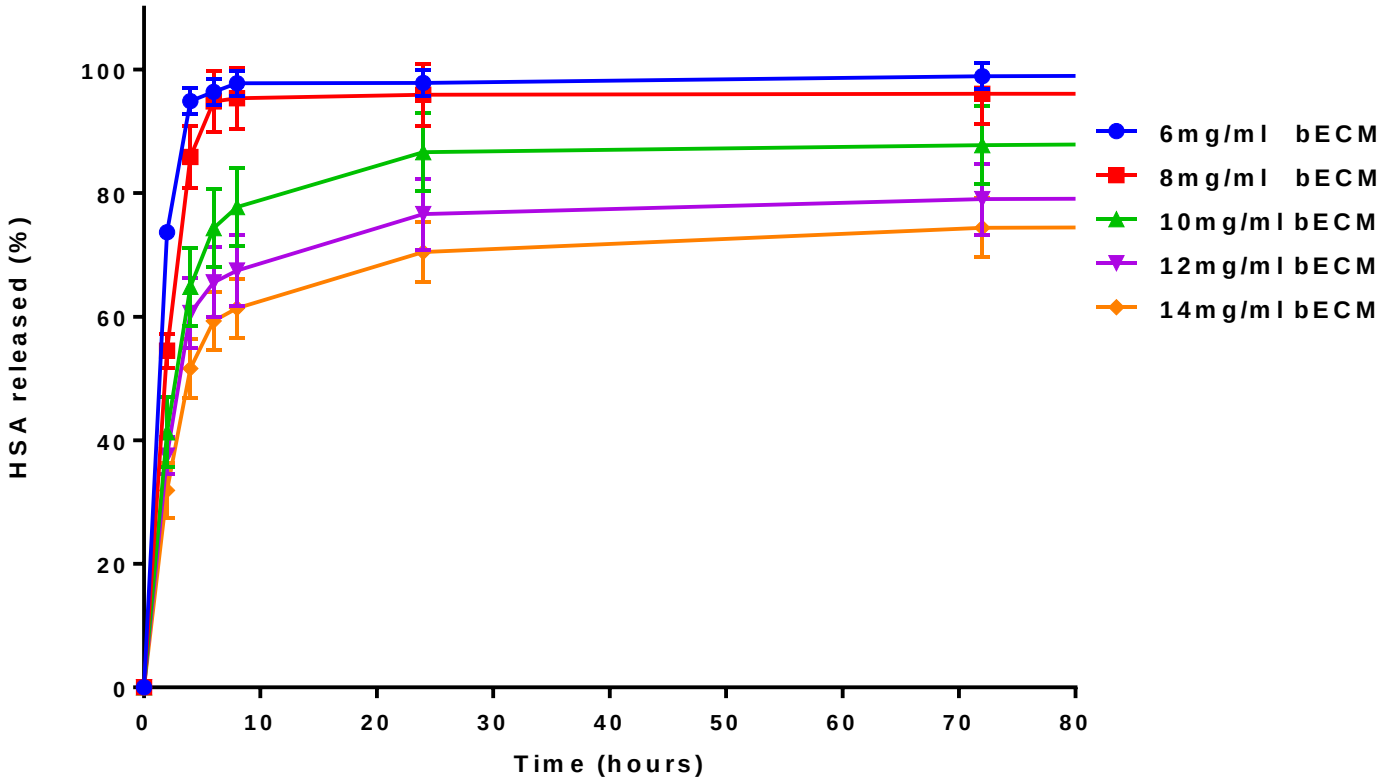



**Figure 18:** The cumulative mass release of HSA expressed as a percentage of the theoretical loading mass, release was assessed alternative days until day 11.

## 3.4 Discussion

ECM based materials hold great promise for bone regeneration because of the bioactive properties of the native material providing cells with adhesion sites and biological factors that aid in cell proliferation and differentiation [160, 161]. bECM, and DBM hydrogels were prepared from bovine bone, using an adapted acidic demineralization process [153], and an enzymatic decellularization protocol [154]. Demineralized and decellularized bone granules were solubilized and induced by neutralizing the pH and salt concentration as previously reported [162] (Figure 9)**.** BCA assay and SDS-PAGE results showed that the bECM hydrogel contains most of the proteins presents in the DBM, the similar protein profile between DBM and bECM indicated the preservation of biochemical composition of bone tissue after decellularization process (Figure 11).

Cell morphology, proliferation, differentiation and apoptosis are modulated by chemical and mechanical cues secreted from surrounding ECM, these biomacromolecules provide various bio-signals guiding cellular behaviour [163, 164]. Morphological differences can be noted between C2C12 cells cultured on bECM gels compared to cells cultured on collagen. This may be an indication that C2C12 cells were differentiated into osteoblast-like phenotype cells on bECM gels, while C2C12 cells grown on collagen differentiated into myoblastic cells in both media. C2C12 cells cultured on collagen in different culture conditions appeared to be in spatially resolved colonies, with well spread

morphology, and tight packing (Figure 12A and B). Whereas C2C12 cells on bECM in different culture conditions appeared to be more irregular in shape, more elongated and less highly spread, with long stress fibres running in many different directions (Figure 12C and D). The changes in morphology observed may be the effect of an osteogenic response to bECM hydrogels [165].

Previous studies have shown that the presence of specific factors can stimulate transdifferentiation of C2C12 myoblasts into osteoblasts [166-168]. The osteogenic capability of bECM hydrogels was measured *in vitro* with the myoblastic C2C12 cell line, by co-incubation of bECM and type I collagen with C2C12 cells with low and rich serum mediums. Differentiation was assessed by activity of alkaline phosphatase (ALP), ALP is an enzyme found in bone and it catalyses the hydrolysis of phosphate monoesters [155], the *p*-nitrophenyl phosphate (*p*NPP) assay can be used to detect ALP enzyme, *p*NPP acts as a phosphatase substrate.

The results indicate that C2C12 myoblasts cultured on bECM in the presence of both media had higher induction levels of ALP activity compared to C2C12 myoblasts grown on collagen type I, this can be an indication that bECM hydrogel induced transdifferentiation of C2C12 myoblasts into osteoblasts (Figure 13).

The osteogenic differentiation was further assessed by immunocytochemistry staining for osteogenic proteins osteocalcin (OCN) and osteopontin (OPN), these two proteins are expressed and localised within nodular structures [169].

In primary calvarial cells, OPN and OCN were expressed in DBM and bECM gels, the level of expression in samples induced with osteogenic media was higher than the samples treated with basal media (Figure 14). mPCs cultured on TCP and collagen I only expressed OPN and OCN when treated with osteogenic media (Figure 14).

This observation was enhanced by quantitative RT-PCR analysis for four osteogenic markers (ALP, RUNX-2, OCN and OPN), these four markers are expressed during osteogenesis, and they range from early markers: ALP and RUNX-2, intermediate: OPN, and late marker OCN [170-172].

The four genes were expressed on bECM and DBM, with and without the induction of the osteogenic medium. In addition, mPCs cultured on bECM hydrogels expressed higher level of the four genes compared to mPCs cultured on DBM. Moreover, the osteogenic differentiation was further enhanced in the presence of osteogenic supplements (Figure 16). ALP, RUNX2, OCN, and OPN were upregulated in mPCs cultured on TCP and collagen I hydrogel with osteogenic medium, and minimum expression of the four genes was seen in mPCs cultured on collagen I hydrogel with basal medium (Figure 16).

Previous studies have revealed that ECM act as a reservoir for growth factors [102, 173] and bECM hydrogel scaffolds retain endogenous growth factors that may give these scaffolds their osteoinductive properties [88]. It is hypothesised that adding exogenous growth factors like BMP2 will enhance the osteogenesis, and VEGF vasculagenseis of the cells seeded in bECM scaffolds. Moreover, number of growth factors has been used previously to induce and enhance osteogenic differentiation, such as transforming growth factor-β (TGF-β), insulin like growth factor-2 (IGF-2), and fibroblast growth factor (FGF) [172, 174-177]. In this study, we assessed the ability of bECM as a carrier for local delivery of proteins, HSA protein was studied as a model protein and the release kinetic was analysed to different hydrogels with bECM concentration range between 6 and 14mg/ml.

The results of this chapter reveal that the presence of bECM and DBM hydrogels can enhance the osteogenic differentiation of two cell types: mPCs and C2C12 without the induction of osteogenic supplements. Furthermore, bECM hydrogels demonstrated stable release of HSA; the release kinetics of proteins from hydrogels was dependent on the bECM hydrogel concentration. These findings support the potential to use bECM and DBM as scaffolds for bone tissue engineering.

# Chapter 4. Hydrogel Scaffolds Derived from Decellularized Tendon and Bone Extracellular Matrices Selectively Enhance MSC Tenogenic and Osteogenic Differentiation for Tendon-to-Bone Interface Tissue Engineering

## 4.1 Introduction

Rotator cuff tears (RCT) are among the most common shoulder injuries. Despite various surgical techniques for rotator cuff (RC) repairs, incomplete healing after the rotator cuff repair has been reported with rate of structural failure ranged from 20% to 90% [178-183]. A number of factors play a role in the RC repairs such as patient age, tear size, tendon quality, muscle atrophy, degradation and chronicity [183-185].

Tissue engineering techniques provide a promising future for the rotator cuff repair; previously successful results have been reported in treating tendon injuries with the use of combination of cells, biomaterials and bioactive factors [66, 186-188]. However, most of these studies described the regeneration of the tendon tissue but not the tendon insertion site that links between two tissues differ in their physical, chemical and biological properties [189].

As mentioned previously, tendon/ligament-to-bone interface exhibits gradient in tissue with specific cellular composition, structural, and biomechanical properties for each tissue type, this gradations in structure facilitates joint movement. Injuries are very common in the anterior cruciate ligament (ACL), the Achilles' tendon and the rotator cuff group, and they require surgical repair and regeneration of soft tendon/ligament-to hard bone tissue in order to restore the original strength of the junction [17, 26, 189, 190]. Current methods for ACL repair include autograft, allograft, xenograft, or synthetic graft. However, allografts and xenografts have led to immunogenic responses [191, 192]. Moreover, ACL reconstruction failure rate increased from 6 to 20% following the utilization of allografts compared to autografts [193]. The most common procedure in ACL reconstruction is autografting technique [194, 195]. However, reconstruction using autografts has been shown to be limited by donor-site morbidity [196].

An alternative approach is the use of manufactured scaffolds [197, 198]. However, few scaffolds have shown success in clinical studies [199]. Although there are a number of approved devices (e.g. Intergraft (carbon fiber), Gore-Tex ACL (polytetrafluoroethylene), and Kennedy Ligament Augmentation Device (polypropylene)) the devices have shown poor results with high rupture rate associated with the use of Intergraft [200], and joint instability and high rate of inflammation with the use of Gore-Tex and Kennedy[201].

Previous preclinical studies have suggested that tissue-engineered scaffolds hold promises over traditional autograft reconstruction due to the elimination of donor-site morbidity risk, the ability to manufacture these scaffolds to mimic the structural and mechanical properties of the native enthesis, and the possible incorporation of biological or chemical in tissue-engineered scaffold to enhance cellular proliferation and differentiation [197, 202, 203].

Recently, adult mesenchymal stem cells (MSCs) have been used widely for tissue regeneration; MSCs can be directed to differentiate into a specific lineage *in vitro* through growth factors stimulation [175, 176, 204-206].

To date, a number of biomaterials has been used as scaffolds to direct the differentiation of stem cells to desired lineage to regenerate hard and soft tissues [205, 207-209]. Among these scaffolds biological scaffold materials composed of extracellular matrix (ECM) are considered as a promising method to regulate the differentiation of stem cells [88, 210-212].

Currently, ECM bioscaffolds are processed and marketed for rotator cuff repair[213]. Such scaffolds have the advantages of providing the chemical and structure environment for host cells, due to the retention of the biological factors, and the 3D structure, which believed to enhance the biology of repair healing [213, 214]. However, number of limitations were associated with these scaffolds as described previously.

The hypothesis of this chapter was that decellularized ECM scaffolds derived from decellularized bone and tendon extracellular matrix seeded with MSCs could aid the reconstruction of tendon-bone insertion. To test this hypothesis we produced a hydrogel from decellularized equine tendon extracellular matrix (tECM), and determined its structure and mechanical properties. We tested the ability of these hydrogels to induce tenogenic differentiation in MSCs, and compared that with decellularized bone extracellular matrix (bECM); we also analysed the potential of bECM to induce osteogenic differentiation in MSCs. The long-term aim of this work is to design a gradient scaffold with these two hydrogels for tendon-bone insertion engineering.

## 4.2 Materials and methods

### 4.2.1 Preparation of tendon extracellular matrix hydrogel

Tendon samples were decellularized using a previously reported method [215]. Briefly, Equine flexor digitorum superficialis tendons were aseptically harvested from the forelimbs of horses (Figure 19A) and the samples were sectioned into 4 mm thick pieces.

Tendon samples were sorted into untreated group to serve as control and treated group. Four freeze/thaw cycles were applied to tendon samples, then they were covered with the detergent solution made of 2% Sodium dodecyl sulfate (SDS, Sigma) in 1M Tris-HCl (Sigma) pH 7.8 under agitation at 4°C for

48h. Tendon samples were then rinsed in PBS six times to remove residual detergent before incubation in a solution of 0.05% trypsin, 0.05% EDTA (Sigma–Aldrich, Poole, UK) for 10 minutes then washed with water.

These were then incubated at 4°C for 24 hours with 1 µl/ml of a mammalian tissue protease inhibitor cocktail (Sigma, USA), to inhibit any residual trypsin then incubated in 0.2 mg/ml DNase-I (AppliChem, Germany) for 30 min. The samples were washed with 95% ethanol (Sigma-Aldrich) for 2h at 4°C, then with PBS with 1% w/v penicillin/streptomycin under agitation for 24 h at 4 °C. The resulting tECM then was snap frozen, lyophilized for 24h and stored at -20°C until required (Figure 19B). Gels were produced following the method of enzymic digestion, solubilization and neutralisation given in 2.1.1 (Figure 19C).

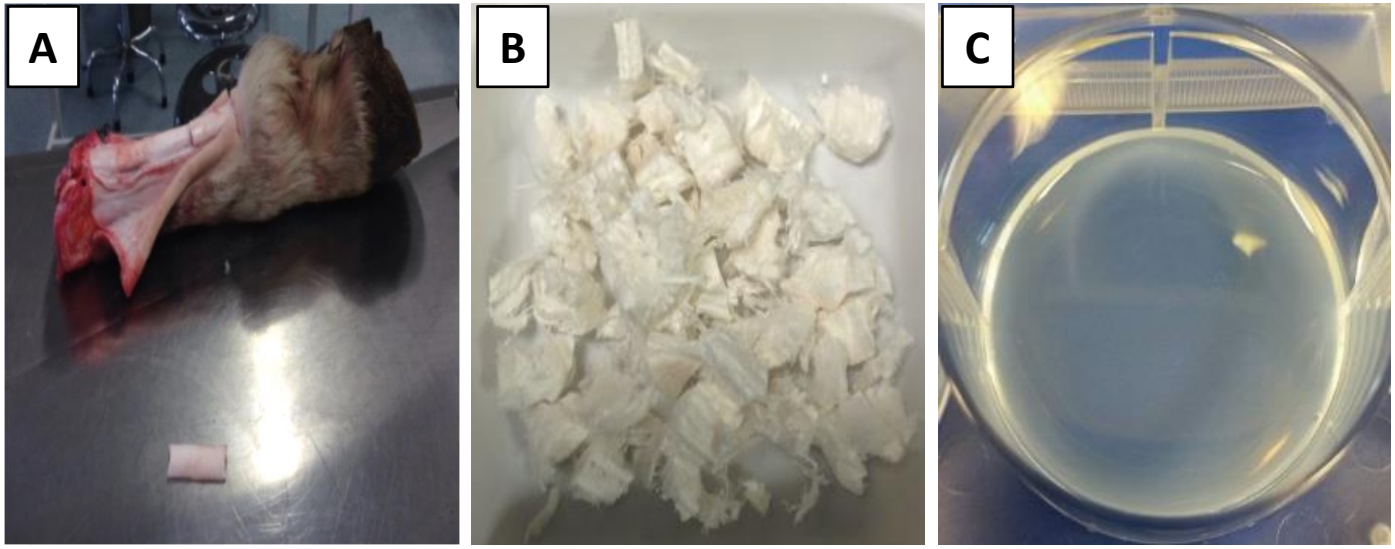



**Figure 19:** Production of ECM hydrogel from tendon. (A) Equine flexor digitorum superficialis tendons were subjected to cell removal procedures to produce (B) decellularized tendon (tECM) prior to pepsin digestion and solubilization to form an ECM hydrogel (C).

### 4.2.2 Assessment of Cellular content

Representative samples of the treated group and untreated group were fixed with 10% neutral buffered formalin and embedded in 30% sucrose over night at 4°C, then transferred into custom-made mould filled with optimum cutting temperature compound (OCT), samples were then frozen in a bath of Isopentane (Sigma), which has been cooled in liquid $N_2$. Sections were cut with cryostat at 8-10 um thickness transferred to a glass slide then stained with haematoxylin and eosin (H&E), followed by 3 washes in PBS, nuclei were stained blue, whereas the cytoplasm and extracellular matrix had varying degrees of pink staining. Diamidino-2-phenylindole, dilactate (DAPI, Invitrogen) was added in mounting solution for nuclear staining. The samples were viewed using an inverted fluorescence microscope.

### 4.2.3 Assessment of collagen content

Solubilized collagen in pepsin digests of the tECM was determined using Sircol collagen assay kit (Biocolor Ltd., UK), following the manufacturer's instructions. Blank pepsin solution was prepared and served as negative control.

### 4.2.4 Scanning electron microscopy (SEM)

The surface morphology of tECM and collagen type I were analysed by scanning electron microscopy (SEM). 300µl of gels were fixed with 5% glutaraldehyde for 1h at room temperature, followed by 3.7% paraformaldehyde at 4°C overnight. Fixed hydrogels were washed with Milli Q water and dehydrated using ethanol baths (20-100%). Samples were gold-coated with blazers SCD030 gold sputter coater after performing critical point drying (CPD). The surface morphology of the hydrogels was examined by scanning electron microscopy (SEM), using a JEOL 6060LV imaging system.

### 4.2.5 Turbidimetric gelation kinetics

tECM and collagen type I gels were formed by neutralizing the salt concentration and pH of the pre-gel solution as described previously [81, 124, 128]. Pre-gel solutions were prepared at 4 and 8mg/ml on ice, 100ml was transferred to cold 96-well plates, the plates were then placed in 37°C Tecan Infinite M200 plate reader (Tecan UK, Reading, UK).

Turbidimetric gelation kinetics was evaluated spectrophotometrically at 405 nm every 3 min for 1 h and 30 min. Six measurements (n=6) were performed for each hydrogel and concentration, the readings were then scaled from 0 (at time 0) to 1 (at maximum absorbance); $(NA=( A-A_0)/ (A_{max}-A_0))$ where *NA* is the normalized absorbance, *A* is the absorbance at a given time, $A_0$ is the initial absorbance, and $A_{max}$ is the maximum absorbance [128].

The time to half gelation ($t_{1/2}$) defined as the time to 50% absorbance, gelation rate ($S$) was defined as the slope of linear region of the gelation curve, and the lag time ($t_{lag}$) was defined as the intercept of the linear region of the gelation curve with 0% absorbance [128].

### 4.2.6 *In vitro* hMSCs culture and viability

hMSCs were cultured on the surface of 4 and 8mg/ml tECM and collagen type I hydrogels with mesenchymal stem cell growth medium (MSCGM) (PT-3001, Lonza). The proliferation of hMSCs was assessed with PrestoBlue (ThermoFisher) over several days as described in section (2.2.6). Cells used in this work were between passage three and five.

### 4.2.7 hMSCs multipotent differentiation and cellular morphology on bECM and tECM

hMSCs were tested for the potential to differentiate towards the osteogenic, adipogenic and chondrogenic lineages, all procedures were performed following Lonza's Poietics human mesenchymal stem cells instructions.

hMSCs were cultured on the surface of 8mg/ml bECM, and tECM hydrogels. Briefly, the pre-gels were kept on ice at 4°C and transferred to 12-well plates; 0.5ml of 8mg/ml gel was added to each well. Once the hydrogels were formed $4x10^3$ hMSCs were added to the surface of the gels and cultured for 7 days in basal medium (MSCGM), cells were maintained at 37°C and 5% $CO_2$. The

morphology and distribution of hMSCs cultured on bECM and tECM hydrogels were observed and imaged on an inverted microscope.

### 4.2.8 Quantitative PCR analysis

The expression levels of tenogenic and osteogenic gene markers in hMSCs cultured on tissue culture plate (TCP) and surface of 8mg/ml tECM, bECM and collagen type I were assessed by qPCR analysis on day 7, 15 and 21 as described in section (3.2.7). For osteogenic differentiation basal and osteogenic medium were obtained from Lonza (PT-3001 and PT-3002, Lonza), for tenogenic differentiation basal medium was prepared as: Alpha MEM (αMEM, Lonza), supplemented with 10% fetal bovine serum (FBS), 1% penicillin/streptomycin, 0.1mM L-ascorbic acid (Sigma-Aldrich) and 1mM L-Glutamine. Tenogenic medium: basal medium supplemented with 50ng/ml BMP12 (Fisher scientific), 100ng/ml IGFI (R&D systems), and 2ng/ml FGF2 (R&D systems).

Taqman PCR primers (Applied Biosystems, Life Technologies) were used; primers for tenogenesis marker genes including scleraxis (SCX) (Assay ID: Hs03054634_g1), tenascin-C (TNC) (Assay ID: Hs01115665_m1), and tenomodulin (TNMD) (Assay ID: Hs00223332_m1). Osteogenesis marker genes including runt-related transcription factor2 (RUNX2) (Assay ID: Hs00231692_m1), alkaline phosphatase (ALP) (Assay ID: Hs01029144_m1), osteopontin (SSP1) (Assay ID: Hs00959010_m1) and osteocalcin (Bglap) (Assay ID: Hs01587813_g1). The ΔΔCt method was used to calculate relative gene expression normalized to β-actin (Assay ID: Hs01060665_g1).

## 4.3 Results

### 4.3.1 Cellular and collagen content of decellularized tendon extracellular matrix

Successful decellularization process should result in having extracellular matrix (ECM) free from its inhabiting cells [104, 169]. This can be assessed by DAPI and (H&E) staining for cell nuclei.

Images shows that the decellularization has removed all cell nuclei (Figure 20B & D), while cell nuclei appears in the untreated tendon sections (Figure 20A & C).

The soluble collagen content was quantified; every mg of the decellularized tECM had 0.62 ± 0.09 mgs of collagen.

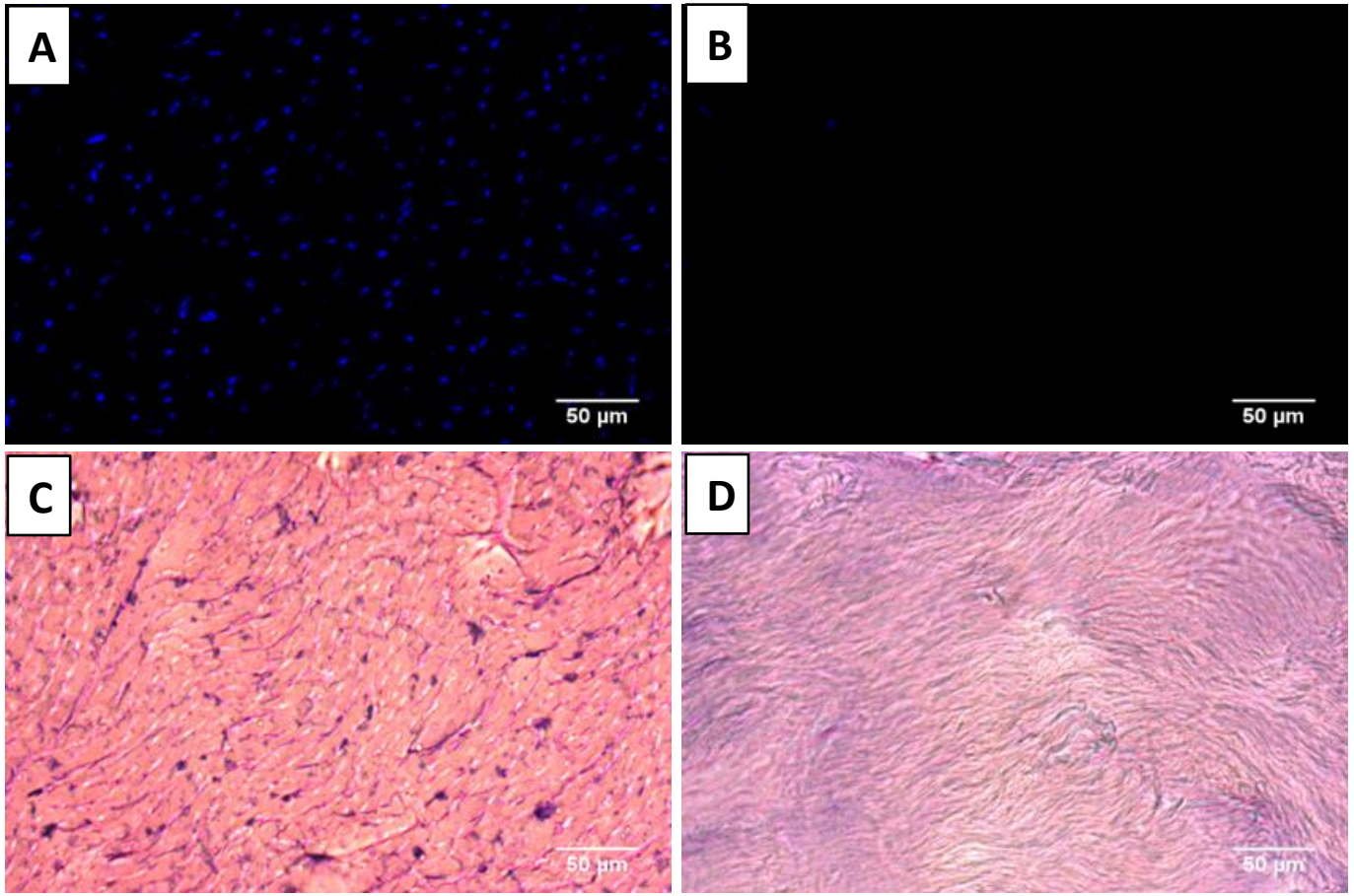



**Figure 20:** Decellularization of tendon ECM sections was assessed by imaging and analysis of DAPI staining (A and B) and (H&E) staining (C and D). (A and C) images represent a control untreated sample, (B and D) represent the decellularized samples.

### 4.3.2 Hydrogel morphology

Scanning electron microscopy (SEM) evaluation of the surface of tECM and collagen type I hydrogels showed that tECM hydrogel possessed a randomly oriented fibrillar structure similar to collagen type I [216] at 4 mg/ml (Figure 21A & C) and 8mg/ml (Figure 21B & D). Both hydrogels formed fiber network with interconnecting pores, tECM fiber organization (Figure 21C & D) appeared to be similar to collagen fiber organization (Figure 21A & B).

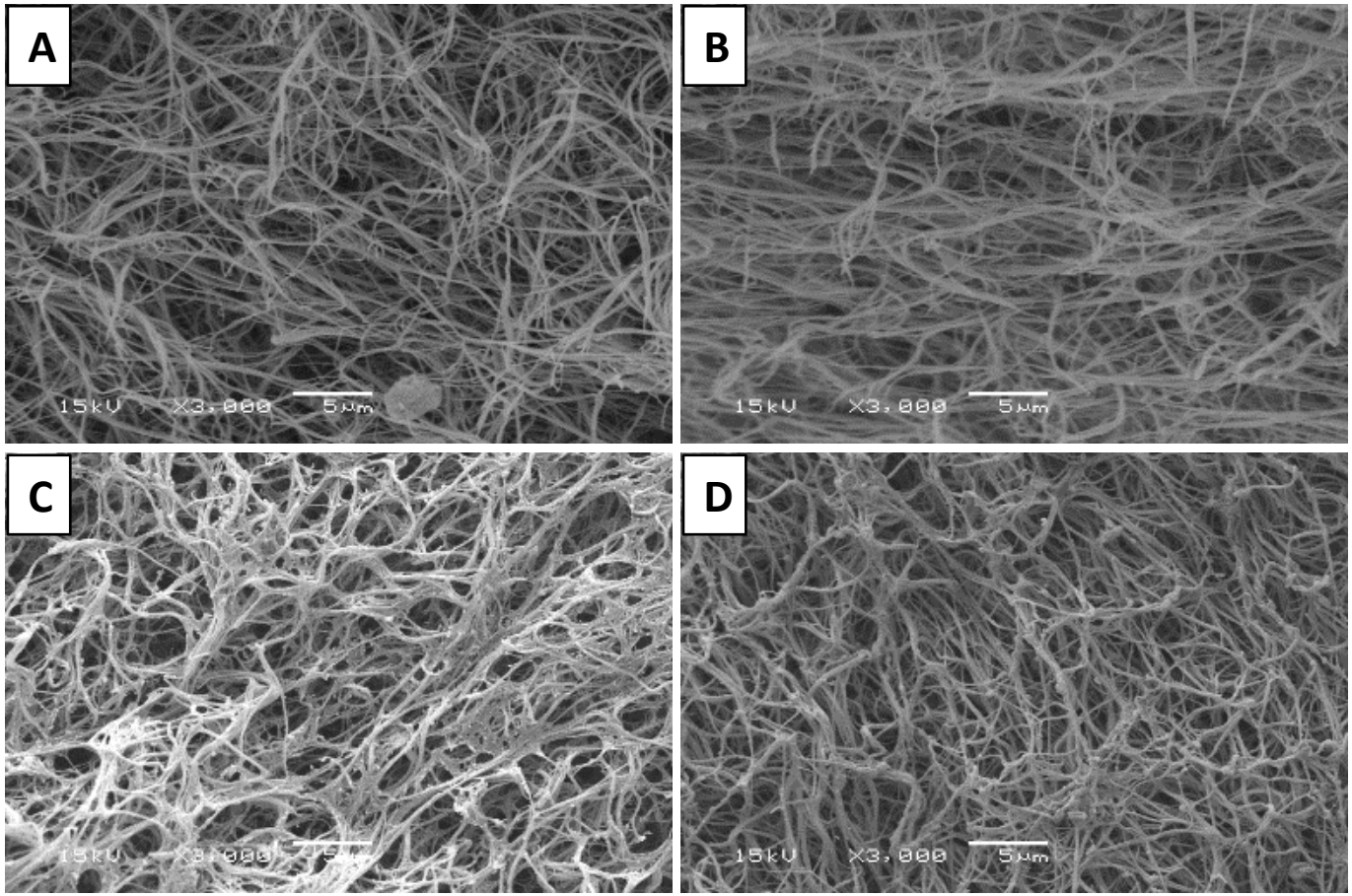



**Figure 21:** Scanning electron micrographs of (A) Coll I hydrogel 4mg/ml, (B) Coll I hydrogel 8mg/ml, (C) tECM hydrogel 4mg/ml, (D) tECM hydrogel 8mg/ml. All images 3000x magnification.

### 4.3.3 Turbidimetric gelation kinetics

The turbidimetric gelation kinetics of tECM and collagen type I were characterized spectrophotometrically at 4 (Figure 22A) and 8mg/ml (Figure 22B). Gelation parameters: lag time, gelation rate, and time to 50% gelation were calculated (Table 1). The turbidimetric gelation kinetics for tECM and collagen type I gels at both concentrations showed a sigmoidal shape (Figure 22A & B). The lag phase ($t_{lag}$) and time to 50% gelation was shorter in collagen type I than tECM hydrogels at 4 and 8mg/ml (Table 1), with higher gelation rate (*S*) in collagen type I when compared to tECM hydrogel at both concentrations (Table 1). Gelation kinetics showed to be independent of concentration.

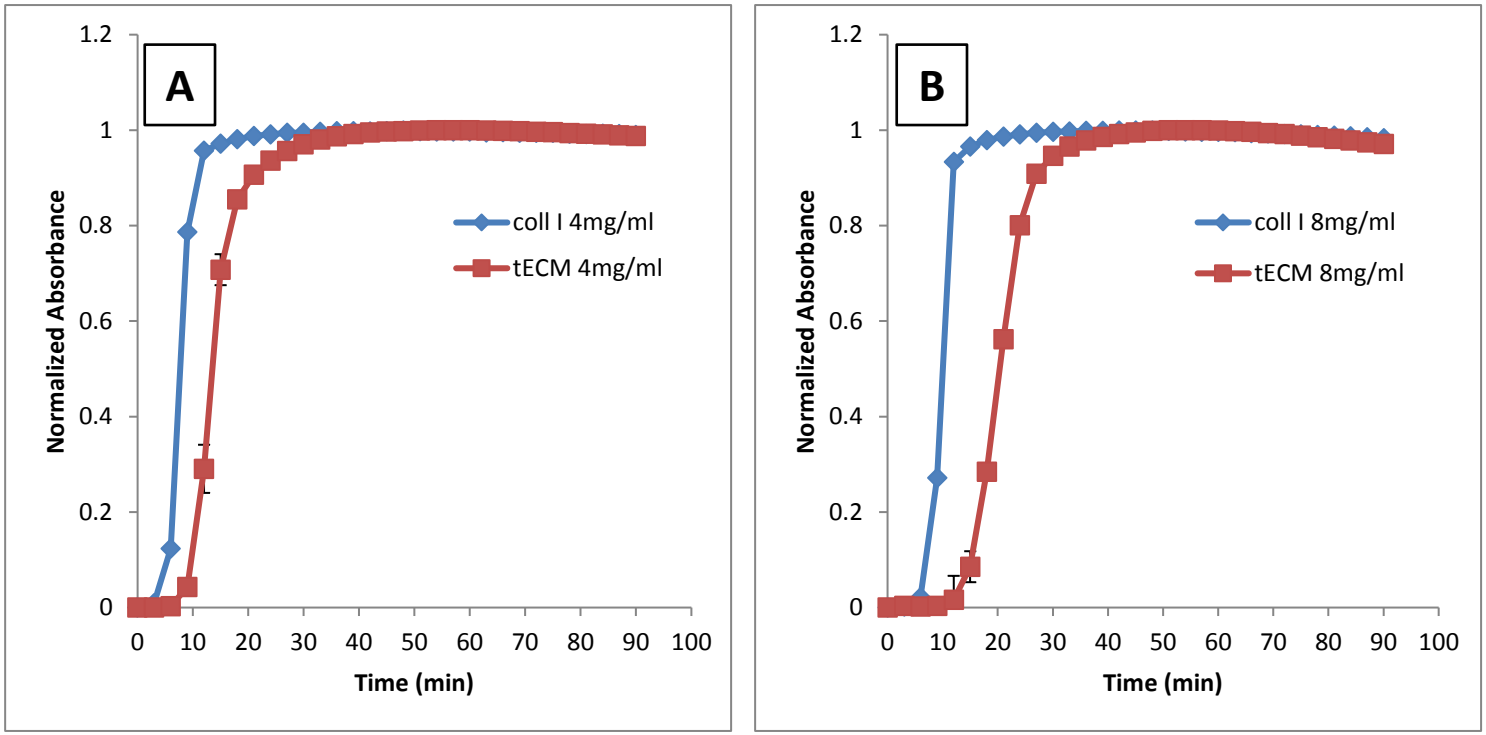



**Figure 22:** Turbidimetric gelation kinetics of tECM and Coll I hydrogels at 4mg/ml (A) and 8mg/ml (B) concentrations. Data represent means ± SD for n = 6.

**Table 1:** Results from the turbidimetric analysis of the tECM and collagen type I gelation kinetics.

| Material | S | $t_{1/2}$ | $t_{lag}$ |
|---|---|---|---|
| Coll I 4mg/ml | 0.1169 | 6.02 | 4.54 |
| Coll I 8mg/ml | 0.1165 | 7.17 | 5.98 |
| tECM 4mg/ml | 0.0442 | 13.15 | 10.24 |
| tECM 8mg/ml | 0.0417 | 15.92 | 9.90 |

### 4.3.4 *In vitro* hMSCs culture and viability

hMSCs cultured on tECM and collagen type I hydrogels at 4 and 8mg/ml were viable after day 3 and day 7 (Figure 23A & B). Increased proliferation was observed between day 3 and day 7, with no significance differences in viability based on hydrogel concentration or type (Figure 23A & B).

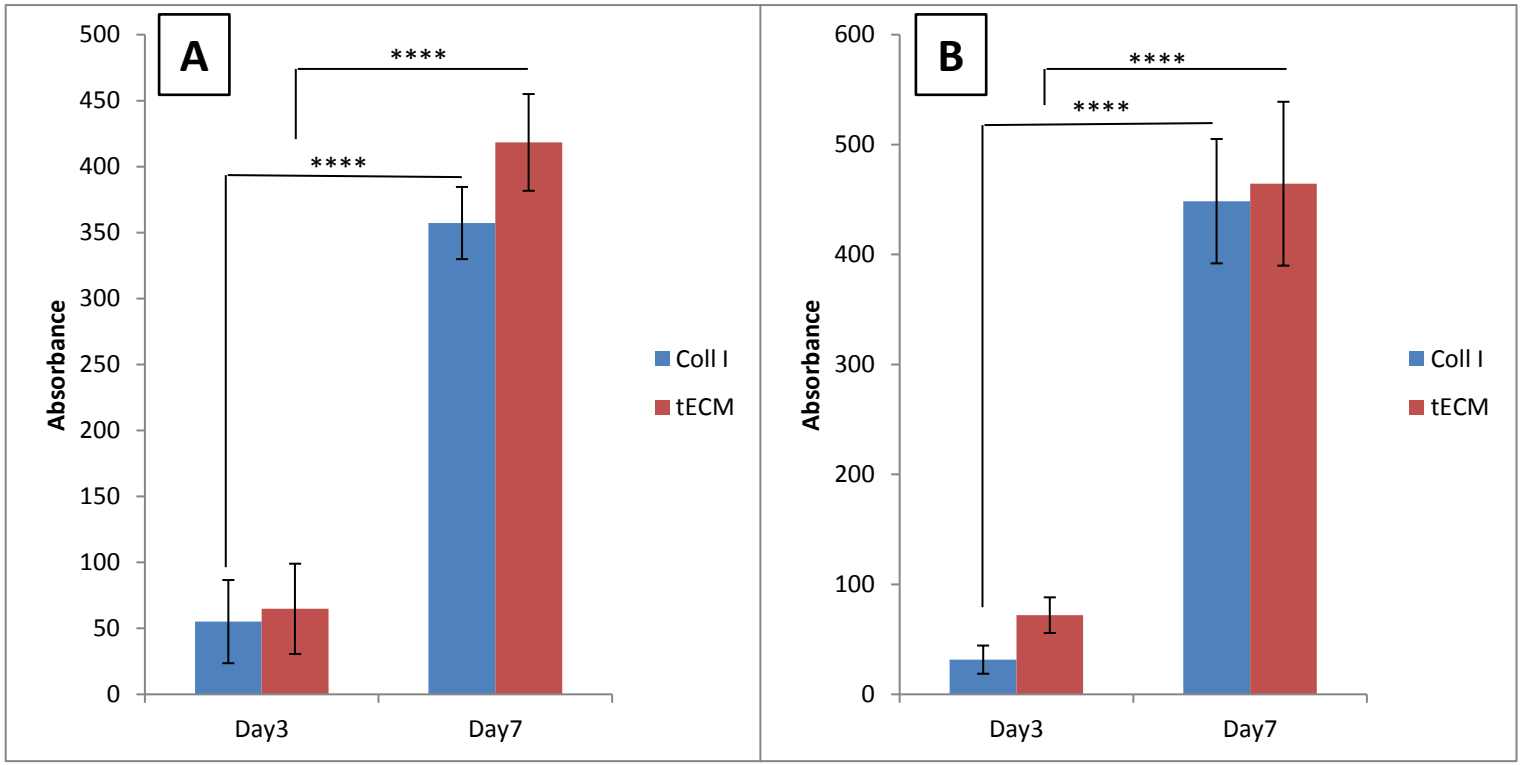



**Figure 23:** Proliferation of hMSCs on (A) Coll I and tECM 4mg/ml hydrogels, (B) Coll I and tECM 8mg/ml hydrogels after 3 and 7 days.

### 4.3.5 hMSCs multipotent differentiation and cellular morphology on bECM and tECM

Multi-lineage differentiation assays demonstrated that hMSCs were able to differentiate into chondrocytes, adipocytes and osteoblasts. Chondrogenic differentiation was assessed by Alcian Blue staining (Figure 24A), adipogenic differentiation was assessed by Oil Red O staining (Figure 24B), and osteogenic differentiation was assessed by Alizarin Red staining (Figure 24C).

hMSCs were cultured at low density on the surface of tECM and bECM hydrogels and treated with basal medium, to observe the effect of each hydrogel on hMSCs differentiation.

hMSCs cultured on tECM were observed to be elongated fibroblasts similar in shape to tenocytes (Figure 25A), while hMSCs cultured on bECM were observed to have morphology similar to osteoblasts (Figure 25B); this may be an indication that hMSCs were differentiated into tenogenic lineage on tECM hydrogels (Figure 25A), while hMSCs cultures on bECM differentiated into osteogenic lineage (Figure 25B).

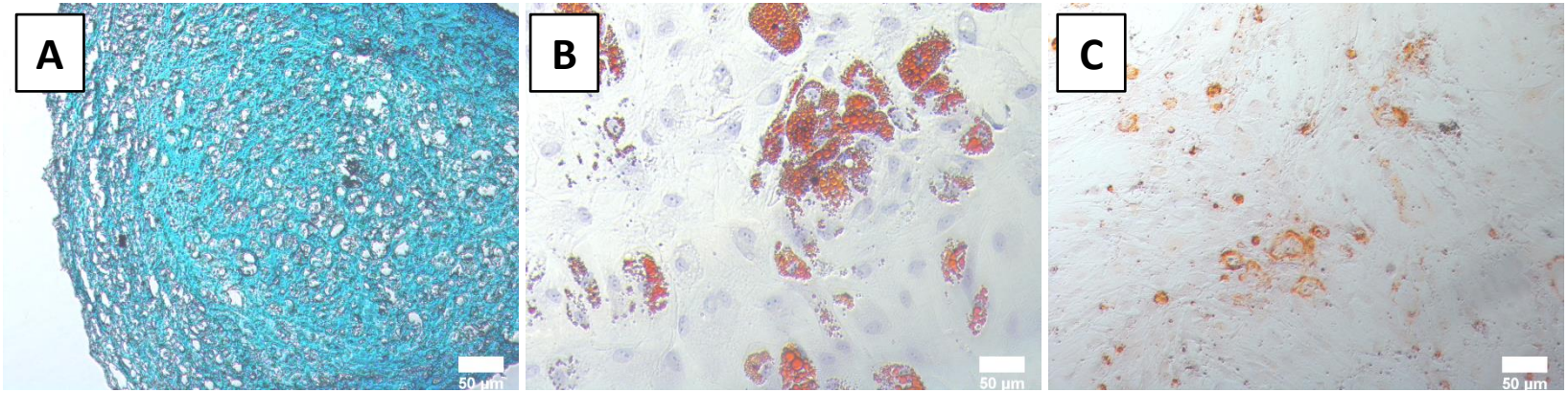
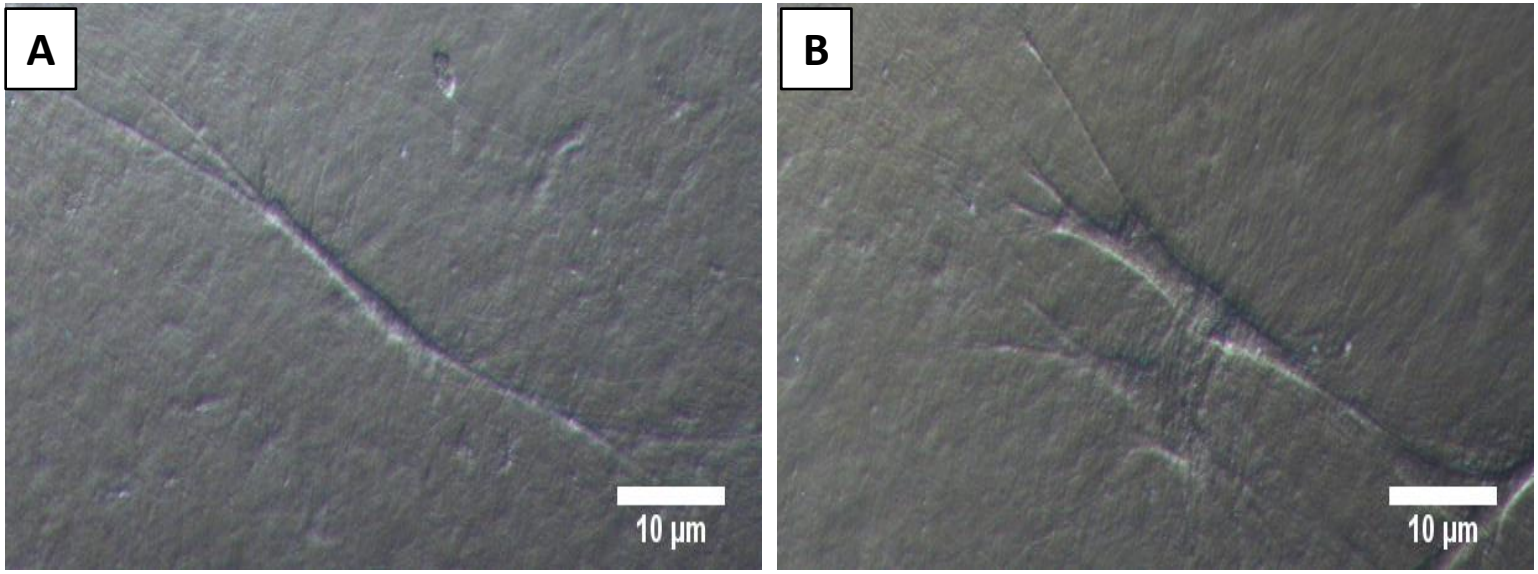



**Figure 24:** Multi-lineage differentiation of hMSCs, (A) Alcian blue staining showing chondrogenic differentiation of hMSCs. (B) Oil red O staining showing adipogenic differentiation of hMSCs. (C) Alizarin Red S staining showing osteogenic differentiation of hMSCs (Scale bar = 50µm).




F**igure 25:** Morphology of hMSCs cultured on (A) 8mg/ml tECM hydrogel, (B) 8mg/ml bECM hydrogel (n = 6).

### 4.3.6 Gene expression

hMSCs tenogenic and osteogenic differentiation was further assessed by RT-qPCR analysis for expression of eight genes, three specific for tenogenic differentiation: scleraxis (SCX), tenascin-C (TNC), and tenomodulin (TNMD). In addition, four specific for osteogenic differentiation: osteopontin (OPN), osteocalcin (OCN), Runt related transcription factor 2 (RUNX-2) and Alkaline phosphatase (ALP). hMSCs were cultured for 7, 15 and 21 days on 8mg/ml bECM, tECM, and coll type I hydrogel in osteogenic, tenogenic and basal medium, hMSCs were cultured on TCPs as well and used as a control.

Figure 26A shows the expression of SCX is upregulated in hMSCs cultured on coll I and tECM with both basal and tenogenic media. However, significant differences were observed in the expression level between cell cultures on tECM and coll I at day 7, 15, and 21 in both media. TMND and TNC showed similar expression, they were expressed in cells cultured on coll I and tECM with basal and tenogenic media (Figure 26B and C), TMND expression was significantly higher in hMSCs cultured on tECM compared to coll I at day 7 and 15 in both media (Figure 26B).

Osteogenic gene markers (ALP, OCN, OPN, and RUNNX2) were expressed at lower levels in hMSCs cultured on tECM and coll I hydrogels at day 7, 15 , and 21 in both basal and tenogenic media (Figure 27).

Different results can be observed in Figure 28, the expression of ALP was upregulated in all cells cultured on bECM, coll I, and TCP and treated with osteogenic media, with minimal expression seen at day 15. In basal media ALP

was upregulated in all samples but the expression was maximised at day 7 (Figure 28A).

Upregulation in OCN expression levels were seen at day 15 and 21, hMSCs had significantly higher expression levels of OCN when cultured on bECM compared to coll I in basal media at day 21 (Figure 28B). Similar results were seen in Figure 26C the highest expression levels of OPN were observed at day 21 in cells cultured on bECM with basal and osteogenic media. Furthermore, hMSCs cultured on coll I expressed OPN only when treated with osteogenic media, with minimal expression seen with basal media. RUNX2 was upregulated in all cells cultured on bECM and coll I with basal and osteogenic media, highest level of expression were observed in cells cultured on bECM and treated with osteogenic media Figure 28D .

Figure 29 shows downregulation in tendon specific gene markers (SCX, TNMD, and TNC) in hMSCs cultured on bECM hydrogels. However, hMSCs cultured on coll I with basal media expressed both tenogenic gene markers SCX at day 7, 15 and 21 (Figure 29A), and TNC at day 7 and 15 (Figure 29C).

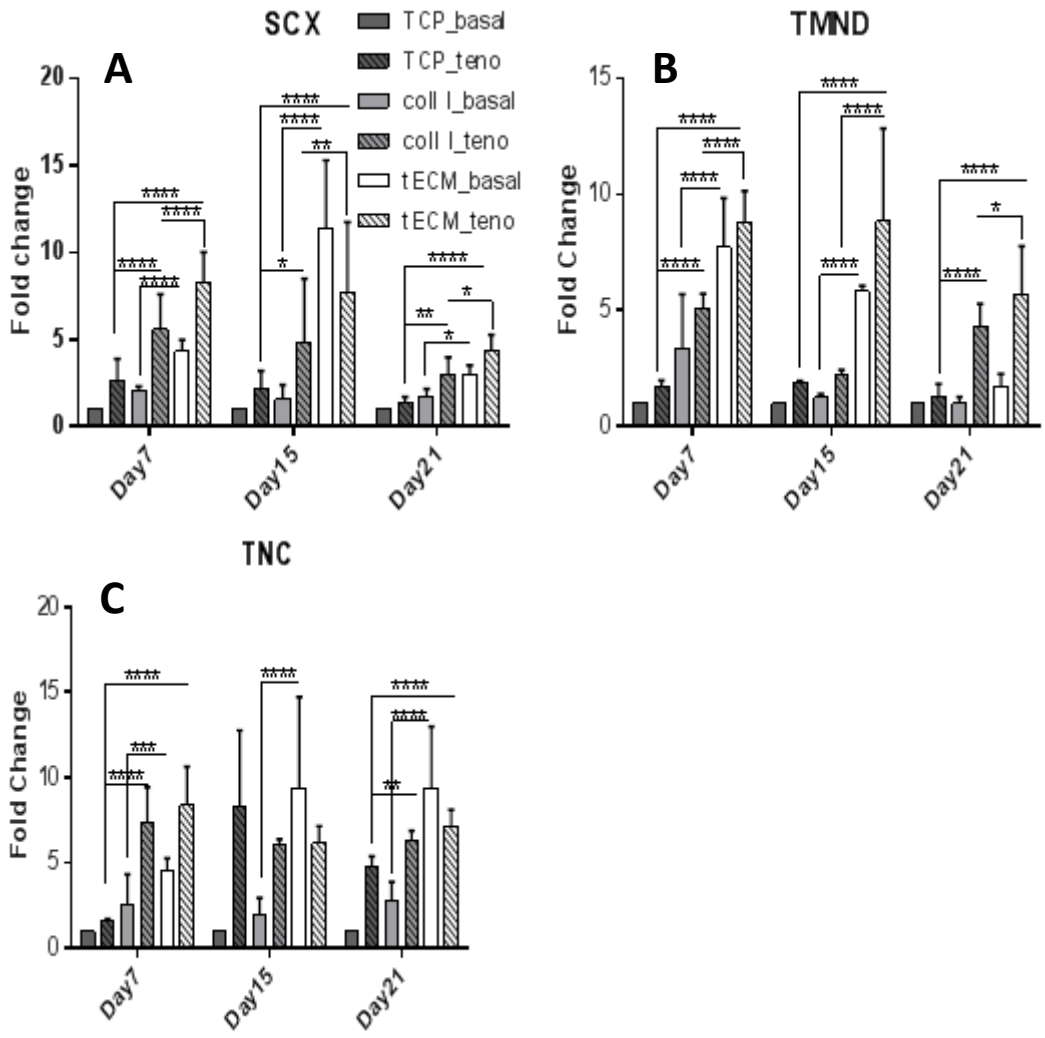



**Figure 26:** RT-qPCR of tenogenic gene markers SCX (A), TNMD (B), and TNC (C) expression in human mesenchymal stem cells (hMSCs) seeded on tECM, coll I hydrogels and TCP cultured in basal and tenogenic medium. Expression of each target gene normalised to β-actin. Data shown is mean±SD of 3 independent experiments (n=3). Statistical significance of expression **** indicates $p<0.0001$; *** indicates $p<0.001$; ** indicates $p<0.01$; and * indicates $p<0.05$

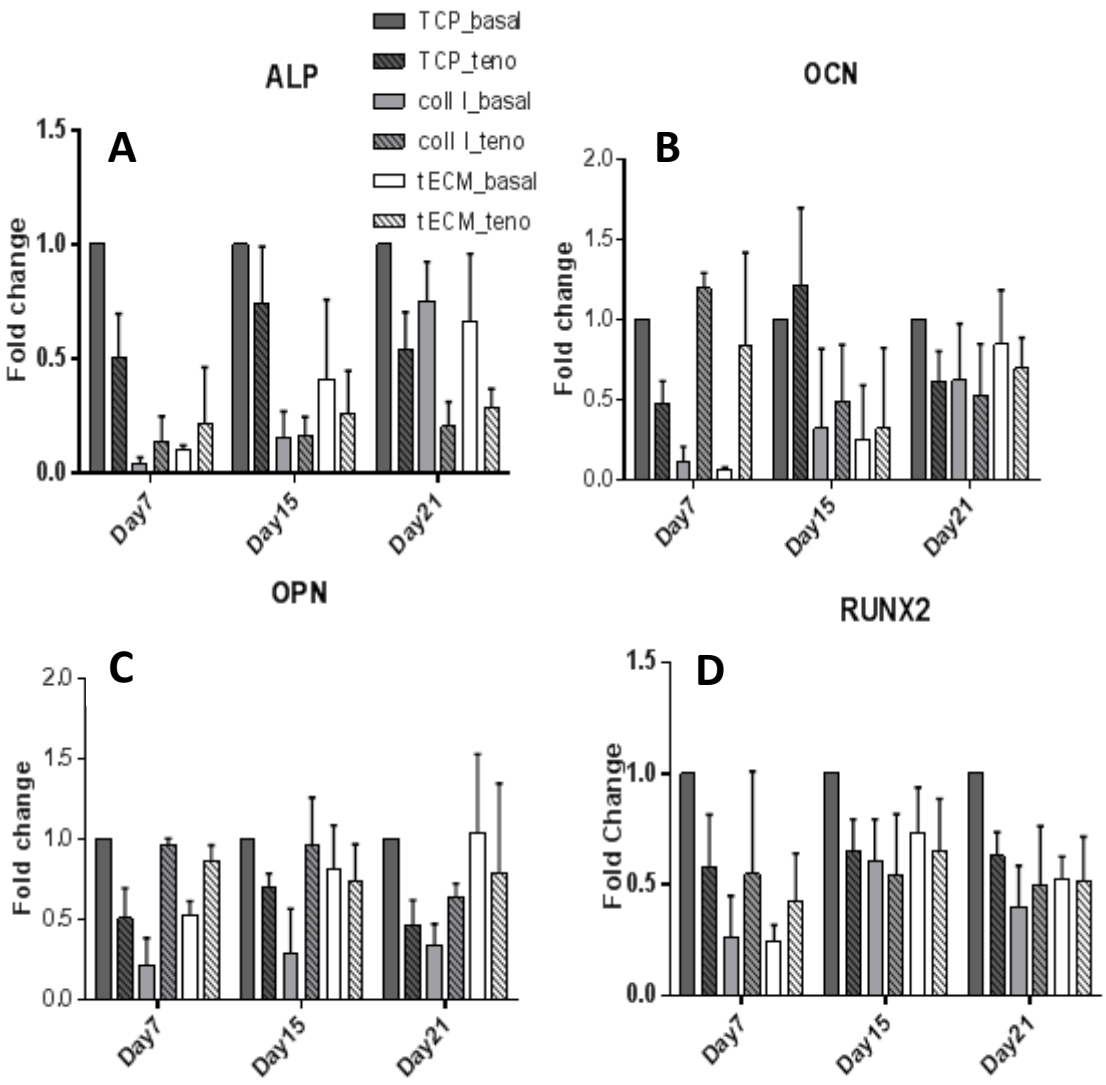



**Figure 27:** RT-qPCR of osteogenic gene markers: ALP (A), OCN (B), OPN (C), and RUNX2 (D) expression in human mesenchymal stem cells (hMSCs) seeded on tECM, coll I hydrogels and TCP cultured in basal and tenogenic medium. Expression of each target gene normalised to β-actin. Data shown is mean±SD of 3 independent experiments (n=3). Statistical significance of expression **** indicates $p<0.0001$; *** indicates $p<0.001$; ** indicates $p<0.01$; and * indicates $p<0.05$

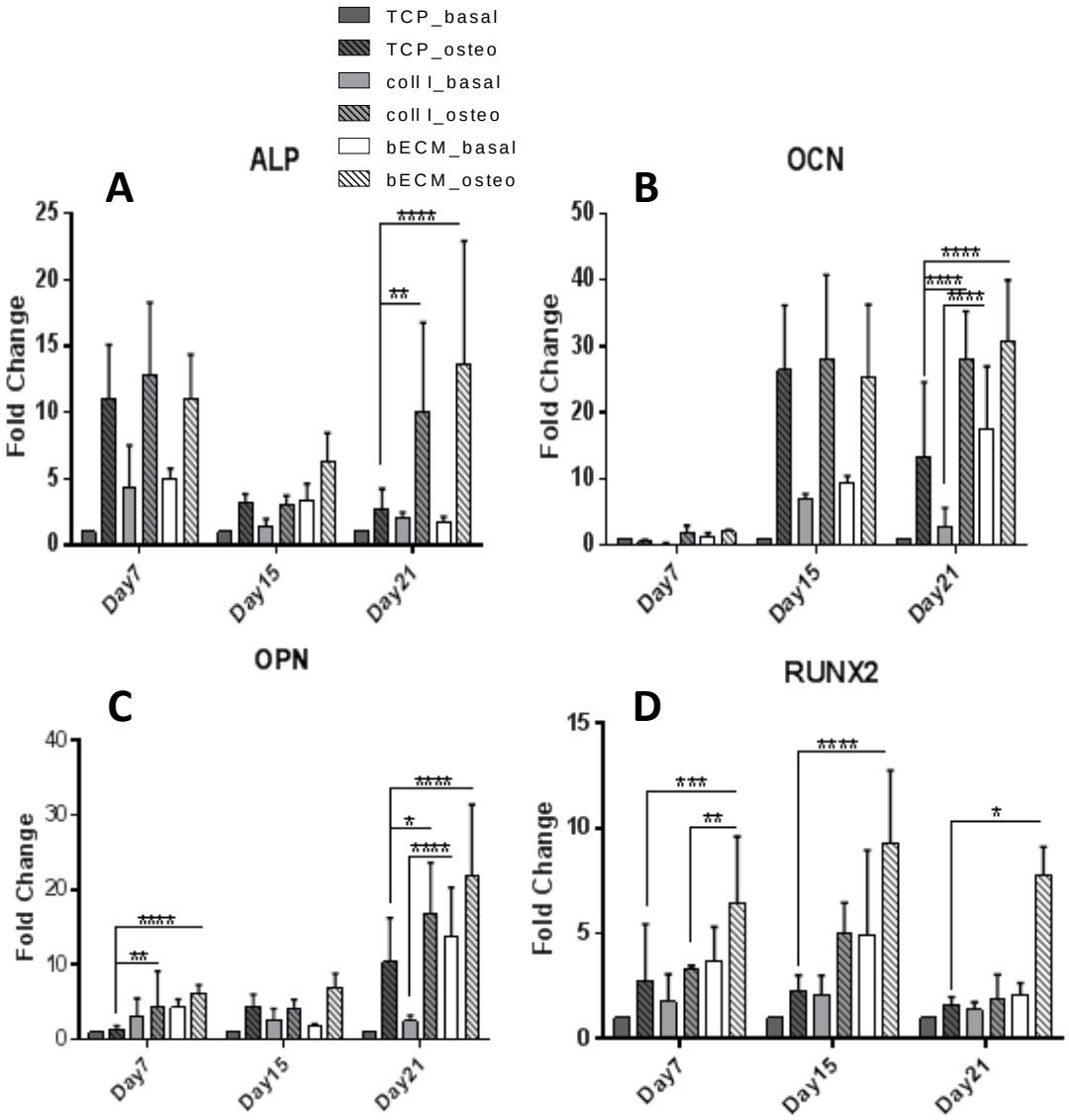



**Figure 28:** RT-qPCR of osteogenic gene markers: ALP (A), OCN (B), OPN (C), and RUNX2 (D) expression in human mesenchymal stem cells (hMSCs) seeded on bECM, coll I hydrogels and TCP cultured in basal and osteogenic medium. Expression of each target gene normalised to β-actin. Data shown is mean±SD of 3 independent experiments (n=3). Statistical significance of expression **** indicates $p<0.0001$; *** indicates $p<0.001$; ** indicates $p<0.01$; and * indicates $p<0.05$

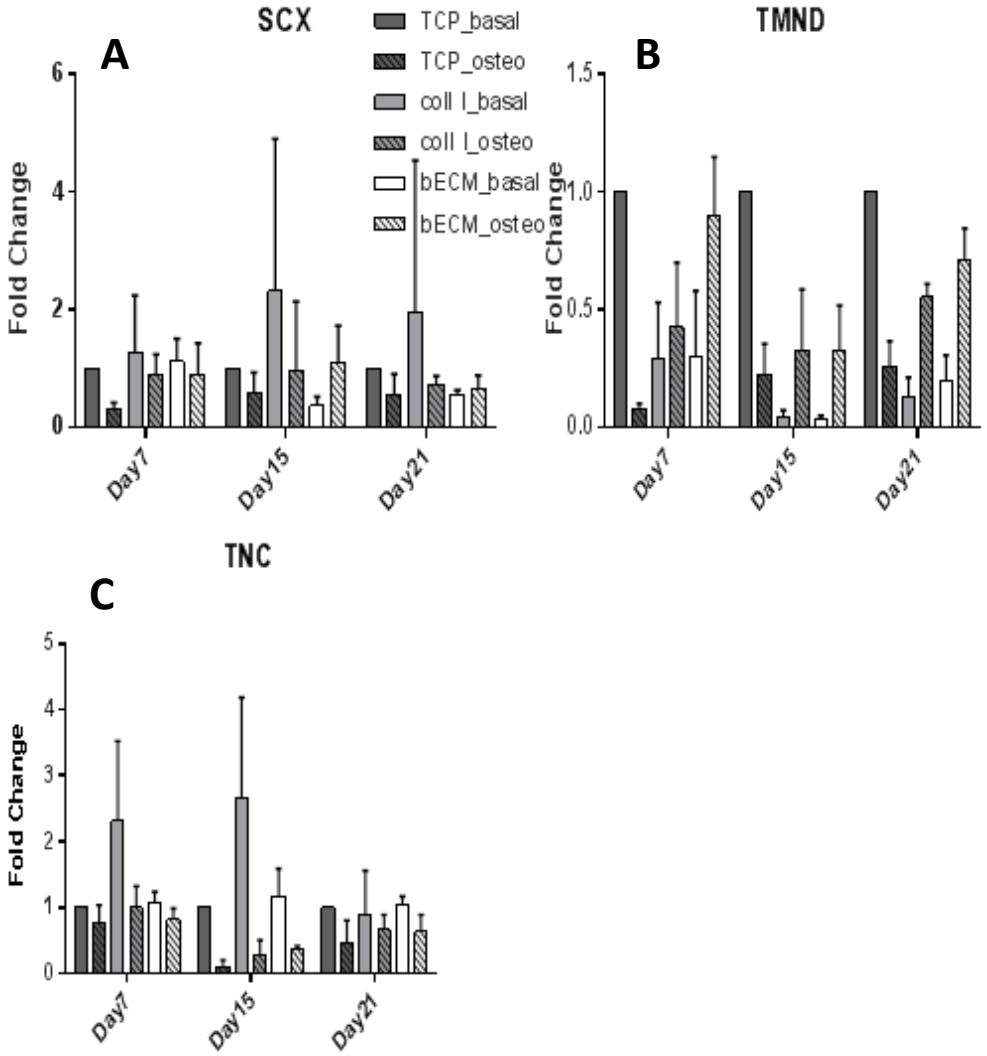



**Figure 29:** RT-qPCR of tenogenic gene markers SCX (A), TNMD (B), and TNC (C) expression in human mesenchymal stem cells (hMSCs) seeded on bECM, coll I hydrogels and TCP cultured in basal and osteogenic medium. Expression of each target gene normalised to β-actin. Data shown is mean±SD of 3 independent experiments (n=3). Statistical significance of expression **** indicates $p<0.0001$; *** indicates $p<0.001$; ** indicates $p<0.01$; and * indicates $p<0.05$

## 4.4 Discussion

The goal of this study was to engineer a hydrogel scaffold to mimic the natural tendon-to-bone interface tissue. In an effort to achieve this goal we have produced a hydrogel derived from decellularized tendon extracellular matrix (tECM), and determined its structural and biological properties. We hypothesize that tECM hydrogel will enhance the tenogenic differentiation of hMSCs, and a hydrogel derived from decellularized bone extracellular matrix (bECM) will enhance the osteogenic differentiation of hMSCs. While MSCs have been widely studied in bone tissue engineering [217-220], less study has been carried out in the field of engineering a 3D biomaterial to enhance MSC tenogenic differentiation. Previous work has suggested that tenogenic differentiation can be enhanced through cell alignment and elongation using two dimensional substrate [221-223] and growth factors such as bFGF, IGF-1, GDF-5, GDF-7 and BMP12 [224-230]. Therefore, the aim of this chapter was to evaluate whether a hydrogel scaffold derived from tendon ECM can induce hMSCs tenogenic differentiation.

Equine flexor digitorum superficialis tendon ECM was decellularized using a previously reported method [215], and a hydrogel was derived from the decellularized material by digesting it with pepsin and inducing the gelation under relevant pH, and salt concentration [162]. The efficiency of the decellularization process is dependent on the type of the tissue and the method used [231]. Cell removal from a tissue can be assessed by staining the

cell nuclei, tECM samples were sectioned and stained with (H&E) and DAPI, control untreated samples were stained as well. Images in Figure 20 show that no cells nuclei can be observed with DAPI staining in the decellularized samples compared to untreated sections (Figure 20A & B). Similar results were obtained with the (H&E) staining (Figure 20C & D).

The soluble collagen content of tECM materials was 0.62 ± 0.09 mg collagen in each 1mg decellularized tECM. Collagen type I is the main component of tendon tissue, and has been previously used as a scaffold in tendon tissue engineering. Therefore, it has been used in this study as comparator material in the evaluation of the structural, mechanical and *in vitro* cell response characteristics.

SEM imaging showed that tECM and coll I have similar fiber node density at 4 and 8mg/ml. Fiber node density can influence the mechanical strength of the scaffold [232], which in turn may have implications on *in vivo* cell behaviour.

The components responsible of tECM gelation are unknown but it is most likely due to the presence of self-assembly collagen monomers, previous work demonstrated the ability of collagen molecules to self-assemble into fibrils and form fibrous network [233-236].

The turbidimetric gelation kinetics of tECM gels were slower than collagen type I at 4 and 8mg/ml, this is most likely due to the presence of other molecules such as glycosaminoglycans (GAGs) and different type of collagen which can modulate collagen self-assembly[235].

Primary human bone-marrow mesenchymal stem cells (hMSCs) were able to grow and attach to the tECM gels, after 3 and 7 days incubation there was not significance differences in cells number cultured on tECM compared to collagen type I.

To create a functionalized 3D scaffold which promotes the regeneration of the tendon-to-bone interface, MSCs need to proliferate and then undergo appropriate differentiation and specific matrix remodeling on the scaffold in order to replace tissue at site of injury. Extracellular matrix regulates cell behaviour, and it has been found that tissue derived ECM can induce tissue specific differentiation of MSCs [237-239]. Clear morphological differences can be noted between hMSCs cultured on tECM gels compared to cells cultured on bECM, hMSCs appear on tECM more elongated with less fibers (Figure 24A), while hMSCs appear on bECM in more irregular shape, with long stress fibres running in many different directions Figure 24B).

The morphological differences were further supported with the results of real time qPCR analysis, which revealed enhanced tenogenesis of hMSCs cultured on tECM based on the expression of tenogenic gene markers (Figure 26). The expression of SCX a tendon-specific transcription factor [27] was higher in hMSCs cultured on tECM compared to coll I at day 7, 15 and 21. Similar results can be noted with TNMD a transmembrane glycoprotein which has a role in tendon proliferation and maturation [240], TNC an ECM glycoprotein tenascin-C modulates cell migration, proliferation and cellular signalling [241] was

upregulated in tECM group with and without tenogenic medium compared to coll I and TCP group at day 7, 15 and 21 (Figure 26).

Moreover, there was downregulation in osteogenic gene markers (ALP, RUNX2, OCN and OPN) (Figure 27), these four markers are specific markers during osteogenesis, and they range from early markers: ALP and RUNX2, intermediate: OPN and late marker OCN [170-172].

In contrast, hMSCs cultured on bECM expressed higher levels in osteogenic gene markers (ALP, RUNX2, OCN and OPN) compared to coll I and TCP at day 7, 15 and 21 in the presence of basal and osteogenic medium (Figure 28), also bECM reduced tenogenic differentiation of hMSCs when cultured on bECM with very minimal expression levels of tenogenic gene markers (SCX, TNMD and TNC) at day 7, 15 and 21 (Figure 29).

Our findings show that tECM hydrogel induced hMSCs tenogenic differentiation and suppressed osteogenic differentiation and bECM hydrogel induced hMSCs osteogenic differentiation and suppressed tenogenic differentiation. tECM and bECM induced hMSCs differentiation into multiple interface-specific lineage (tendon and bone), which may have potential benefit over the currently used non-site specific ECM grafts, primarily tECM/bECM are site-specific ECM and they supported hMSCs tenogenic and osteogenic differentiation respectively, without the induction of tenogenic and osteogenic media, the ability to regenerate multiple tissue may overcome the limitations

associated with current available grafts for enthesis repair ; together these data provide a new approach to design a gradient hydrogel scaffold for tendon-to-bone interface tissue engineering.

# Chapter 5. Novel Electrospun Decellularized Bone Extracellular Matrix for Bone Tissue Engineering

## 5.1 Introduction

Biological scaffolds composed of ECM are widely used to facilitate the functional reconstruction of numerous tissue types. They are produced by chemical, enzymatic, or physical decellularization process. ECM scaffolds have shown efficacy in both pre-clinical animal studies and human clinical applications [242-245]. However, the decellularization process may alters the biochemical and ultrastructure of the ECM and accordingly, alters the host tissue response to the ECM scaffold following implantation [104, 246, 247]. Therefore, there is a great need to develop new tools to reconstruct the resultant ECM and the tissue architecture after the decellularization process.

Among the currently known fabrication techniques, electrospinning has been shown to be a straightforward and effective way to design and produce nanofibrous scaffolds that recapitulate the native extracellular matrix (ECM) [248, 249]. This approach has been widely employed to fabricate number of polymers such as; natural proteins [250-252], synthetic polymers [253, 254], and combinations of natural and synthetic polymers [255-257].

Electrospun scaffolds have attracted considerable attention in the bone tissue engineering field as it was considered that nanofibrous structure of the electrospun scaffold may provide an appropriate environment for bone-associated cells and their progenitor/stem cells to grow and proliferate [258]. Moreover, it has been reported that osteoblastic differentiation and mineralization were enhanced with the use of nanofibrous scaffolds compared to a dense substrate of polymers [259]. Even though the *in vivo* studies for electrospun scaffolds application in bone regeneration and tissue engineering approach are still an under-researched area, several reports of electrospun scaffolds with large surface area, high porosity, and mechanical and structural properties similar to the native bone ECM have highlighted the potential of these scaffolds to serve as an ideal bone substitutes [260].

Polyurethane and polyesterurethane electrospun scaffolds possessed good mechanical properties. However, the slow degradation of these scaffolds might interfere with tissue turnover and remodeling [261]. Several other polymers have been fabricated with the electrospinning technique for bone tissue engineering such as: poly(ε-caprolactone) (PCL), a degradable polymer that demonstrated good support for MSCs proliferation, and enhanced the osteoblastic differentiation of MSCs in osteogenic media [262, 263]. Similar results were reported with electrospun poly-l-lactide (PLA) and osteoblastic cells [264]. Natural polymers like collagen, silk, and chitosan have also been processed by electrospinning for bone tissue engineering because of their

favourable proprieties as they support cell adhesion, biodegradable, with minimal inflammatory reaction [265-268].

Moreover, electrospinning has facilitated the utilization of (ECM) by either act like a carrier for the ECM or by electrospinning a mixture of ECM and other materials. Baiguera *at al.* have shown that incorporation of gelatin with rat decellularized brain ECM enhanced the differentiative potential of mesenchymal stromal cells [269], further studies has investigated different decellularized ECM particles blended with polycaprolactone polymer [270] and hybrid mat consist of electrospun poly(ester-urethane)urea and electrosprayed decellularized porcine dermis ECM hydrogel [162].

To date, no study has yet been reported that has explored the potential of electrospinning decellularized ECM without the incorporation of other materials. The aims of this chapter were to utilise the results from the previous two chapters and produce an electrospun scaffold using decellularized bovine bone extracellular matrix (bECM) to serve in the long term as a base for the gradient scaffold with bone ECM and tendon ECM hydrogels. In the present research we optimised a method to electrospin decellularized bovine bone extracellular matrix (bECM) without the addition of any other materials as a potential improvement for cell adhesion, proliferation and differentiation. We assessed the biological activity and osteogenic capability *in vitro* of electrospun bECM scaffolds in comparison to electrospun gelatin scaffolds using mouse primary calvarial cells (mPCs) and human mesenchymal stem cells (hMSCs).

## 5.2 Materials and methods

### 5.2.1 Solvent selection for bECM and gelatin materials

Bovine bone extracellular matrix was decellularized as previously mentioned (1.2.1). The lyophilized decellularized bone granules (55mg/ml) were dissolved in Trifluoroacetic acid (TFA) (Thermo Fisher, UK) and Dichloromethane (DCM) (Sigma-Aldrich, UK)/TFA mixture (v/v, 75/25, 50/50, 25/75). In addition, the bone granules were dissolved in 1, 1, 1, 3, 3, 3-Hexafluoro-2-propanol (HFP) (Sigma-Aldrich, UK) and HFP/TFA mixture at different ratios (v/v, 75/25, 50/50, 25/75). Gelatin type A (Sigma, UK) was dissolved in hexafluoro-2-propanol (HFP) at 55mg/ml. The solutions were kept stirring at room temperature for periods range from 4 to 18 hours before the electrospinning process.

### 5.2.2 Electrospinning

bECM and gelatin solutions were loaded into a plastic syringe with a 23-gauge needle (spinneret). The syringe was placed in a syringe pump (Harvard Apparatus, UK) and set to solution flow rate 1ml/hr. A 22 kV voltage was applied to the spinneret and fibres were collected on rotating mandrel positioned 15 cm away from the needle tip, mandrel speed was set to 50 rpm. The solutions were electrospun for 3 hours at 20°C in 40% relative humidity. A schematic of the complete electrospinning equipment is shown in Figure 30.

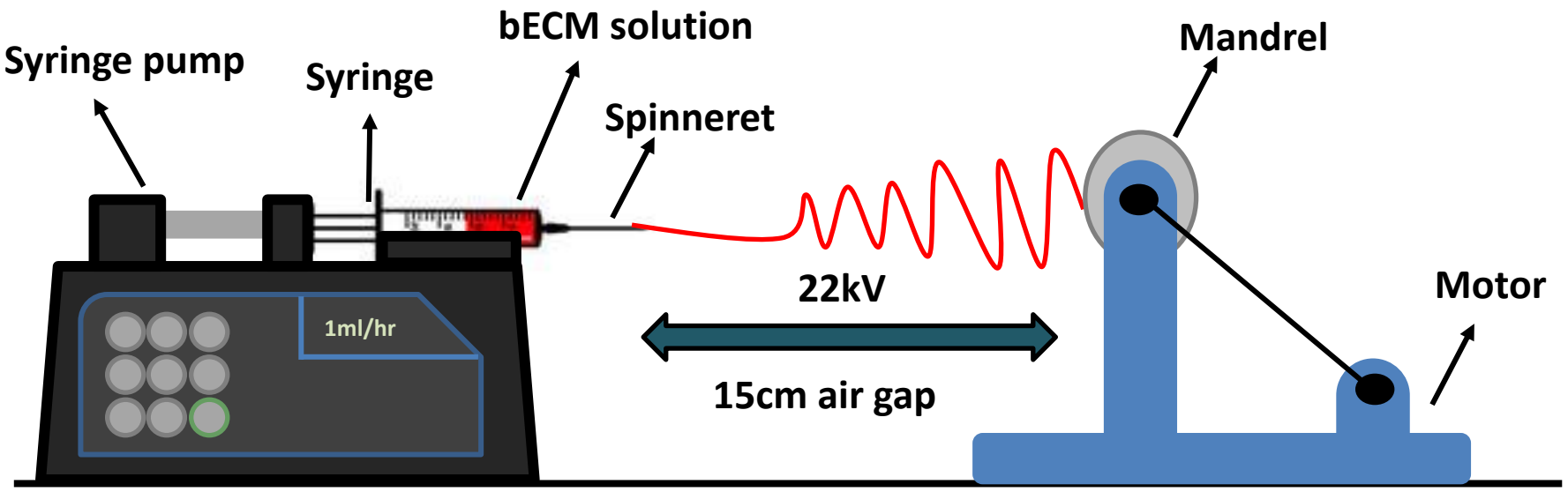



**Figure 30:** A schematic of the electrospinning apparatus. bECM solution is passed through a syringe placed on a syringe pump facing the mandrel, a high voltage supply is applied to the spinneret causing an electric potential between the spinneret and the grounded mandrel forcing the fibers to be ejected from the spinneret and deposited on the rotating mandrel.

### 5.2.3 Crosslinking of the electrospun fibres

Electrospun fibres were crosslinked using a mixture of N-(3-dimethylaminopropyl)-N'-ethyl-carbodiimide hydrochloride (EDC) (Sigma-Aldrich, UK) and N-hydroxysuccinimide (NHS) (Sigma-Aldrich, UK) [271].

Crosslinking was carried out by mounting small circular samples of the mats in the Scaffdex CellCrown™ system, and incubating the samples in 10ml ethanol/water (90% v/v) buffer containing 25mM EDC, 10 mM NHS overnight at 4°C. After removal of the crosslinking solution samples were washed with phosphate-buffered saline (PBS) supplemented with 20% v/v penicillin/streptomycin overnight at 4°C. A further washing step was performed with PBS. The crosslinked samples were sterilized with ultra violet irradiation for 30 min on each side of the scaffold, and soaked in PBS at 4°C until use.

### 5.2.4 Morphology

Samples of electrospun bECM and electrospun gelatin before and after crosslinking were gold-coated with blazers SCD030 gold sputter coater. The morphology of the electrospun scaffolds were examined by scanning electron microscopy (SEM), using a JEOL 6060LV imaging system. The diameter distribution of the electrospun fibre was determined by measuring at least 20 fibers from three different samples using ImageJ software.

### 5.2.5 mPCs and hMSCs seeding onto electrospun scaffolds

mPCs were seeded onto bECM electrospun scaffolds at 100k in 12 plates with basal media.

*in vitro* cell viability was further assessed with hMSCs, cells were cultured on bECM electrospun and gelatin electrospun scaffolds at 100k in 12 well plate with mesenchymal stem cell growth medium (MSCGM). The proliferation of mPCs and hMSCs were assessed with PrestoBlue (ThermoFisher) over several days as described in section (2.2.6).

### 5.2.6 Assessment of mineralisation

The presence of mineralised nodules was assessed with von Kossa staining (Millipore, UK). mPCs were cultured on tissue culture plate (TCP) and electrospun bECM with osteogenic and basal medium, after 21 days cells were fixed in 10% (v/v) formalin. After rinsing the fixed cells were incubated with silver nitrate solution under UV light, then washed three times with deionized water and treated with sodium thiosulfate solution, final wash with deionized water was performed. Mineralized nodules were seen as dark brown to black spots.

### 5.2.7 Immunohistochemical staining for osteopontin and osteocalcin

Immunohistochemical staining for the osteogenic marker proteins osteocalcin (OCN) and osteopontin (OPN) in mPCs and hMSCs was performed as described previously in section (2.2.7). Hoechst (Sigma-Aldrich, UK) applied for nuclei stain.

### 5.2.8 Quantitative PCR analysis

The expression levels osteogenic gene markers in hMSCs seeded onto bECM electrospun and gelatin electrospun scaffolds were assessed by qPCR analysis, on day 21 scaffolds were cut into small pieces and resuspended in TRIZOL reagent, RNA isolation and qPCR analysis were completed as described in (3.2.7).

## 5.3 Results

### 5.3.1 Selection of an appropriate solvent

HFP was used previously as a suitable solvent for collagen type I electrospinning [250, 272, 273], and because collagen type I is the main component of bone ECM, solvents used in the literature to dissolve collagen were screened to find the best solvent.

HFP was not able to fully dissolve bECM, but the resultant solution after filtering showed reasonable viscosity for electrospinning (Figure 31A & B). TFA dissolved bECM granules but the formed solution could not be fabricated into fibers by electrospinning, beads and drops were formed on the collector (Figure 31C & D).

DCM/TFA mixture with the volume ratio of 50/50 dissolved bECM powder, but it was not an appropriate solvent because a number of beads were formed on the collector after the electrospinning process (Figure 31E & F).

The best solvent used in this study was HFP/TFA with the volume ratio of 50/50; TFA improved the solubility of bECM and formed a proper solution for electrospinning (Figure 31G & H).

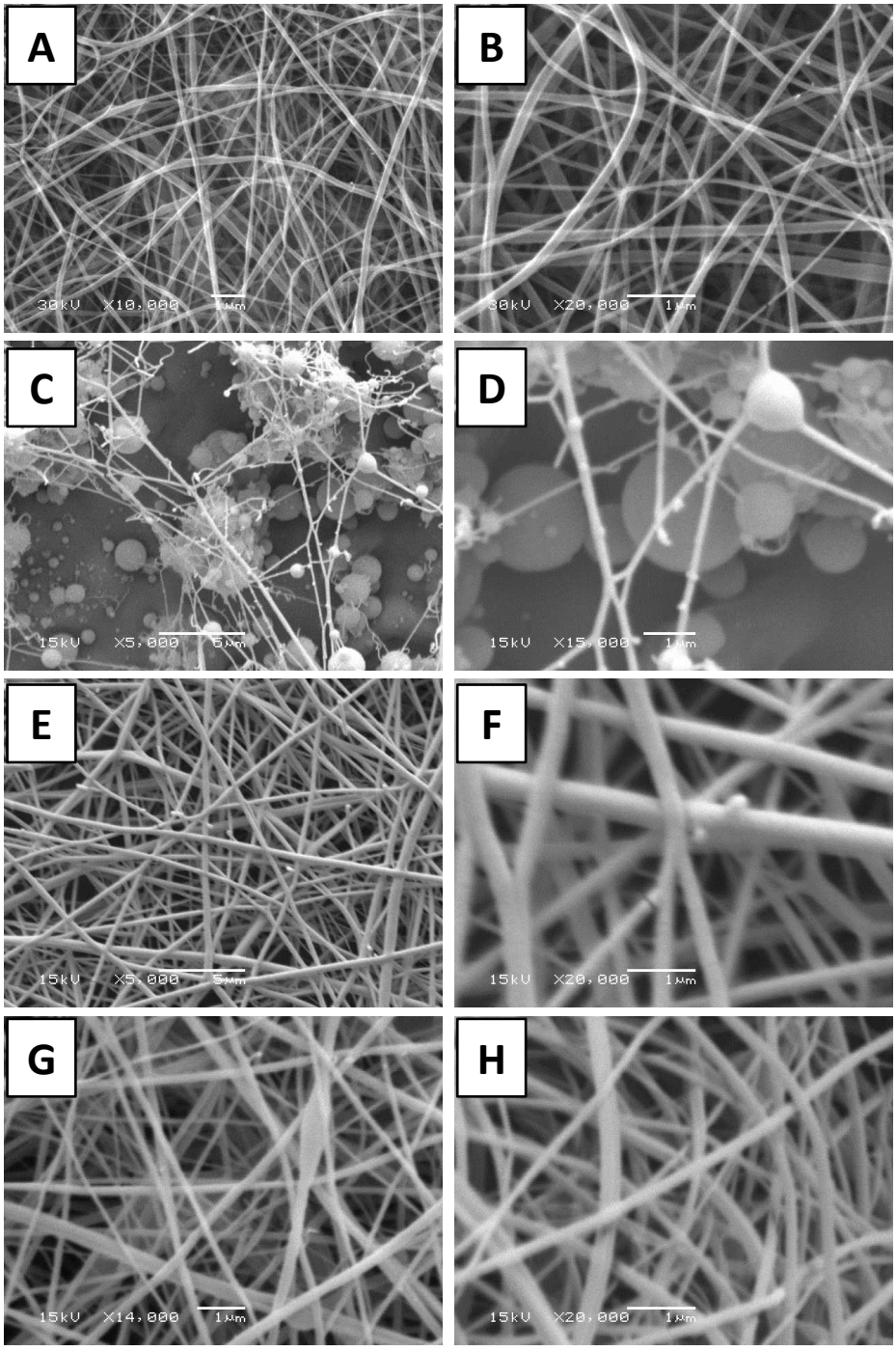



**Figure 31:** Selection of an appropriate solvent for bECM electrospinning. (A & B) 100% HFP, (C & D), 100% TFA, (E & F) DCM/TFA with the volume ratio of 50/50, (G & H) HFP/TFA with the volume ratio of 50/50.

### 5.3.2 Electrospinning and crosslinking of bECM and gelatin fibers

The solution of bECM granules in HFP/TFA with different volume ratio and different concentrations were electrospun under specific spinning parameters. It was found that smooth nanofibers were obtained with 55mg/ml bECM concentration and 50/50 HFP/TFA volume ratio (Figure 32). Gelatin type A was dissolved in 100% HFP at 55mg/ml and electrospun under the same conditions to be used as a comparator material in some experiments (Figure 35). The morphology of electrospun scaffolds were assessed by means of SEM analysis, the spun scaffolds were characterized by random arrangement of fibers, free of beads, and diameter range between 200_700nm before and after crosslinking. (Figure 32, Figure 33, Figure 35, and Figure 36). The mean diameter of the spun fibers was measured from SEM micrograph, which showed a slight reduction in fiber diameter after crosslinking process in both bECM and gelatin fibers (Figure 34 and Figure 37).

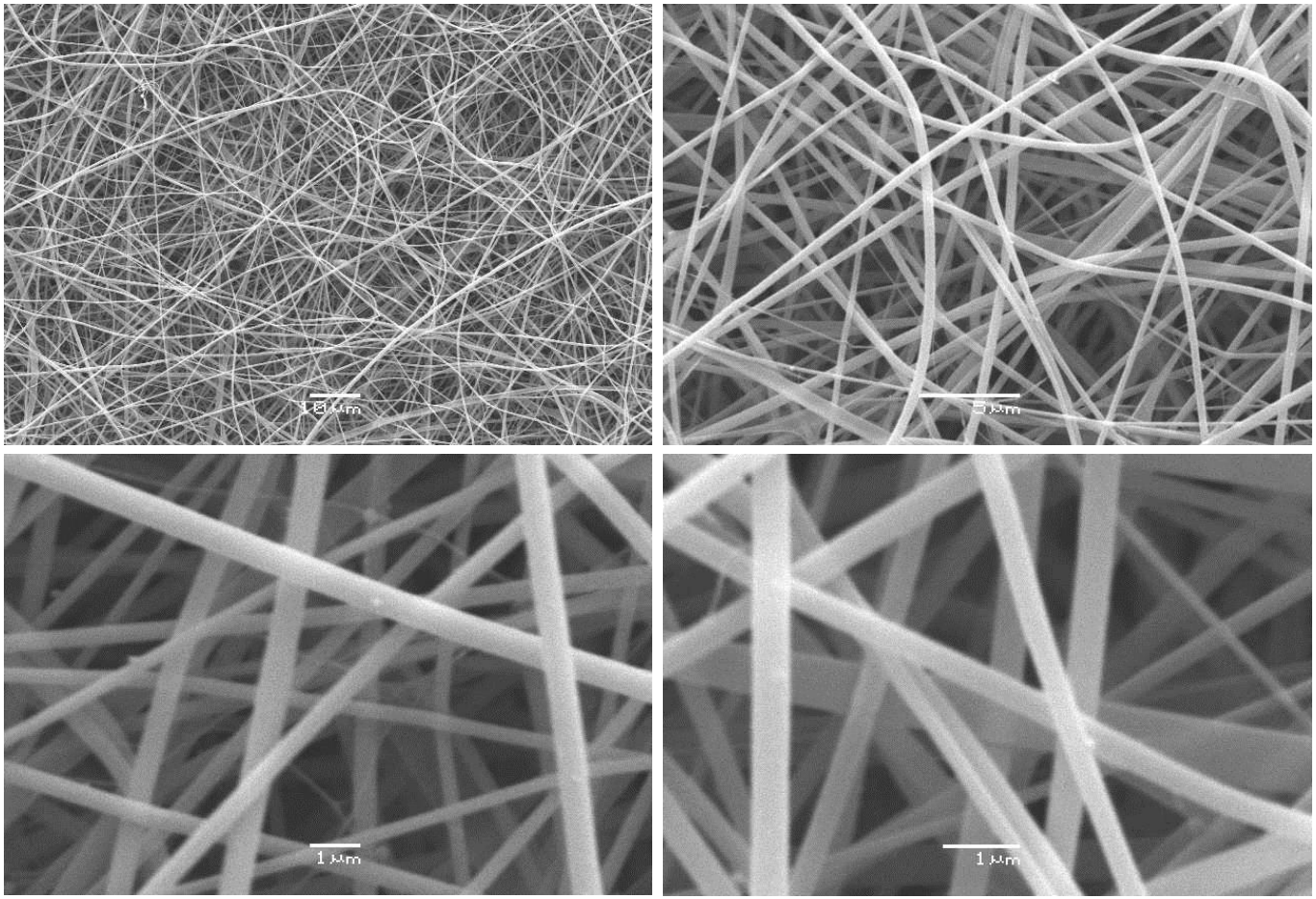



**Figure 32:** Electrospinning of bECM. 55mg/ml bECM dissolved in 50/50 HFP/TFA volume ratio, 22 kV voltage was applied to the spinneret and fibres were collected on rotating mandrel positioned 15 cm away from the needle tip, mandrel speed was set to 50 rpm. The solutions were electrospun for 3 hours at 20°C in 40% relative humidity.

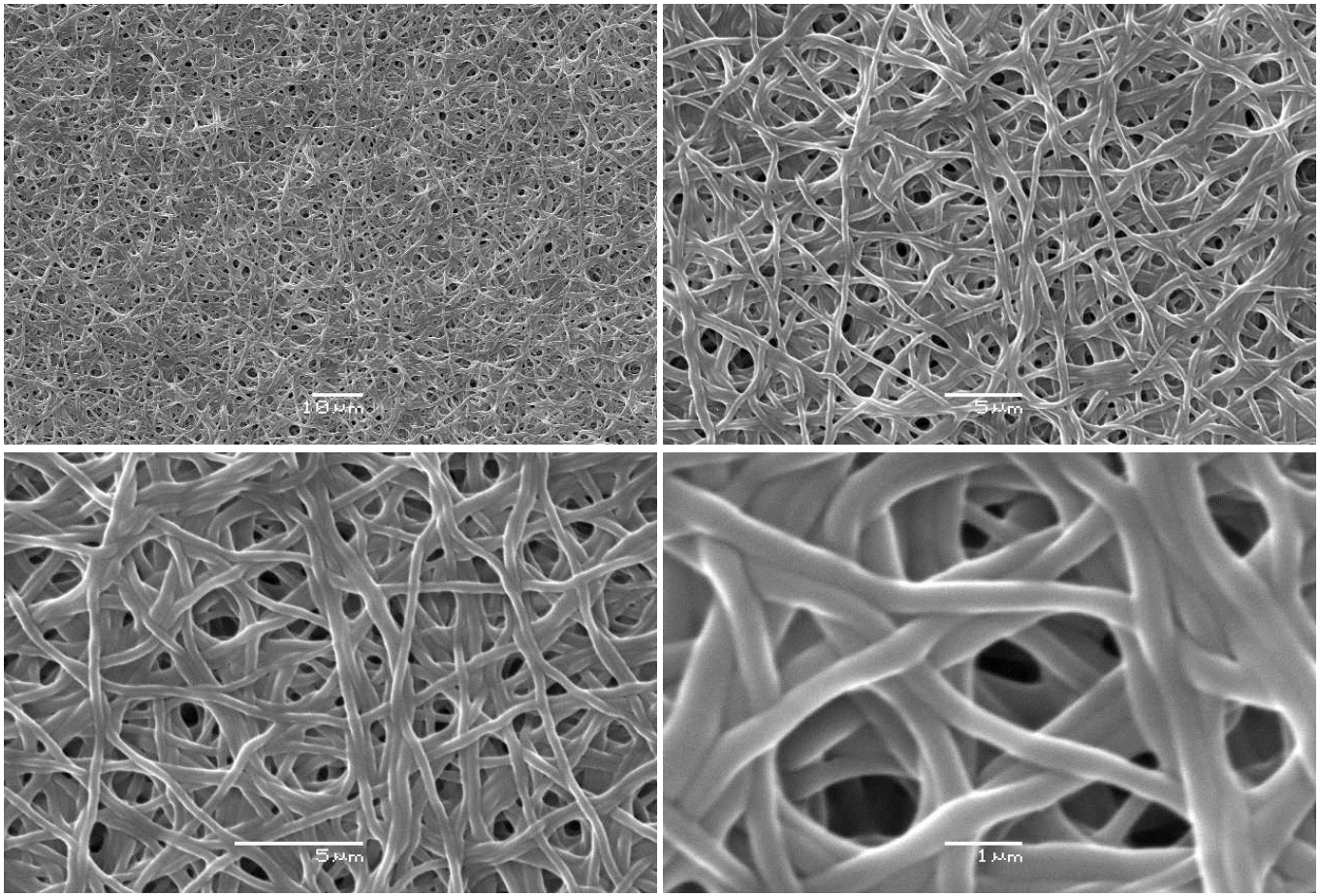



**Figure 33:** SEM images of bECM electrospun fibers after crosslinking. Electrospun bECM were crosslinked using a mixture of 25mM N-(3-dimethylaminopropyl)-N'-ethyl-carbodiimide hydrochloride (EDC) and 10mM N-hydroxysuccinimide (NHS).

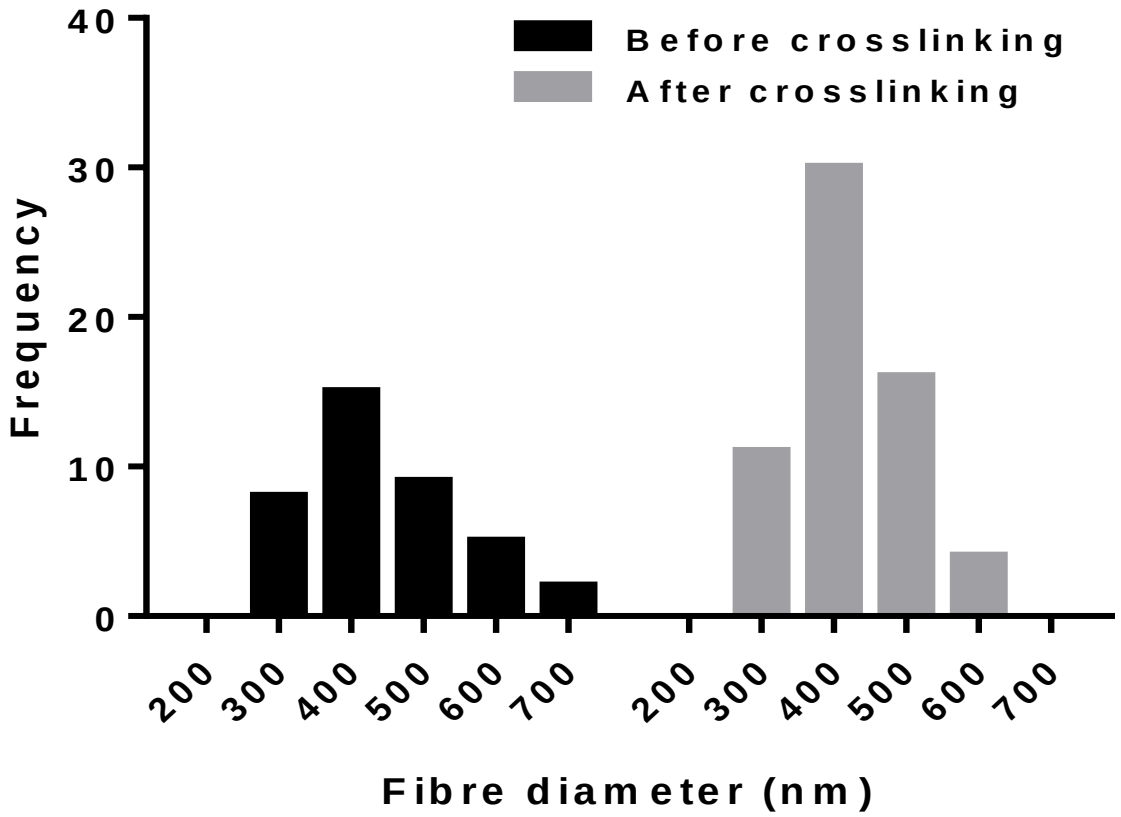



**Figure 34:** Distribution of fibre diameters of electrospun bECM before and after crosslinking.

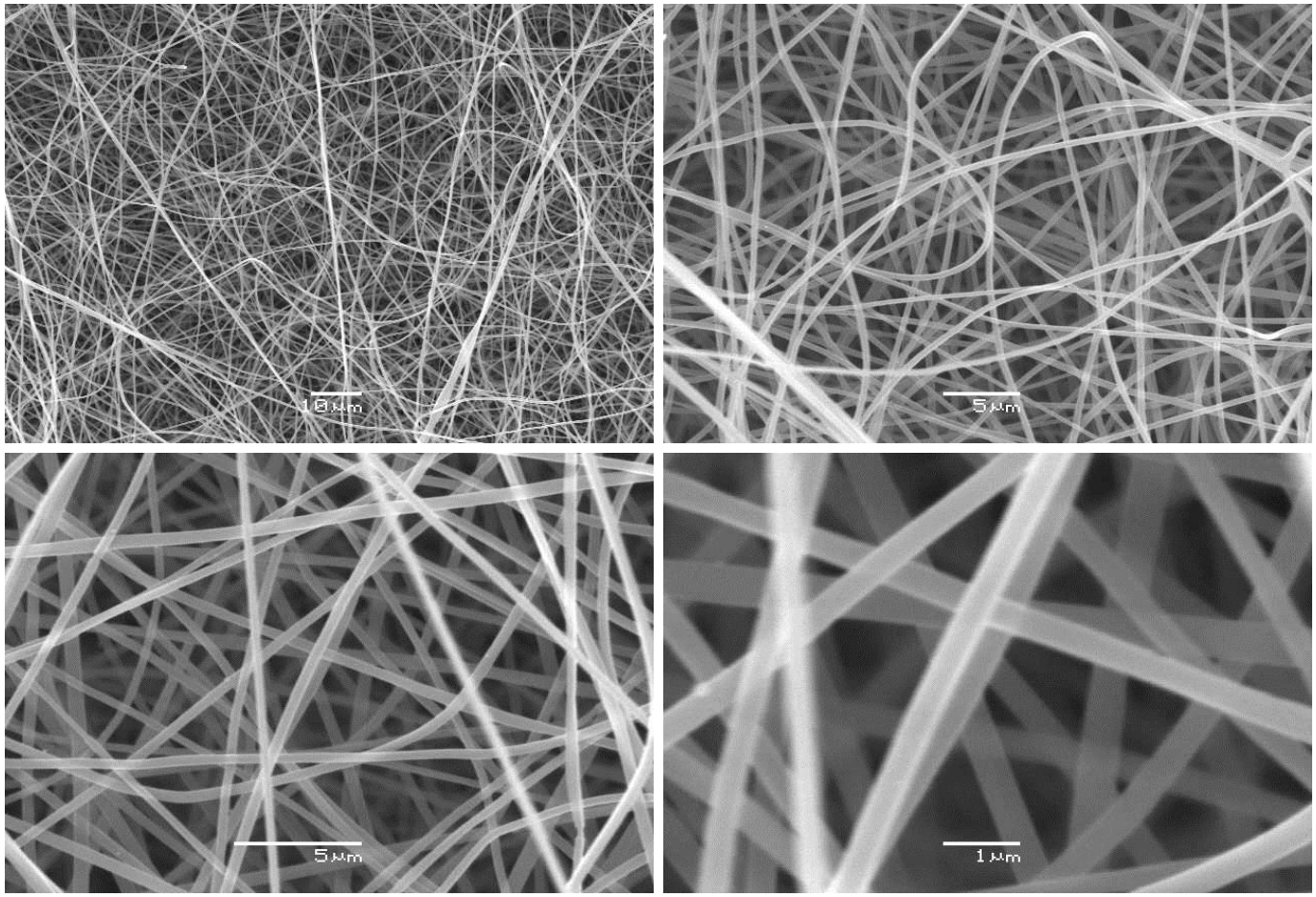



**Figure 35:** Electrospinning of gelatin type A. 55mg/ml gelatin A was dissolved in 100% HFP, 22 kV voltage was applied to the spinneret and fibres were collected on rotating mandrel positioned 15 cm away from the needle tip, mandrel speed was set to 50 rpm. The solutions were electrospun for 3 hours at 20°C in 40% relative humidity.

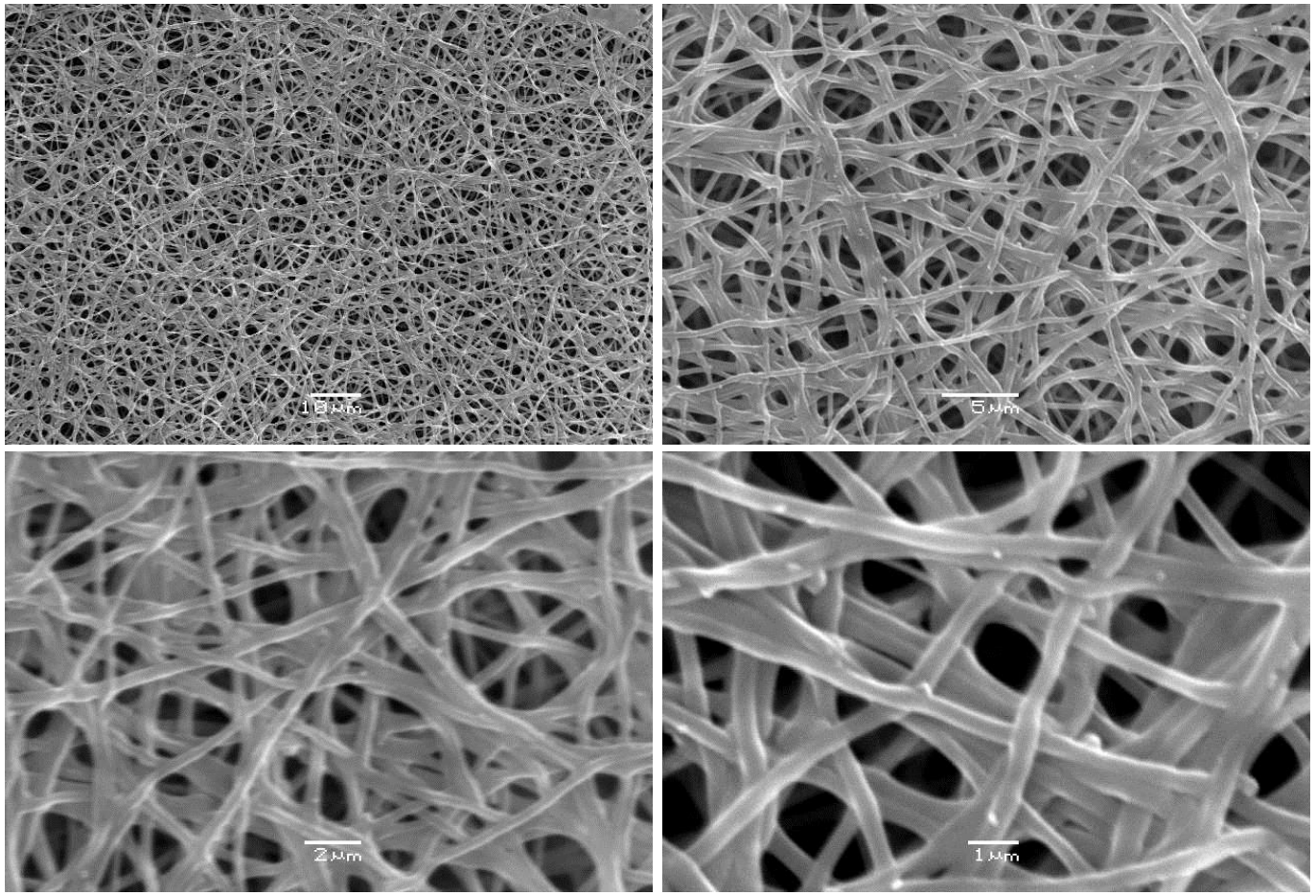



**Figure 36:** SEM images of gelatin electrospun fibers after crosslinking. Electrospun gelatin were crosslinked using a mixture of 25mM N-(3-dimethylaminopropyl)-N'-ethyl-carbodiimide hydrochloride (EDC) and 10mM N-hydroxysuccinimide (NHS).

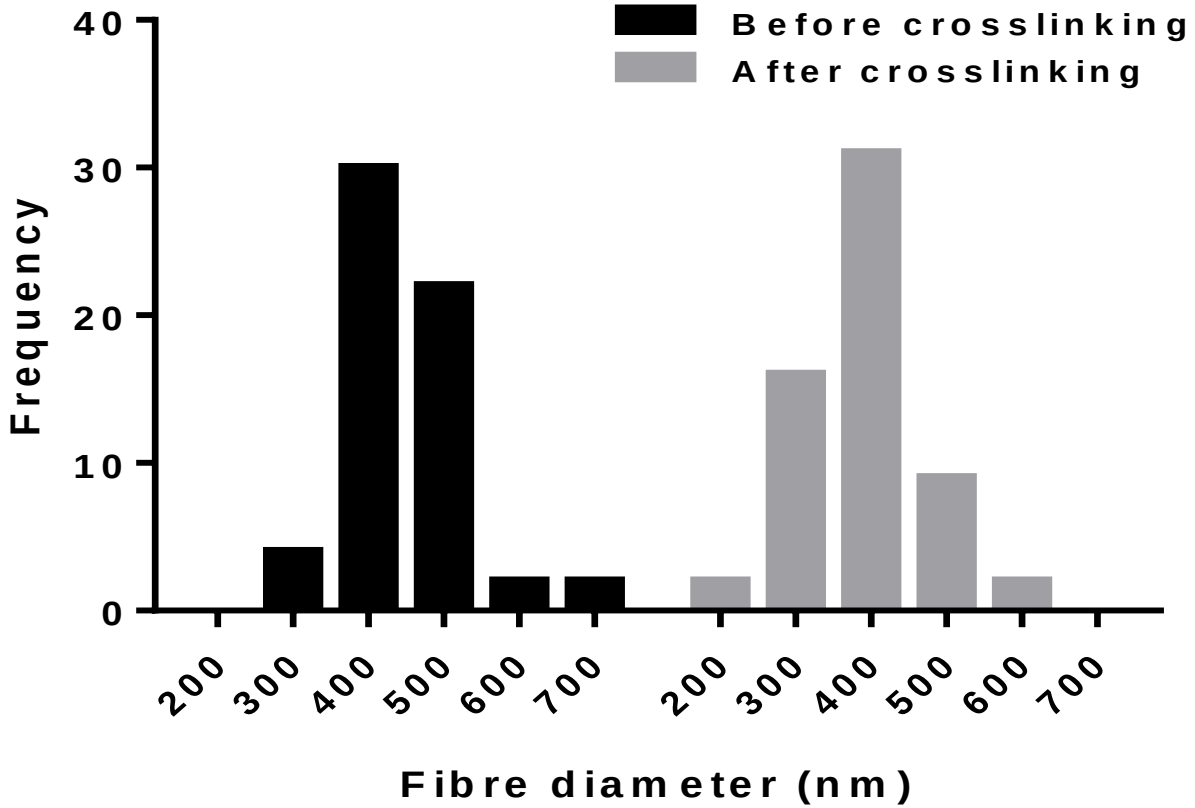



**Figure 37:** Distribution of fibre diameters of electrospun gelatin before and after crosslinking.

### 5.3.3 mPCs and hMSCs seeding onto electrospun scaffolds

mPCs cultured on electrospun bECM were viable after day 2 and day 4, with increased proliferation between day 2 and day 4 (Figure 38).

hMSCs seeded onto electrospun bECM and electrospun gelatin were also viable after day 3 and day 7, with significant increase in proliferation between hMSCs cultured onto spun bECM and gelatin on day 7 (Figure 39).

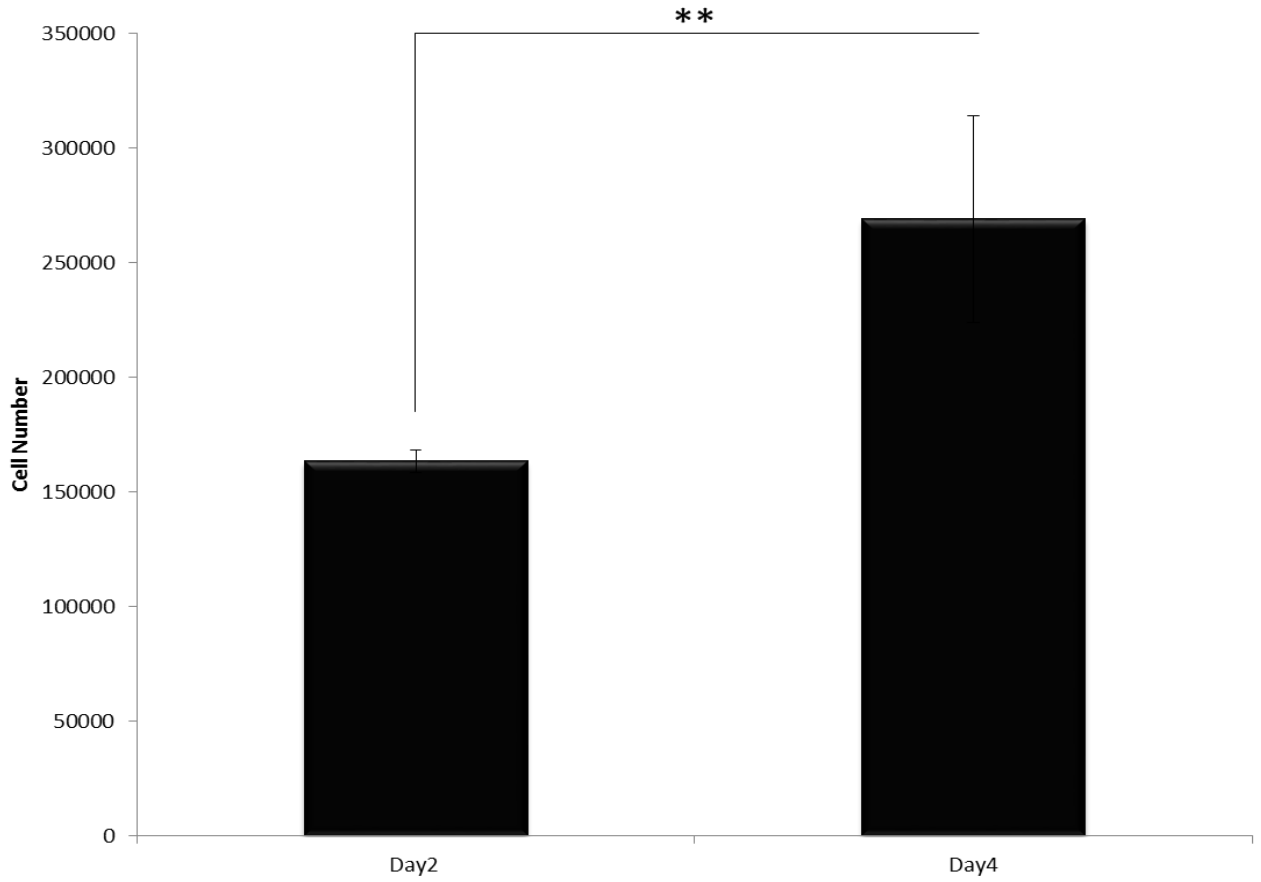



**Figure 38:** Proliferation of mPCs on electrospun bECM after 2 and 4 days.

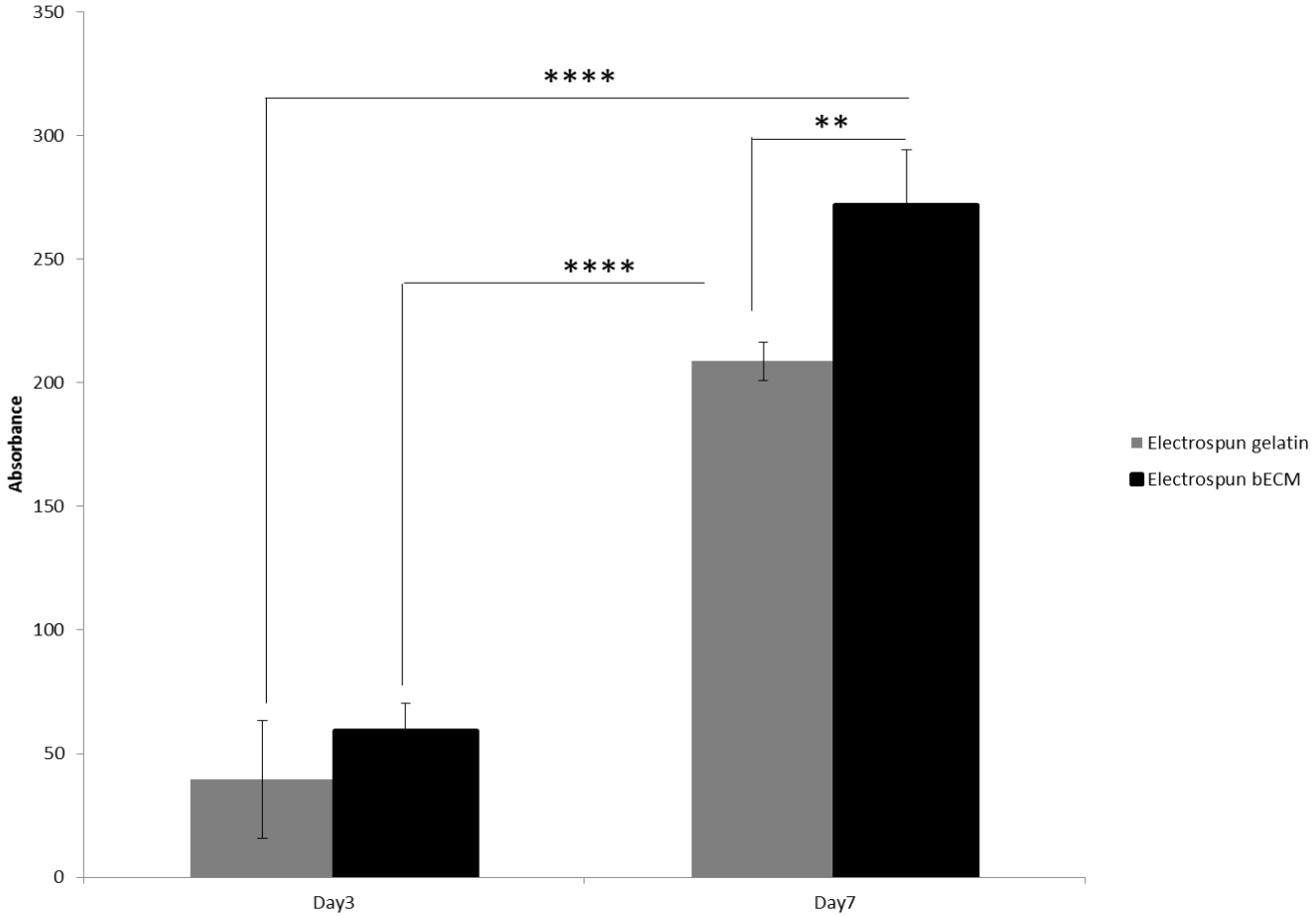



**Figure 39:** Proliferation of hMSCs on electrospun gelatin and electrospun bECM after 3 and 7 days.

### 5.3.4 Von Kossa staining

Mineralisation was assessed by von Kossa staining after 21 days of mPCs culture on tissue culture plate (TCP) and spun bECM with basal and osteogenic media. All samples exhibited positive staining when treated with osteogenic medium (Figure 40A & C). However, mineral deposition represented with black colour was only observed in cells cultured on spun bECM when treated with basal medium (Figure 40B & D).

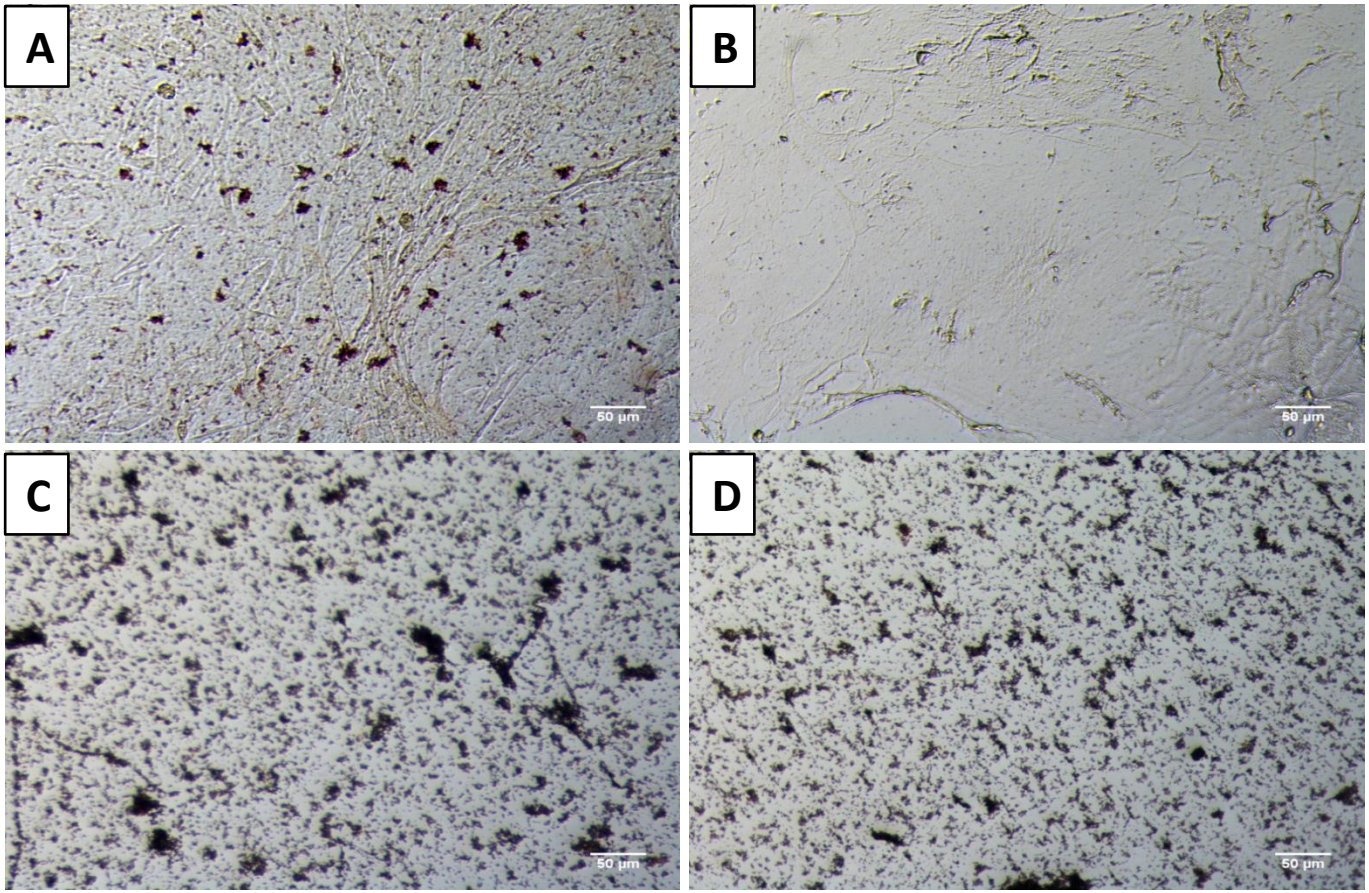



**Figure 40:** Von Kossa staining of mPCs cultured on tissue culture plate (TCP) (A & B) and electrospun bECM (C & D), with osteogenic medium (A & C ), and basal medium (B and D). Black colour indicates mineral deposition. Scale bar: 50µm.

### 5.3.5 Expression of osteogenic proteins in mPCs and hMSCs

Osteocalcin and osteopontin expression in mPCs cultured on electrospun bECM was assessed by immunocytochemistry on day 21, staining of expressed ECM proteins OPN and OCN were observed in all cells cultured on spun bECM with basal and osteogenic medium (Figure 41).

Similar results were observed with hMSCs when cultured on spun bECM, OCN was expressed in all samples with basal and osteogenic medium (Figure 42A & E). However, staining of expressed OCN was only observed in hMSCs cultured on electrospun gelatin when treated with osteogenic medium (Figure 42C & G).

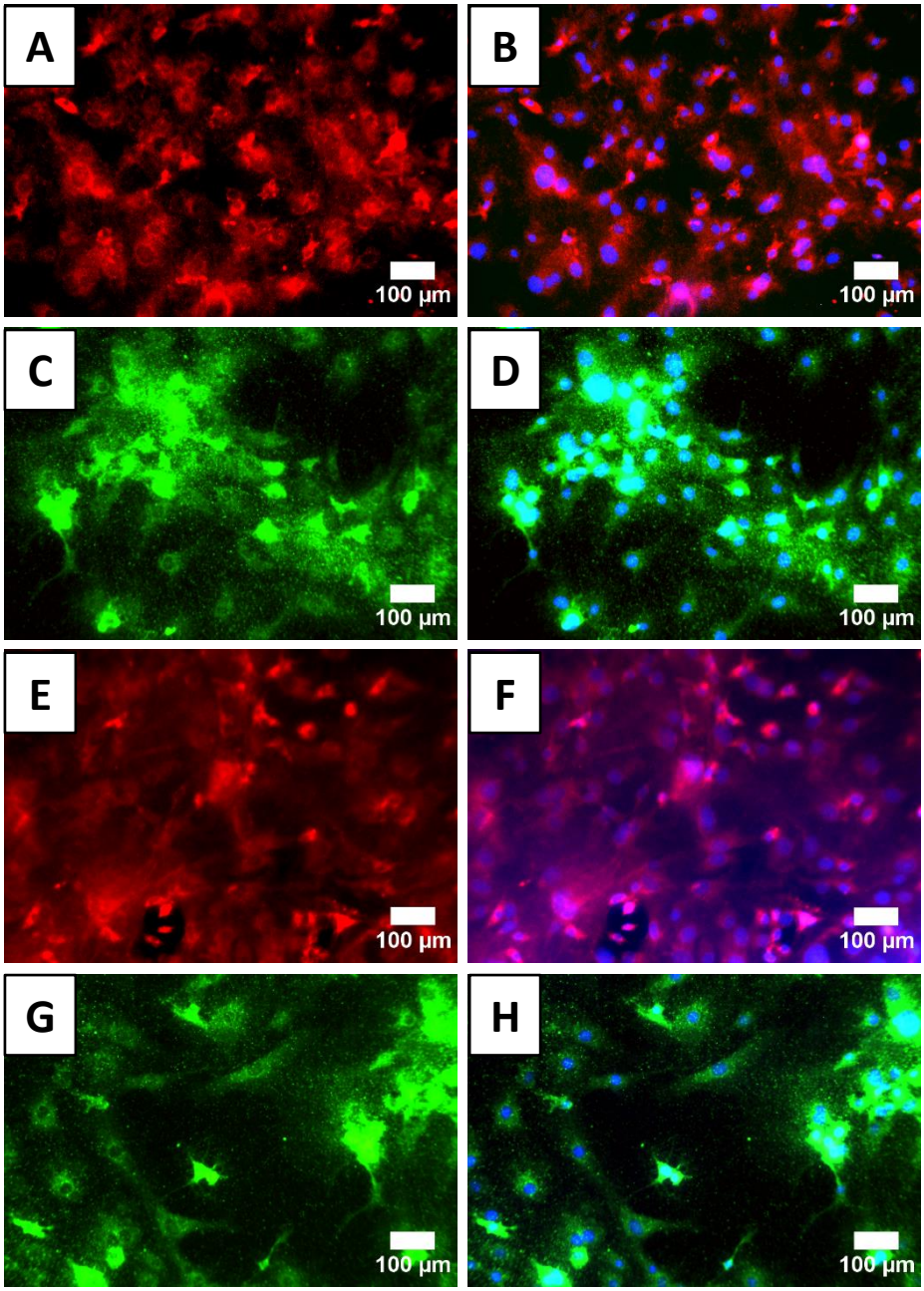



**Figure 41:** Expression of osteopontin (A & E) and osteocalcin (C & G) in mPCs cultured on electrospun bECM with osteogenic medium (A & C) and basal medium (E & G). Merge image shows OPN and OCN with Hoechst nuclear staining (B, D, F & H).

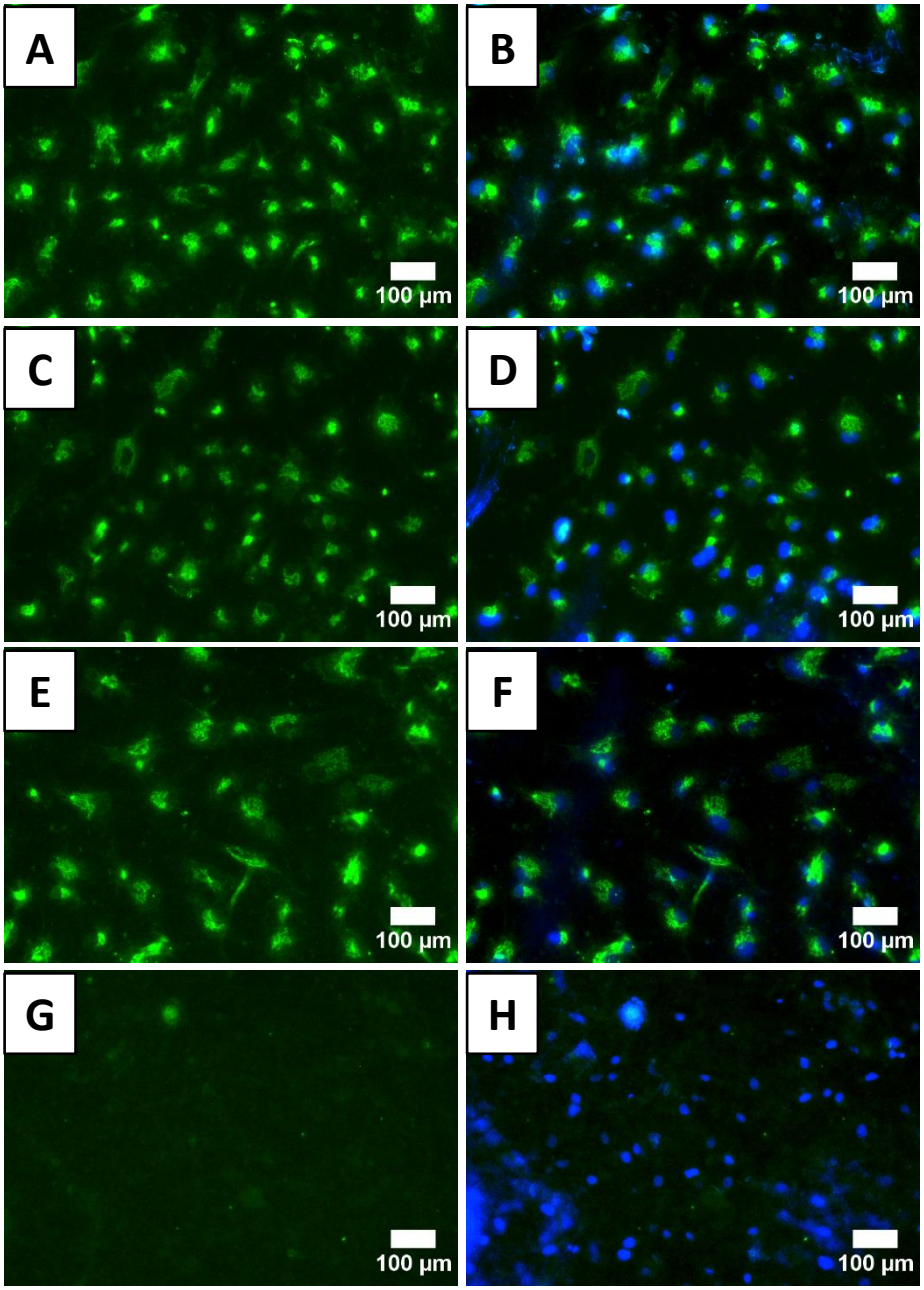



**Figure 42:** Expression of osteocalcin in hMSCs cultured on electrospun bECM (A & E) and electrospun gelatin (C & G) with osteogenic medium (A & C) and basal medium (E & G). Merge image shows OPN and OCN with Hoechst nuclear staining (B, D, F & H).

### 5.3.6 mRNA expression of osteogenic markers

Osteogenesis was further evaluated by RT-qPCR analysis for expression of four genes: osteopontin (OPN), osteocalcin (OCN), runt related transcription factor 2 (RUNX-2) and alkaline phosphatase (ALP). hMSCs were cultured for 21 days on electrospun bECM and electrospun gelatin in osteogenic and basal media.

Figure 43 shows the expression of the four genes is upregulated in all cultures treated with osteogenic medium, but this expression was highest in hMSCs seeded onto spun bECM with osteogenic medium. Moreover, there was significant differences in the four genes expression between hMSCs cultured on spun bECM compared to spun bECM when treated with basal medium.

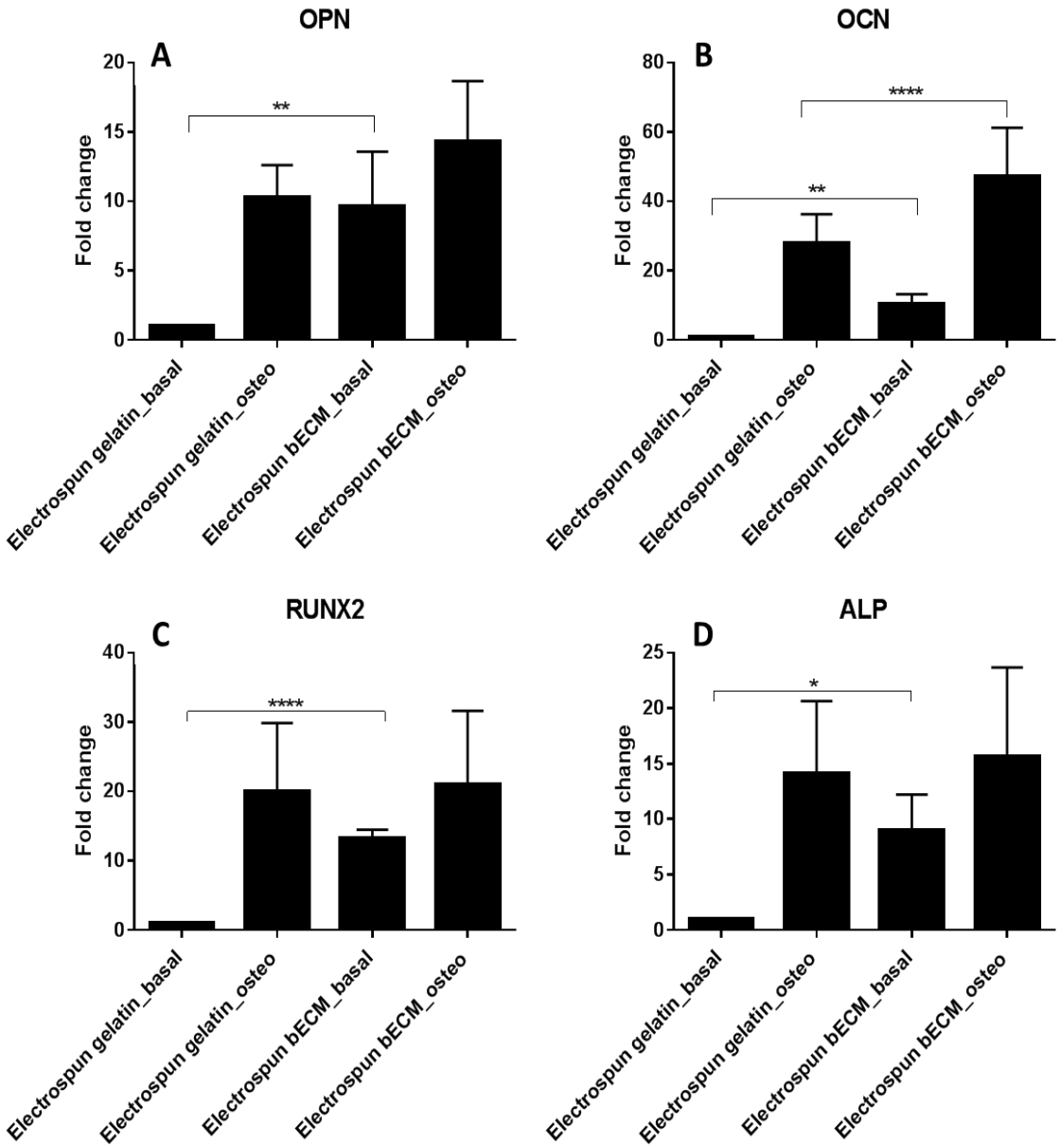



**Figure 43:** RT-qPCR of osteogenic markers OPN (A), OCN (B), RUNX2 (C), and ALP (D) expression in hMSCs seeded onto electrospun gelatin and electrospun bECM cultured in basal and osteogenic medium. Expression of each target gene normalised to β-actin. Data shown is mean±SD of 3 independent experiments (n=3). Statistical significance of expression **** indicates $p<0.0001$; *** indicates $p<0.001$; ** indicates $p<0.01$; and * indicates $p<0.05$

## 5.4 Discussion

Biomaterials derived from decellularized ECM contain complex cues that influence cellular activity. These materials retain the biological and architectural features that highly bioactive. This bioactivity cannot be imitated by adding biomolecules to synthetic scaffolds because it is almost impossible to replicate the exact biomolecules and their concentration contained in ECM [112, 274-276]. The major limitation with decellularized ECM associated with difficulties to control shape and physical properties.

On the other hand, electrospinning process has been widely used as a technique to produce nanofibrous scaffolds mimicking ECM structure, number of materials have been electrospun to fabricate scaffolds for applications in a variety of tissue engineering such as: bone [277], tendon [278], and cartilage [279].

To address the limitations associated with decellularized ECM, we electrospun these materials to improve porosity and handling and presented them within a platform that allows a control over ECM material properties.

The aim of this chapter was the evaluation of electrospinning decellularized bone ECM, to obtain highly porous nanofibrous scaffolds that support mouse PCs and human MSCs adhesion, proliferation and osteogenic differentiation.

The choice of solvent plays a crucial role in the electrospinning process, it should be able to dissolve the polymer into solution and carry it towards the collector, then to vaporize quickly to leave the polymer fibers. No study has been reported yet that electrospin decellularized bone ECM. Therefore, number of solvents has been screened to find the appropriate solvent to dissolve bECM and form a solution suitable for electrospinning.

Several parameters can influence the morphology of the collected fibers, like the voltage applied, solvent, air gap distance and flow rate [280, 281]. Volatile solvents such as chloroform or 1, 1, 1, 3, 3, 3-Hexafluoro-2-propanol were appropriate solvents for electrospinning natural and synthetic polymers [282-284].

Collagen type I is the most abundant protein in bone ECM [101, 285]. Therefore, we were interested in solvents used previously to dissolve collagen type I. HFP partially dissolved bECM powder and produced an appropriate solution for electrospinning bECM after filtering the solution. However, the protein component of bone ECM after the decellularization process is yet unknown and the undissolved granules could contain essential proteins for bone ECM (Figure 31A & B).

Though bECM granules could be dissolved in TFA solvent, the resultant solution could not be fabricated by electrospinning into nanofibers, only beads and drops were formed on the collector (Figure 31C & D).

DCM/TFA mixture with the volume ratio of 50/50 also dissolved bECM powder and produced better solution for electrospinning. However, beads formation on the collector remain a problem with this solvent (Figure 31E & F). The addition of TFA to HFP with the volume ratio of 50/50 improved bECM solubility and formed a solution suitable for electrospinning (Figure 31G & H).

The solution of bECM in HFP/TFA with different concentration and volume ratio of the solvent were electrospun. It was found that the nanofibers were obtained with no beads and drops, and showed typical fiber morphology under SEM when the concentration of bECM used was 55mg/ml with 50/50 volume ratio of HFP/TFA Figure 32.

The electrospun bECM scaffolds were water soluble. Therefore, the nanofibrous scaffolds were crosslinked using EDC/NHS in in ethanol/water (90% v/v) Figure 33.

The fibrous, beads free structure was retained after the crosslinking, the mean diameter of the electrospun bECM before and after electrospinning was measured from SEM micrographs, which was decreased slightly after crosslinking process (Figure 34), which is a common result previously discussed [286].

Gelatin Type A also processed uniform fibers that retained after crosslinking and it showed similar results in terms of the decrease of fiber diameter after crosslinking process as showed in Figure 35, Figure 36, and Figure 37.

Our results showed that seeding mPCs and hMSCs into electrospun bECM scaffolds was successful after *in vitro* culturing (Figure 38 and Figure 39), suggesting that the decellularization and electrospinning process preserved ECM structural component and did not remove or damage cellular binding sites crucial for cell adhesion and proliferation, which explains the significant increase in hMSCs proliferation on spun bECM compared to spun gelatin Figure 39.

We discussed in the first chapter the osteoinductive activity of bECM hydrogels, and we focused in this chapter in presenting bone ECM in new application while retaining their osteogenic potential.

Mineralisation and nodule formation was assessed with Von Kossa staining in mPCs cultured on spun bECM; results showed electrospun bECM induced osteogenic differentiation in without the enhancement of osteogenic medium compared to mPCs cultured on TCP Figure 40.

These results were further supported with immunocytochemistry staining for osteogenic proteins osteocalcin (OCN) and osteopontin (OPN), which were expressed in mPCs seeded into spun bECM with both basal and osteogenic media.

hMSCs showed similar results when cultured on spun bECM, osteocalcin was expressed in all cells. However, hMSCs seeded into spun gelatin only expressed osteogenic protein osteocalcin when induced with osteogenic medium (Figure 41 and Figure 42).

qPCR analysis revealed enhanced osteogenesis of hMSCs cultured on spun bECM based on the expression of four osteogenic gene markers: ALP, RUNX2, OPN and OCN compared to hMSCs cultured on spun gelatin (Figure 43).

Our findings show that decellularized bovine bone extracellular matrix retained the osteogenic potential upon electrospinning, electrospun bECM scaffolds supported the attachment, proliferation, and osteogenic differentiation of two cell types: mPCs and hMSCs. These results open up opportunities to use decellularized bone ECM in new and wider range of clinical application, consequently enhance their contribution toward bone regeneration and repair.

# Chapter 6. Summary and Future Direction

Tendon-to-bone entheses allow proper transmission of forces from muscle to bone in the musculoskeletal system. Although injuries to the tendon-to-bone interface are very common in the orthopaedic field, their repair is often associated with high failure rates. Reconstruction of entheses, with the four zones of soft tendon tissue, fibrocartilage, mineralized fibrocartilage, and hard bone tissue is essential to restore the original strength of the insertion site. Therefore, enthesis regeneration represent a great challenge in the orthopaedic field.

Tissue engineering provides an attractive platform for tendon-to-bone interface regeneration; it offers number of strategies to recapitulate the structural and cellular heterogeneity of the native tissue. Current clinical techniques used for enthesis repair, such as bridging and grafting, had high failure rate due to poor integration between the graft and the insertion site. Therefore, replicating the native biological, structural, and mechanical features of the tendon-to-bone interface is believed to be the ideal technique for designing tissue-engineered scaffold for enthesis repair. Development and investigation of scaffolds with multiple phases that direct MSCs differentiation, is needed to design a construct with multiple zones, multiple cell types, and consequently multiple mechanical properties to functionally restore the structural, cellular, and mechanical properties of the enthesis in order to improve the repair of this complex and unique interface site.

The aim of this work was to address the limitation associated with current available strategies for tendon-to-bone interface tissue engineering, by designing a gradient hydrogel bioscaffold with different conditions to induce mesenchymal stem cells (MSCs) differentiation into multiple interface-specific lineages.

The first experimental chapter of this project focused on investigating the osteoinductive activity of demineralized and decellularized bone extracellular matrix, they were solubilized and induced to form a hydrogel. C2C12 myoblasts cultured on bECM in the presence of low and rich serum mediums appeared to be converted the differentiation pathway into osteoblast lineage compared to C2C12 cells cultured on collagen type I. Exposure to DBM and bECM hydrogels promoted mPCs osteogenic differentiation *in vitro* compared to cells cultured on collagen type I.

The second experimental chapter focused on producing hydrogel derived from equine tendon ECM, to get the two forms of hydrogels essential for the gradient bioscaffold. Tendon ECM was decellularized, solubilized and induced to form a hydrogel, with distinct structural and biological proprieties, tECM enhanced hMSCs attachment, proliferation and tenogenic differentiation. tECM and bECM induced hMSCs differentiation into multiple interface-specific lineage (tendon and bone).

The third experimental chapter focused on optimising a method to electrospin bone ECM, to enable control of material properties. Electrospun bECM scaffolds have shown to retain the osteogenic potential upon electrospinning, and they supported the attachment, proliferation, and osteogenic differentiation of two cell types: mPCs and hMSCs.

The findings of this work demonstrated the ability of bECM, tECM hydrogels and electrospun bECM to influence hMSCs osteogenic and tenogenic differentiation without the additional of biological factors, making these materials promising bioactive scaffolds for use in tendon-to-bone interface tissue engineering applications. Together these data provide all the elements needed to design a gradient hydrogel scaffold for tendon-to- bone interface tissue engineering.

## 6.1 Future direction

Previous studies on tendon-to-bone insertion site have demonstrated the graded structure of these entheses, and its importance in the joint mobilization [30, 287]. However, the gradation in properties at repaired entheses was not established in most animal studies [32, 33, 288]. The most promising methods used in entheses repair are the use of extracellular matrix (ECM) derived materials as a scaffold [289, 290]. Our research aimed to apply the positive effect of the ECM scaffolds at the insertion site, to develop a gradient tECM/bECM hydrogel scaffold; it is likely that gradations in ECM hydrogel promote gradations in cell differentiation and tissue remodelling, which would provide a possibility to develop a material-regulated cell behaviour.

We also aim to develop a method to electrospin tendon extracellular matrix (tECM) with aligned fibers, previous studies have shown that aligned electrospun polymer scaffolds demonstrate better tenogenic effect compared to non-aligned scaffolds [94, 223, 291]. Further aim is to produce an aligned-to-random electrospun scaffolds, aligned fibers with tendon ECM and randomly oriented fibers with bone ECM to mimic the structural and compositional organization at the tendon-to-bone insertion site.

Promising experimental data support the concept of using graded materials for tendon-to-bone insertion repair [97, 99]. The final aim of this work is to design multi-phased bioscaffold, with aligned-to-random electrospun nanofibrous scaffold, coated with gradient concentration of bone and tendon ECM hydrogels and seeded with human mesenchymal stem cells.

We propose that the aligned-to-random nanofibrous structure of the scaffold, together with the gradation in the tECM/bECM hydrogels could promote graded stem cell lineage differentiation into tenogenic, chondrogenic, and osteogenic lineages respectively, and as a result, enhance the regeneration and mechanical properties of the four distinct zones of the interface tissue.

Overall, this multi-phased scaffold could be a great development for the future engineering of tendon-to-bone insertions sites.

## References


1. Thomopoulos, S., *The role of mechanobiology in the attachment of tendon to bone.* IBMS BoneKEy, 2011. **8**(6): p. 271-285.
2. Wolf, M.T., et al., *Naturally derived and synthetic scaffolds for skeletal muscle reconstruction.* Advanced drug delivery reviews, 2015. **84**: p. 208-221.
3. Cooper, J.O., et al., *Co-cultured tissue-specific scaffolds for tendon/bone interface engineering.* Journal of tissue engineering, 2014. **5**: p. 2041731414542294.
4. Viola, J., B. Lal, and O. Grad, *The emergence of tissue engineering as a research field.* National Science Foundation, Arlington, VA, 2003.
5. Stock, U.A. and J.P. Vacanti, *Tissue engineering: current state and prospects.* Annual review of medicine, 2001. **52**(1): p. 443-451.
6. Langer, R. and J.P. Vacanti, *Tissue engineering.* Science, 1993. **260**(5110): p. 920-926.
7. Mason, C. and P. Dunnill, *A brief definition of regenerative medicine.* 2008.
8. Merrill, J.P., et al., *Successful homotransplantation of the kidney in an identical twin.* Transactions of the American Clinical and Climatological Association, 1956. **67**: p. 166.
9. Vacanti, C.A., *History of tissue engineering and a glimpse into its future.* Tissue engineering, 2006. **12**(5): p. 1137-1142.
10. Lu, H.H. and S. Thomopoulos, *Functional attachment of soft tissues to bone: development, healing, and tissue engineering.* Annual review of biomedical engineering, 2013. **15**: p. 201.
11. Thomopoulos, S., V. Birman, and G.M. Genin, *Structural interfaces and attachments in biology*. 2012: Springer Science & Business Media.
12. Doschak, M. and R. Zernicke, *Structure, function and adaptation of bone-tendon and bone-ligament complexes.* J Musculoskelet Neuronal Interact, 2005. **5**(1): p. 35-40.
13. Benjamin, M., et al., *The skeletal attachment of tendons—tendon 'entheses'.* Comparative Biochemistry and Physiology Part A: Molecular & Integrative Physiology, 2002. **133**(4): p. 931-945.

14. Hems, T. and B. Tillmann, *Tendon entheses of the human masticatory muscles.* Anatomy and Embryology, 2000. **202**(3): p. 201-208.
15. Benjamin, M. and J. Ralphs, *Fibrocartilage in tendons and ligaments—an adaptation to compressive load.* Journal of anatomy, 1998. **193**(04): p. 481-494.
16. Benjamin, M. and D. McGonagle, *Entheses: tendon and ligament attachment sites.* Scandinavian journal of medicine & science in sports, 2009. **19**(4): p. 520-527.
17. Yang, P.J. and J.S. Temenoff, *Engineering orthopedic tissue interfaces.* Tissue Engineering Part B: Reviews, 2009. **15**(2): p. 127-141.
18. Angeline, M.E. and S.A. Rodeo, *Biologics in the management of rotator cuff surgery.* Clinics in sports medicine, 2012. **31**(4): p. 645-663.
19. Shaw, H. and M. Benjamin, *Structure–function relationships of entheses in relation to mechanical load and exercise.* Scandinavian journal of medicine & science in sports, 2007. **17**(4): p. 303-315.
20. Smith, L., et al., *Tissue-engineering strategies for the tendon/ligament-to-bone insertion.* Connective tissue research, 2012. **53**(2): p. 95-105.
21. Padulo, J., et al., *Muscle, Ligaments and Tendons Journal. Basic principles and recommendations in clinical and field science research.* MLTJ Muscles, Ligaments and Tendons Journal, 2013. **3**(4): p. 250-252.
22. Benjamin, M. and J. Ralphs, *Entheses--the bony attachments of tendons and ligaments.* Italian journal of anatomy and embryology= Archivio italiano di anatomia ed embriologia, 2000. **106**(2 Suppl 1): p. 151-157.
23. Lu, H.H., et al., *Tissue engineering strategies for the regeneration of orthopedic interfaces.* Annals of biomedical engineering, 2010. **38**(6): p. 2142-2154.
24. Juneja, S.C. and C. Veillette, *Defects in tendon, ligament, and enthesis in response to genetic alterations in key proteoglycans and glycoproteins: a review.* Arthritis, 2013. **2013**.
25. Fujioka, H., et al., *Comparison of surgically attached and non-attached repair of the rat Achilles tendon-bone interface. Cellular organization and type X collagen expression.* Connective tissue research, 1998. **37**(3-4): p. 205-218.

26. Thomopoulos, S., G.M. Genin, and L.M. Galatz, *The development and morphogenesis of the tendon-to-bone insertion What development can teach us about healing.* Journal of musculoskeletal & neuronal interactions, 2010. **10**(1): p. 35.
27. Schweitzer, R., et al., *Analysis of the tendon cell fate using Scleraxis, a specific marker for tendons and ligaments.* Development, 2001. **128**(19): p. 3855-3866.
28. Kim, H.M., et al., *Recovery potential after postnatal shoulder paralysis.* J Bone Joint Surg Am, 2009. **91**(4): p. 879-891.
29. Genin, G.M., et al., *Functional grading of mineral and collagen in the attachment of tendon to bone.* Biophysical journal, 2009. **97**(4): p. 976-985.
30. Thomopoulos, S., et al., *Variation of biomechanical, structural, and compositional properties along the tendon to bone insertion site.* Journal of Orthopaedic Research, 2003. **21**(3): p. 413-419.
31. Carpenter, J.E. and K.D. Hankenson, *Animal models of tendon and ligament injuries for tissue engineering applications.* Biomaterials, 2004. **25**(9): p. 1715-1722.
32. Galatz, L.M., et al., *Characteristics of the rat supraspinatus tendon during tendon-to-bone healing after acute injury.* Journal of orthopaedic research, 2006. **24**(3): p. 541-550.
33. Thomopoulos, S., et al., *The localized expression of extracellular matrix components in healing tendon insertion sites: an in situ hybridization study.* Journal of orthopaedic research, 2002. **20**(3): p. 454-463.
34. Aune, A.K., et al., *Nerve regeneration during patellar tendon autograft remodelling after anterior cruciate ligament reconstruction: an experimental and clinical study.* Journal of orthopaedic research, 1996. **14**(2): p. 193-199.
35. Gulotta, L.V. and S.A. Rodeo, *Growth factors for rotator cuff repair.* Clinics in sports medicine, 2009. **28**(1): p. 13-23.
36. Wen, C.-Y., et al., *Grafted tendon healing in tibial tunnel is inferior to healing in femoral tunnel after anterior cruciate ligament reconstruction: a histomorphometric study in rabbits.* Arthroscopy: The Journal of Arthroscopic & Related Surgery, 2010. **26**(1): p. 58-66.
37. Deehan, D. and T. Cawston, *The biology of integration of the anterior cruciate ligament.* Bone & Joint Journal, 2005. **87**(7): p. 889-895.

38. Carofino, B. and J. Fulkerson, *Medial hamstring tendon regeneration following harvest for anterior cruciate ligament reconstruction: fact, myth, and clinical implication.* Arthroscopy: The Journal of Arthroscopic & Related Surgery, 2005. **21**(10): p. 1257-1265.
39. Edwards, S.L., et al., *Biologic and pharmacologic augmentation of rotator cuff repairs.* Journal of the American Academy of Orthopaedic Surgeons, 2011. **19**(10): p. 583-589.
40. Gulotta, L.V., et al., *Application of bone marrow-derived mesenchymal stem cells in a rotator cuff repair model.* The American journal of sports medicine, 2009. **37**(11): p. 2126-2133.
41. Gulotta, L.V., et al., *Bone marrow–derived mesenchymal stem cells transduced with scleraxis improve rotator cuff healing in a rat model.* The American journal of sports medicine, 2011. **39**(6): p. 1282-1289.
42. Robbe, R. and D.L. Johnson, *Graft fixation alternatives in anterior cruciate ligament reconstruction.* Univ Pa Orthop J, 2002. **15**: p. 21-27.
43. Butler, D.L., S.A. Goldstein, and F. Guilak, *Functional tissue engineering: the role of biomechanics.* Journal of biomechanical engineering, 2000. **122**(6): p. 570-575.
44. Smith, M.A. and W.T. Smith, *Rotator cuff tears: an overview.* Orthopaedic nursing, 2010. **29**(5): p. 319-322.
45. Clark, J. and D.n. Harryman, *Tendons, ligaments, and capsule of the rotator cuff. Gross and microscopic anatomy.* J Bone Joint Surg Am, 1992. **74**(5): p. 713-725.
46. Blevins, F.T., et al., *Biology of the rotator cuff tendon.* Orthopedic Clinics of North America, 1997. **28**(1): p. 1-16.
47. Matyas, J., et al., *Stress governs tissue phenotype at the femoral insertion of the rabbit MCL.* Journal of biomechanics, 1995. **28**(2): p. 147-157.
48. Ghodadra, N.S., et al., *Open, mini-open, and all-arthroscopic rotator cuff repair surgery: indications and implications for rehabilitation.* journal of orthopaedic & sports physical therapy, 2009. **39**(2): p. 81-A6.
49. Freemont, A.J. and J. Hoyland, *Lineage plasticity and cell biology of fibrocartilage and hyaline cartilage: its significance in cartilage repair and replacement.* European journal of radiology, 2006. **57**(1): p. 32-36.

50. Iwakura, T., R. Sakata, and A.H. Reddi, *Induction of chondrogenesis and expression of superficial zone protein in synovial explants with TGF-β1 and BMP-7.* Tissue Engineering Part A, 2013. **19**(23-24): p. 2638-2644.
51. Petrou, M., et al., *Mesenchymal stem cell chondrogenesis: composite growth factor–bioreactor synergism for human stem cell chondrogenesis.* Regenerative medicine, 2013. **8**(2): p. 157-170.
52. Cicione, C., et al., *Alternative protocols to induce chondrogenic differentiation: transforming growth factor-β superfamily.* Cell and tissue banking, 2015. **16**(2): p. 195-207.
53. Brady, K., et al., *Human fetal and adult bone marrow-derived mesenchymal stem cells use different signaling pathways for the initiation of chondrogenesis.* Stem cells and development, 2013. **23**(5): p. 541-554.
54. Demoor, M., et al., *Cartilage tissue engineering: molecular control of chondrocyte differentiation for proper cartilage matrix reconstruction.* Biochimica et Biophysica Acta (BBA)-General Subjects, 2014. **1840**(8): p. 2414-2440.
55. Hashimoto, Y., et al., *Generation of tendon-to-bone interface "enthesis" with use of recombinant BMP-2 in a rabbit model.* Journal of Orthopaedic Research, 2007. **25**(11): p. 1415-1424.
56. Seeherman, H.J., et al., *rhBMP-12 accelerates healing of rotator cuff repairs in a sheep model.* J Bone Joint Surg Am, 2008. **90**(10): p. 2206-2219.
57. Sasaki, K., et al., *Enhancement of tendon-bone osteointegration of anterior cruciate ligament graft using granulocyte colony-stimulating factor.* The American journal of sports medicine, 2008. **36**(8): p. 1519-1527.
58. Manning, C.N., et al., *Sustained delivery of transforming growth factor beta three enhances tendon-to-bone healing in a rat model.* Journal of Orthopaedic Research, 2011. **29**(7): p. 1099-1105.
59. Ide, J., et al., *The effects of fibroblast growth factor-2 on rotator cuff reconstruction with acellular dermal matrix grafts.* Arthroscopy: The Journal of Arthroscopic & Related Surgery, 2009. **25**(6): p. 608-616.
60. O'brien, F.J., *Biomaterials & scaffolds for tissue engineering.* Materials today, 2011. **14**(3): p. 88-95.

61. Wang, I.N.E., et al., *Role of osteoblast–fibroblast interactions in the formation of the ligament-to-bone interface.* Journal of Orthopaedic Research, 2007. **25**(12): p. 1609-1620.
62. Rothrauff, B.B. and R.S. Tuan, *Cellular therapy in bone-tendon interface regeneration.* Organogenesis, 2014. **10**(1): p. 13-28.
63. Soon, M.Y., et al., *An analysis of soft tissue allograft anterior cruciate ligament reconstruction in a rabbit model a short-term study of the use of mesenchymal stem cells to enhance tendon osteointegration.* The American journal of sports medicine, 2007. **35**(6): p. 962-971.
64. Nourissat, G., et al., *Mesenchymal stem cell therapy regenerates the native bone-tendon junction after surgical repair in a degenerative rat model.* PloS one, 2010. **5**(8): p. e12248.
65. Gulotta, L.V., et al., *Stem cells genetically modified with the developmental gene MT1-MMP improve regeneration of the supraspinatus tendon-to-bone insertion site.* The American journal of sports medicine, 2010. **38**(7): p. 1429-1437.
66. James, R., et al., *Tendon tissue engineering: adipose-derived stem cell and GDF-5 mediated regeneration using electrospun matrix systems.* Biomedical Materials, 2011. **6**(2): p. 025011.
67. Raabe, O., et al., *Tenogenic differentiation of equine adipose-tissue-derived stem cells under the influence of tensile strain, growth differentiation factors and various oxygen tensions.* Cell and tissue research, 2013. **352**(3): p. 509-521.
68. Little, D., F. Guilak, and D.S. Ruch, *Ligament-derived matrix stimulates a ligamentous phenotype in human adipose-derived stem cells.* Tissue Engineering Part A, 2010. **16**(7): p. 2307-2319.
69. Wei, Y., et al., *Cartilage regeneration of adipose-derived stem cells in a hybrid scaffold from fibrin-modified PLGA.* Cell transplantation, 2009. **18**(2): p. 159-170.
70. Yoon, H.H., et al., *Enhanced cartilage formation via three-dimensional cell engineering of human adipose-derived stem cells.* Tissue Engineering Part A, 2012. **18**(19-20): p. 1949-1956.
71. Hutton, D.L., et al., *Platelet-derived growth factor and spatiotemporal cues induce development of vascularized bone tissue by adipose-derived stem cells.* Tissue Engineering Part A, 2013. **19**(17-18): p. 2076-2086.

72. Rodrigues, A., et al., *Bioactive starch-based scaffolds and human adipose stem cells are a good combination for bone tissue engineering.* Acta biomaterialia, 2012. **8**(10): p. 3765-3776.
73. Ding, X., et al., *Integrated trilayered silk fibroin scaffold for osteochondral differentiation of adipose-derived stem cells.* ACS applied materials & interfaces, 2014. **6**(19): p. 16696-16705.
74. Erisken, C., et al., *Osteochondral tissue formation through adipose-derived stromal cell differentiation on biomimetic polycaprolactone nanofibrous scaffolds with graded insulin and beta-glycerophosphate concentrations.* Tissue Engineering Part A, 2011. **17**(9-10): p. 1239-1252.
75. Min, H.K., et al., *Porous membrane with reverse gradients of PDGF-BB and BMP-2 for tendon-to-bone repair: in vitro evaluation on adipose-derived stem cell differentiation.* Acta biomaterialia, 2014. **10**(3): p. 1272-1279.
76. Sulaiman, S.B., et al., *Tricalcium phosphate/hydroxyapatite (TCP-HA) bone scaffold as potential candidate for the formation of tissue engineered bone.* The Indian journal of medical research, 2013. **137**(6): p. 1093.
77. Sumanasinghe, R.D., S.H. Bernacki, and E.G. Loboa, *Osteogenic differentiation of human mesenchymal stem cells in collagen matrices: effect of uniaxial cyclic tensile strain on bone morphogenetic protein (BMP-2) mRNA expression.* Tissue engineering, 2006. **12**(12): p. 3459-3465.
78. Long, T., et al., *Fabrication of three-dimensional porous scaffold based on collagen fiber and bioglass for bone tissue engineering.* Journal of Biomedical Materials Research Part B: Applied Biomaterials, 2015. **103**(7): p. 1455-1464.
79. Daei-farshbaf, N., et al., *Bioceramic-collagen scaffolds loaded with human adipose-tissue derived stem cells for bone tissue engineering.* Molecular biology reports, 2014. **41**(2): p. 741-749.
80. Valente, J., et al., *Alginate based scaffolds for bone tissue engineering.* Materials Science and Engineering: C, 2012. **32**(8): p. 2596-2603.
81. Sawkins, M., et al., *Hydrogels derived from demineralized and decellularized bone extracellular matrix.* Acta biomaterialia, 2013. **9**(8): p. 7865-7873.

82. Jose, M.V., et al., *Aligned PLGA/HA nanofibrous nanocomposite scaffolds for bone tissue engineering.* Acta biomaterialia, 2009. **5**(1): p. 305-315.
83. Kim, S.-S., et al., *Poly (lactide-co-glycolide)/hydroxyapatite composite scaffolds for bone tissue engineering.* Biomaterials, 2006. **27**(8): p. 1399-1409.
84. Chen, X., et al., *Scleraxis-overexpressed human embryonic stem cell–derived mesenchymal stem cells for tendon tissue engineering with knitted silk-collagen scaffold.* Tissue Engineering Part A, 2014. **20**(11-12): p. 1583-1592.
85. Kwon, S.-Y., et al., *Silk and collagen scaffolds for tendon reconstruction.* Proceedings of the Institution of Mechanical Engineers, Part H: Journal of Engineering in Medicine, 2014: p. 0954411914528890.
86. Inui, A., et al., *Potency of double-layered Poly L-lactic Acid scaffold in tissue engineering of tendon tissue.* International orthopaedics, 2010. **34**(8): p. 1327-1332.
87. Schulze-Tanzil, G., et al., *Decellularized tendon extracellular matrix—a valuable approach for tendon reconstruction?* Cells, 2012. **1**(4): p. 1010-1028.
88. Yang, G., et al., *Enhancement of tenogenic differentiation of human adipose stem cells by tendon-derived extracellular matrix.* Biomaterials, 2013. **34**(37): p. 9295-9306.
89. Gimbel, J.A., et al., *The tension required at repair to reappose the supraspinatus tendon to bone rapidly increases after injury.* Clinical orthopaedics and related research, 2004. **426**: p. 258-265.
90. Gimbel, J.A., et al., *The role of repair tension on tendon to bone healing in an animal model of chronic rotator cuff tears.* Journal of biomechanics, 2007. **40**(3): p. 561-568.
91. Omi, R., et al., *Rotator cuff repair augmentation in a rat model that combines a multilayer xenograft tendon scaffold with bone marrow stromal cells.* Journal of Shoulder and Elbow Surgery, 2016. **25**(3): p. 469-477.
92. Peterson, D.R., et al., *Evaluation of a collagen-coated, resorbable fiber scaffold loaded with a peptide basic fibroblast growth factor mimetic in a sheep model of rotator cuff repair.* Journal of Shoulder and Elbow Surgery, 2015. **24**(11): p. 1764-1773.
93. Xie, J., et al., *"Aligned-to-random" nanofiber scaffolds for mimicking the structure of the tendon-to-bone insertion site.* Nanoscale, 2010. **2**(6): p. 923-926.

94. Moffat, K.L., et al., *Novel nanofiber-based scaffold for rotator cuff repair and augmentation.* Tissue Engineering Part A, 2008. **15**(1): p. 115-126.
95. Ma, B., et al., *Rational design of nanofiber scaffolds for orthopedic tissue repair and regeneration.* Nanomedicine, 2013. **8**(9): p. 1459-1481.
96. Kolluru, P.V., et al., *Strong and tough mineralized PLGA nanofibers for tendon-to-bone scaffolds.* Acta biomaterialia, 2013. **9**(12): p. 9442-9450.
97. Soo Kim, B., et al., *Human collagen-based multilayer scaffolds for tendon-to-bone interface tissue engineering.* Journal of Biomedical Materials Research Part A, 2014. **102**(11): p. 4044-4054.
98. Sahoo, S., J.G. Cho-Hong, and T. Siew-Lok, *Development of hybrid polymer scaffolds for potential applications in ligament and tendon tissue engineering.* Biomedical materials, 2007. **2**(3): p. 169.
99. Li, X., et al., *Nanofiber scaffolds with gradations in mineral content for mimicking the tendon-to-bone insertion site.* Nano letters, 2009. **9**(7): p. 2763-2768.
100. Erisken, C., D.M. Kalyon, and H. Wang, *Functionally graded electrospun polycaprolactone and β-tricalcium phosphate nanocomposites for tissue engineering applications.* Biomaterials, 2008. **29**(30): p. 4065-4073.
101. Frantz, C., K.M. Stewart, and V.M. Weaver, *The extracellular matrix at a glance.* Journal of cell science, 2010. **123**(24): p. 4195-4200.
102. Badylak, S.F., *The extracellular matrix as a biologic scaffold material.* Biomaterials, 2007. **28**(25): p. 3587-3593.
103. Badylak, S.F., et al., *Engineered whole organs and complex tissues.* The Lancet, 2012. **379**(9819): p. 943-952.
104. Crapo, P.M., T.W. Gilbert, and S.F. Badylak, *An overview of tissue and whole organ decellularization processes.* Biomaterials, 2011. **32**(12): p. 3233-3243.
105. Keane, T.J., et al., *Consequences of ineffective decellularization of biologic scaffolds on the host response.* Biomaterials, 2012. **33**(6): p. 1771-1781.
106. Sellaro, T.L., et al., *Maintenance of human hepatocyte function in vitro by liver-derived extracellular matrix gels.* Tissue Engineering Part A, 2009. **16**(3): p. 1075-1082.

107. Reing, J.E., et al., *Degradation products of extracellular matrix affect cell migration and proliferation.* Tissue Engineering Part A, 2008. **15**(3): p. 605-614.
108. Brown, B.N., et al., *Macrophage phenotype as a predictor of constructive remodeling following the implantation of biologically derived surgical mesh materials.* Acta biomaterialia, 2012. **8**(3): p. 978-987.
109. Keane, T.J. and S.F. Badylak. *Biomaterials for tissue engineering applications*. in *Seminars in pediatric surgery*. 2014. Elsevier.
110. Hodde, J., et al., *Vascular endothelial growth factor in porcine-derived extracellular matrix.* Endothelium, 2001. **8**(1): p. 11-24.
111. Badylak, S.F., D.O. Freytes, and T.W. Gilbert, *Extracellular matrix as a biological scaffold material: structure and function.* Acta biomaterialia, 2009. **5**(1): p. 1-13.
112. Crapo, P.M., et al., *Biologic scaffolds composed of central nervous system extracellular matrix.* Biomaterials, 2012. **33**(13): p. 3539-3547.
113. Choi, J.S., et al., *Full-thickness skin wound healing using human placenta-derived extracellular matrix containing bioactive molecules.* Tissue Engineering Part A, 2012. **19**(3-4): p. 329-339.
114. Agrawal, V., et al., *An isolated cryptic peptide influences osteogenesis and bone remodeling in an adult mammalian model of digit amputation.* Tissue engineering Part A, 2011. **17**(23-24): p. 3033-3044.
115. Hoganson, D.M., et al., *Preserved extracellular matrix components and retained biological activity in decellularized porcine mesothelium.* Biomaterials, 2010. **31**(27): p. 6934-6940.
116. Xing, Q., et al., *Highly aligned nanofibrous scaffold derived from decellularized human fibroblasts.* Advanced functional materials, 2014. **24**(20): p. 3027-3035.
117. Gilbert, T.W., et al., *Production and characterization of ECM powder: implications for tissue engineering applications.* Biomaterials, 2005. **26**(12): p. 1431-1435.
118. Badylak, S.F., et al., *The use of xenogeneic small intestinal submucosa as a biomaterial for Achille's tendon repair in a dog model.* Journal of biomedical materials research, 1995. **29**(8): p. 977-985.

119. Badylak, S.F., et al., *Esophageal reconstruction with ECM and muscle tissue in a dog model.* Journal of Surgical Research, 2005. **128**(1): p. 87-97.
120. Schmidt, C.E. and J.M. Baier, *Acellular vascular tissues: natural biomaterials for tissue repair and tissue engineering.* Biomaterials, 2000. **21**(22): p. 2215-2231.
121. Ott, H.C., et al., *Regeneration and orthotopic transplantation of a bioartificial lung.* Nature medicine, 2010. **16**(8): p. 927-933.
122. Ott, H.C., et al., *Perfusion-decellularized matrix: using nature's platform to engineer a bioartificial heart.* Nature medicine, 2008. **14**(2): p. 213-221.
123. Uygun, B.E., et al., *Organ reengineering through development of a transplantable recellularized liver graft using decellularized liver matrix.* Nature medicine, 2010. **16**(7): p. 814-820.
124. Freytes, D.O., et al., *Preparation and rheological characterization of a gel form of the porcine urinary bladder matrix.* Biomaterials, 2008. **29**(11): p. 1630-1637.
125. Okada, M., et al., *Differential efficacy of gels derived from small intestinal submucosa as an injectable biomaterial for myocardial infarct repair.* Biomaterials, 2010. **31**(30): p. 7678-7683.
126. Medberry, C.J., et al., *Hydrogels derived from central nervous system extracellular matrix.* Biomaterials, 2013. **34**(4): p. 1033-1040.
127. Singelyn, J.M., et al., *Naturally derived myocardial matrix as an injectable scaffold for cardiac tissue engineering.* Biomaterials, 2009. **30**(29): p. 5409-5416.
128. Wolf, M.T., et al., *A hydrogel derived from decellularized dermal extracellular matrix.* Biomaterials, 2012. **33**(29): p. 7028-7038.
129. Gothard, D., et al., *In Vivo Assessment of Bone Regeneration in Alginate/Bone ECM Hydrogels with Incorporated Skeletal Stem Cells and Single Growth Factors.* PloS one, 2015. **10**(12): p. e0145080.
130. Smith, E., et al., *Evaluation of skeletal tissue repair, Part 1: Assessment of novel growth-factor-releasing hydrogels in an ex vivo chick femur defect model.* Acta biomaterialia, 2014. **10**(10): p. 4186-4196.
131. Smith, E., et al., *Evaluation of skeletal tissue repair, Part 2: Enhancement of skeletal tissue repair through dual-growth-*

*factor-releasing hydrogels within an ex vivo chick femur defect model.* Acta biomaterialia, 2014. **10**(10): p. 4197-4205.
132. Derwin, K.A., et al., *Extracellular matrix scaffold devices for rotator cuff repair.* Journal of shoulder and elbow surgery, 2010. **19**(3): p. 467-476.
133. Bond, J.L., et al., *Arthroscopic replacement of massive, irreparable rotator cuff tears using a GraftJacket allograft: technique and preliminary results.* Arthroscopy: The Journal of Arthroscopic & Related Surgery, 2008. **24**(4): p. 403. e1-403. e8.
134. Wong, I., J. Burns, and S. Snyder, *Arthroscopic GraftJacket repair of rotator cuff tears.* Journal of Shoulder and Elbow Surgery, 2010. **19**(2): p. 104-109.
135. Omae, H., et al., *Biomechanical effect of rotator cuff augmentation with an acellular dermal matrix graft: a cadaver study.* Clinical Biomechanics, 2012. **27**(8): p. 789-792.
136. Barber, F.A., M.A. Herbert, and D.A. Coons, *Tendon augmentation grafts: biomechanical failure loads and failure patterns.* Arthroscopy: The Journal of Arthroscopic & Related Surgery, 2006. **22**(5): p. 534-538.
137. Fisher, M.B., et al., *Potential of healing a transected anterior cruciate ligament with genetically modified extracellular matrix bioscaffolds in a goat model.* Knee Surgery, Sports Traumatology, Arthroscopy, 2012. **20**(7): p. 1357-1365.
138. Sclamberg, S.G., et al., *Six-month magnetic resonance imaging follow-up of large and massive rotator cuff repairs reinforced with porcine small intestinal submucosa.* Journal of shoulder and elbow surgery, 2004. **13**(5): p. 538-541.
139. Iannotti, J.P., et al., *Porcine small intestine submucosa augmentation of surgical repair of chronic two-tendon rotator cuff tears.* J Bone Joint Surg Am, 2006. **88**(6): p. 1238-1244.
140. Sidney, L.E., G.R. Kirkham, and L.D. Buttery, *Comparison of osteogenic differentiation of embryonic stem cells and primary osteoblasts revealed by responses to IL-1β, TNF-α, and IFN-γ.* Stem cells and development, 2013. **23**(6): p. 605-617.
141. Griffin, M., S. Iqbal, and A. Bayat, *Exploring the application of mesenchymal stem cells in bone repair and regeneration.*

Journal of Bone & Joint Surgery, British Volume, 2011. **93**(4): p. 427-434.
142. Khan, Y., et al., *Tissue engineering of bone: material and matrix considerations.* The Journal of Bone & Joint Surgery, 2008. **90**(Supplement 1): p. 36-42.
143. Nandi, S., et al., *Orthopaedic applications of bone graft & graft substitutes: a review.* Indian J Med Res, 2010. **132**(1): p. 15-30.
144. Lichtenberg, A., et al., *Biological scaffolds for heart valve tissue engineering*, in *Tissue Engineering*. 2007, Springer. p. 309-317.
145. Ingenito, E.P., et al., *Design and testing of biological scaffolds for delivering reparative cells to target sites in the lung.* Journal of tissue engineering and regenerative medicine, 2010. **4**(4): p. 259-272.
146. Schlie-Wolter, S., A. Ngezahayo, and B.N. Chichkov, *The selective role of ECM components on cell adhesion, morphology, proliferation and communication in vitro.* Experimental cell research, 2013. **319**(10): p. 1553-1561.
147. Sellaro, T.L., et al., *Maintenance of hepatic sinusoidal endothelial cell phenotype in vitro using organ-specific extracellular matrix scaffolds.* Tissue engineering, 2007. **13**(9): p. 2301-2310.
148. Zhang, Y., et al., *Tissue-specific extracellular matrix coatings for the promotion of cell proliferation and maintenance of cell phenotype.* Biomaterials, 2009. **30**(23): p. 4021-4028.
149. Moroni, F. and T. Mirabella, *Decellularized matrices for cardiovascular tissue engineering.* American journal of stem cells, 2014. **3**(1): p. 1.
150. Wong, D.A., et al., *Neurologic impairment from ectopic bone in the lumbar canal: a potential complication of off-label PLIF/TLIF use of bone morphogenetic protein-2 (BMP-2).* The Spine Journal, 2008. **8**(6): p. 1011-1018.
151. Kaneko, H., et al., *Direct stimulation of osteoclastic bone resorption by bone morphogenetic protein (BMP)-2 and expression of BMP receptors in mature osteoclasts.* Bone, 2000. **27**(4): p. 479-486.
152. Vaidya, R., et al., *Complications of anterior cervical discectomy and fusion using recombinant human bone morphogenetic protein-2.* European spine journal, 2007. **16**(8): p. 1257-1265.

153. Pietrzak, W.S., et al., *BMP depletion occurs during prolonged acid demineralization of bone: characterization and implications for graft preparation.* Cell and tissue banking, 2011. **12**(2): p. 81-88.
154. Schenke-Layland, K., et al., *Impact of decellularization of xenogeneic tissue on extracellular matrix integrity for tissue engineering of heart valves.* Journal of structural biology, 2003. **143**(3): p. 201-208.
155. Yang, X., et al., *Human osteoprogenitor growth and differentiation on synthetic biodegradable structures after surface modification.* Bone, 2001. **29**(6): p. 523-531.
156. Price, J., B. Oyajobi, and R. Russell, *The cell biology of bone growth.* European journal of clinical nutrition, 1994. **48**: p. S131-49.
157. Aubin, J.E., *Regulation of osteoblast formation and function.* Reviews in Endocrine and Metabolic Disorders, 2001. **2**(1): p. 81-94.
158. Granéli, C., et al., *Novel markers of osteogenic and adipogenic differentiation of human bone marrow stromal cells identified using a quantitative proteomics approach.* Stem cell research, 2014. **12**(1): p. 153-165.
159. Pèrié, L., et al., *Enhancement of C2C12 myoblast proliferation and differentiation by GASP-2, a myostatin inhibitor.* Biochemistry and Biophysics Reports, 2016. **6**: p. 39-46.
160. Benders, K.E., et al., *Extracellular matrix scaffolds for cartilage and bone regeneration.* Trends in biotechnology, 2013. **31**(3): p. 169-176.
161. Datta, N., et al., *Effect of bone extracellular matrix synthesized in vitro on the osteoblastic differentiation of marrow stromal cells.* Biomaterials, 2005. **26**(9): p. 971-977.
162. Hong, Y., et al., *Mechanical properties and in vivo behavior of a biodegradable synthetic polymer microfiber–extracellular matrix hydrogel biohybrid scaffold.* Biomaterials, 2011. **32**(13): p. 3387-3394.
163. Nakamura, M. and T. Nishida, *Synergistic effects of hyaluronan and fibronectin on epithelial migration in rabbit cornea in vitro.* Cornea, 1999. **18**(6): p. 686-692.
164. Olivero, D.K. and L.T. Furcht, *Type IV collagen, laminin, and fibronectin promote the adhesion and migration of rabbit*

*lens epithelial cells in vitro.* Investigative ophthalmology & visual science, 1993. **34**(10): p. 2825-2834.
165. Tsai, W.-B., et al., *Fibronectin modulates the morphology of osteoblast-like cells (MG-63) on nano-grooved substrates.* Journal of Materials Science: Materials in Medicine, 2009. **20**(6): p. 1367-1378.
166. Okubo, Y., et al., *Expression of bone morphogenetic protein-2 via adenoviral vector in C2C12 myoblasts induces differentiation into the osteoblast lineage.* Biochemical and biophysical research communications, 1999. **262**(3): p. 739-743.
167. Katagiri, T., et al., *Bone morphogenetic protein-2 converts the differentiation pathway of C2C12 myoblasts into the osteoblast lineage.* The Journal of cell biology, 1994. **127**(6): p. 1755-1766.
168. Sondag, G.R., et al., *Osteoactivin induces transdifferentiation of C2C12 myoblasts into osteoblasts.* Journal of cellular physiology, 2014. **229**(7): p. 955-966.
169. Manolagas, S.C., *Birth and death of bone cells: basic regulatory mechanisms and implications for the pathogenesis and treatment of osteoporosis 1.* Endocrine reviews, 2000. **21**(2): p. 115-137.
170. Ichijima, T., et al., *Osteogenic differences in cultured rat periosteal cells under hypoxic and normal conditions.* Experimental and therapeutic medicine, 2012. **3**(2): p. 165-170.
171. Shakibaei, M., et al., *Resveratrol mediated modulation of Sirt-1/Runx2 promotes osteogenic differentiation of mesenchymal stem cells: potential role of Runx2 deacetylation.* PLoS One, 2012. **7**(4): p. e35712.
172. Ye, G., et al., *Bone morphogenetic protein-9 induces PDLSCs osteogenic differentiation through the ERK and p38 signal pathways.* International journal of medical sciences, 2014. **11**(10): p. 1065.
173. Macri, L., D. Silverstein, and R.A. Clark, *Growth factor binding to the pericellular matrix and its importance in tissue engineering.* Advanced drug delivery reviews, 2007. **59**(13): p. 1366-1381.
174. Chen, L., et al., *Insulin-like growth factor 2 (IGF-2) potentiates BMP-9-induced osteogenic differentiation and bone formation.* Journal of Bone and Mineral Research, 2010. **25**(11): p. 2447-2459.

175. Ng, F., et al., *PDGF, TGF-β, and FGF signaling is important for differentiation and growth of mesenchymal stem cells (MSCs): transcriptional profiling can identify markers and signaling pathways important in differentiation of MSCs into adipogenic, chondrogenic, and osteogenic lineages.* Blood, 2008. **112**(2): p. 295-307.
176. Pountos, I., et al., *The effect of bone morphogenetic protein-2, bone morphogenetic protein-7, parathyroid hormone, and platelet-derived growth factor on the proliferation and osteogenic differentiation of mesenchymal stem cells derived from osteoporotic bone.* Journal of orthopaedic trauma, 2010. **24**(9): p. 552-556.
177. Ryoo, H.-M., M.-H. Lee, and Y.-J. Kim, *Critical molecular switches involved in BMP-2-induced osteogenic differentiation of mesenchymal cells.* Gene, 2006. **366**(1): p. 51-57.
178. Tocci, S.L., et al., *Biomechanical comparison of single-row arthroscopic rotator cuff repair technique versus transosseous repair technique.* Journal of Shoulder and Elbow Surgery, 2008. **17**(5): p. 808-814.
179. Domb, B.G., et al., *High-tension double-row footprint repair compared with reduced-tension single-row repair for massive rotator cuff tears.* The Journal of Bone & Joint Surgery, 2008. **90**(Supplement 4): p. 35-39.
180. Nelson, C.O., et al., *Single-row modified Mason-Allen versus double-row arthroscopic rotator cuff repair: a biomechanical and surface area comparison.* Arthroscopy: The Journal of Arthroscopic & Related Surgery, 2008. **24**(8): p. 941-948.
181. Galatz, L.M., et al., *Prospective longitudinal analysis of postoperative shoulder function.* The Journal of Bone & Joint Surgery, 2001. **83**(7): p. 1052-1056.
182. Ozbaydar, M., et al., *A comparison of single-versus double-row suture anchor techniques in a simulated repair of the rotator cuff AN EXPERIMENTAL STUDY IN RABBITS.* Journal of Bone & Joint Surgery, British Volume, 2008. **90**(10): p. 1386-1391.
183. Björnsson, H.C., et al., *The influence of age, delay of repair, and tendon involvement in acute rotator cuff tears: structural and clinical outcomes after repair of 42 shoulders.* Acta orthopaedica, 2011. **82**(2): p. 187-192.

184. Cofield, R.H., et al., *Surgical repair of chronic rotator cuff tears.* The Journal of Bone & Joint Surgery, 2001. **83**(1): p. 71-71.
185. Goutallier, D., et al., *Influence of cuff muscle fatty degeneration on anatomic and functional outcomes after simple suture of full-thickness tears.* Journal of shoulder and elbow surgery, 2003. **12**(6): p. 550-554.
186. Sahoo, S., et al., *Bioactive nanofibers for fibroblastic differentiation of mesenchymal precursor cells for ligament/tendon tissue engineering applications.* Differentiation, 2010. **79**(2): p. 102-110.
187. Liu, Y., H. Ramanath, and D.-A. Wang, *Tendon tissue engineering using scaffold enhancing strategies.* Trends in biotechnology, 2008. **26**(4): p. 201-209.
188. Kuo, C.K., J.E. Marturano, and R.S. Tuan, *Novel strategies in tendon and ligament tissue engineering: Advanced biomaterials and regeneration motifs.* BMC Sports Science, Medicine and Rehabilitation, 2010. **2**(1): p. 20.
189. Apostolakos, J., et al., *The enthesis: a review of the tendon-to-bone insertion.* Muscles, ligaments and tendons journal, 2014. **4**(3): p. 333.
190. Lui, P., et al., *Biology and augmentation of tendon-bone insertion repair.* J Orthop Surg Res, 2010. **5**(1): p. 1-14.
191. Dashe, J., et al., *Allograft tissue irradiation and failure rate after anterior cruciate ligament reconstruction: A systematic review.* World Journal of Orthopedics, 2016. **7**(6): p. 392.
192. Shaerf, D.A., et al., *Anterior cruciate ligament reconstruction best practice: a review of graft choice.* World J Orthop, 2014. **5**(1): p. 23-9.
193. Spindler, K.P., et al., *Prognosis and predictors of ACL reconstructions using the MOON cohort: a model for comparative effectiveness studies.* Journal of Orthopaedic Research, 2013. **31**(1): p. 2-9.
194. Dargel, J., et al., *Biomechanics of the anterior cruciate ligament and implications for surgical reconstruction.* Strategies in Trauma and Limb Reconstruction, 2007. **2**(1): p. 1-12.
195. Freedman, K.B., et al., *Arthroscopic anterior cruciate ligament reconstruction: a metaanalysis comparing patellar tendon and hamstring tendon autografts.* The American journal of sports medicine, 2003. **31**(1): p. 2-11.

196. Kartus, J., T. Movin, and J. Karlsson, *Donor-site morbidity and anterior knee problems after anterior cruciate ligament reconstruction using autografts.* Arthroscopy: The Journal of Arthroscopic & Related Surgery, 2001. **17**(9): p. 971-980.
197. Bi, F., et al., *Anterior cruciate ligament reconstruction in a rabbit model using silk-collagen scaffold and comparison with autograft.* PloS one, 2015. **10**(5): p. e0125900.
198. Ratcliffe, A., et al., *Scaffolds for tendon and ligament repair and regeneration.* Annals of biomedical engineering, 2015. **43**(3): p. 819-831.
199. Batty, L.M., et al., *Synthetic devices for reconstructive surgery of the cruciate ligaments: a systematic review.* Arthroscopy: The Journal of Arthroscopic & Related Surgery, 2015. **31**(5): p. 957-968.
200. Smith, C., et al., *The use of the ligament augmentation and reconstruction system (LARS) for posterior cruciate reconstruction.* Arthroscopy: The Journal of Arthroscopic & Related Surgery, 2014. **30**(1): p. 111-120.
201. Kdolsky, R.K., et al., *Braided polypropylene augmentation device in reconstructive surgery of the anterior cruciate ligament: Long-term clinical performance of 594 patients and short-term arthroscopic results, failure analysis by scanning electron microscopy, and synovial histomorphology.* Journal of orthopaedic research, 1997. **15**(1): p. 1-10.
202. Murray, M.M. and B.C. Fleming, *Use of a bioactive scaffold to stimulate anterior cruciate ligament healing also minimizes posttraumatic osteoarthritis after surgery.* The American journal of sports medicine, 2013. **41**(8): p. 1762-1770.
203. Kiapour, A.M., B.C. Fleming, and M.M. Murray, *Biomechanical outcomes of bridge-enhanced anterior cruciate ligament repair are influenced by sex in a preclinical model.* Clinical Orthopaedics and Related Research®, 2015. **473**(8): p. 2599-2608.
204. Wakitani, S., et al., *Mesenchymal cell-based repair of large, full-thickness defects of articular cartilage.* The Journal of Bone & Joint Surgery, 1994. **76**(4): p. 579-592.
205. Lui, P., et al., *Tenogenic differentiation of stem cells for tendon repair—what is the current evidence?* Journal of

tissue engineering and regenerative medicine, 2011. **5**(8): p. e144-e163.
206. Bruder, S.P., D.J. Fink, and A.I. Caplan, *Mesenchymal stem cells in bone development, bone repair, and skeletal regenaration therapy.* Journal of cellular biochemistry, 1994. **56**(3): p. 283-294.
207. Hwang, N.S., et al., *Biomaterials directed in vivo osteogenic differentiation of mesenchymal cells derived from human embryonic stem cells.* Tissue Engineering Part A, 2013. **19**(15-16): p. 1723-1732.
208. Levenberg, S., et al., *Differentiation of human embryonic stem cells on three-dimensional polymer scaffolds.* Proceedings of the National Academy of Sciences, 2003. **100**(22): p. 12741-12746.
209. Yin, Z., et al., *Stem cells for tendon tissue engineering and regeneration.* Expert opinion on biological therapy, 2010. **10**(5): p. 689-700.
210. Bosnakovski, D., et al., *Chondrogenic differentiation of bovine bone marrow mesenchymal stem cells (MSCs) in different hydrogels: influence of collagen type II extracellular matrix on MSC chondrogenesis.* Biotechnology and bioengineering, 2006. **93**: p. 1152-1163.
211. Kang, Y., et al., *The osteogenic differentiation of human bone marrow MSCs on HUVEC-derived ECM and β-TCP scaffold.* Biomaterials, 2012. **33**(29): p. 6998-7007.
212. Thibault, R.A., et al., *Osteogenic differentiation of mesenchymal stem cells on pregenerated extracellular matrix scaffolds in the absence of osteogenic cell culture supplements.* Tissue Engineering Part A, 2009. **16**(2): p. 431-440.
213. Badylak, S.F. and J.E. Valentin, *Extracellular Matrix Bioscaffolds for Orthopaedic Applications.* J Bone Joint Surg Am, 2010. **92**(5): p. 1317-1318.
214. Badylak, S.F. *The extracellular matrix as a scaffold for tissue reconstruction*. in *Seminars in cell & developmental biology*. 2002. Elsevier.
215. Youngstrom, D.W., et al., *Functional characterization of detergent-decellularized equine tendon extracellular matrix for tissue engineering applications.* PloS one, 2013. **8**(5): p. e64151.

216. D'Amore, A., et al., *Characterization of the complete fiber network topology of planar fibrous tissues and scaffolds.* Biomaterials, 2010. **31**(20): p. 5345-5354.
217. Peter, S.J., et al., *Osteoblastic phenotype of rat marrow stromal cells cultured in the presence of dexamethasone, β-glycerolphosphate, and L-ascorbic acid.* Journal of cellular biochemistry, 1998. **71**(1): p. 55-62.
218. Larsen, K.H., et al., *Identifying a molecular phenotype for bone marrow stromal cells with in vivo bone-forming capacity.* Journal of Bone and Mineral Research, 2010. **25**(4): p. 796-808.
219. Prins, H.-J., et al., *Bone-forming capacity of mesenchymal stromal cells when cultured in the presence of human platelet lysate as substitute for fetal bovine serum.* Tissue Engineering Part A, 2009. **15**(12): p. 3741-3751.
220. Janssen, F., et al., *Human tissue-engineered bone produced in clinically relevant amounts using a semi-automated perfusion bioreactor system: a preliminary study.* Journal of tissue engineering and regenerative medicine, 2010. **4**(1): p. 12-24.
221. Subramony, S.D., et al., *The guidance of stem cell differentiation by substrate alignment and mechanical stimulation.* Biomaterials, 2013. **34**(8): p. 1942-1953.
222. Kapoor, A., et al., *Microtopographically patterned surfaces promote the alignment of tenocytes and extracellular collagen.* Acta biomaterialia, 2010. **6**(7): p. 2580-2589.
223. Yin, Z., et al., *The regulation of tendon stem cell differentiation by the alignment of nanofibers.* Biomaterials, 2010. **31**(8): p. 2163-2175.
224. Molloy, T., Y. Wang, and G.A. Murrell, *The roles of growth factors in tendon and ligament healing.* Sports Medicine, 2003. **33**(5): p. 381-394.
225. Tao, X., et al., *EGR1 induces tenogenic differentiation of tendon stem cells and promotes rabbit rotator cuff repair.* Cellular Physiology and Biochemistry, 2015. **35**(2): p. 699-709.
226. Hagerty, P., et al., *The effect of growth factors on both collagen synthesis and tensile strength of engineered human ligaments.* Biomaterials, 2012. **33**(27): p. 6355-6361.
227. Furumatsu, T., et al., *GDF-5/7 and bFGF activate integrin α2-mediated cellular migration in rabbit ligament*

*fibroblasts.* Journal of Orthopaedic Research, 2010. **28**(2): p. 225-231.
228. Shen, H., et al., *BMP12 induces tenogenic differentiation of adipose-derived stromal cells.* PloS one, 2013. **8**(10): p. e77613.
229. Caliari, S.R. and B.A. Harley, *Composite growth factor supplementation strategies to enhance tenocyte bioactivity in aligned collagen-GAG scaffolds.* Tissue Engineering Part A, 2013. **19**(9-10): p. 1100-1112.
230. Costa, M.A., et al., *Tissue engineering of flexor tendons: optimization of tenocyte proliferation using growth factor supplementation.* Tissue engineering, 2006. **12**(7): p. 1937-1943.
231. Robertus, J., W.R. Browne, and B.L. Feringa, *Dynamic control over cell adhesive properties using molecular-based surface engineering strategies.* Chemical Society Reviews, 2010. **39**(1): p. 354-378.
232. Chandran, P.L. and V.H. Barocas, *Deterministic material-based averaging theory model of collagen gel micromechanics.* Journal of biomechanical engineering, 2007. **129**(2): p. 137-147.
233. Wood, G., *The formation of fibrils from collagen solutions. 2. A mechanism for collagen-fibril formation.* Biochemical Journal, 1960. **75**(3): p. 598.
234. Wood, G. and M. Keech, *The formation of fibrils from collagen solutions 1. The effect of experimental conditions: kinetic and electron-microscope studies.* Biochemical Journal, 1960. **75**(3): p. 588.
235. Brightman, A., et al., *Time-lapse confocal reflection microscopy of collagen fibrillogenesis and extracellular matrix assembly in vitro.* Biopolymers, 2000. **54**(3): p. 222-234.
236. Yang, Y.-l. and L.J. Kaufman, *Rheology and confocal reflectance microscopy as probes of mechanical properties and structure during collagen and collagen/hyaluronan self-assembly.* Biophysical journal, 2009. **96**(4): p. 1566-1585.
237. Stern, M.M., et al., *The influence of extracellular matrix derived from skeletal muscle tissue on the proliferation and differentiation of myogenic progenitor cells ex vivo.* Biomaterials, 2009. **30**(12): p. 2393-2399.

238. Xue, J.X., et al., *Chondrogenic differentiation of bone marrow-derived mesenchymal stem cells induced by acellular cartilage sheets.* Biomaterials, 2012. **33**(24): p. 5832-5840.
239. Omae, H., et al., *Multilayer tendon slices seeded with bone marrow stromal cells: a novel composite for tendon engineering.* Journal of Orthopaedic Research, 2009. **27**(7): p. 937-942.
240. Shukunami, C., et al., *Scleraxis positively regulates the expression of tenomodulin, a differentiation marker of tenocytes.* Developmental biology, 2006. **298**(1): p. 234-247.
241. Pajala, A., et al., *TenascinC and type I and III collagen expression in total Achilles tendon rupture. An immunohistochemical study.* 2009.
242. Badylak, S.F., *Xenogeneic extracellular matrix as a scaffold for tissue reconstruction.* Transplant immunology, 2004. **12**(3): p. 367-377.
243. Chen, F., J.J. Yoo, and A. Atala, *Acellular collagen matrix as a possible "off the shelf" biomaterial for urethral repair.* Urology, 1999. **54**(3): p. 407-410.
244. Harper, C., *Permacol: clinical experience with a new biomaterial.* Hospital medicine (London, England: 1998), 2001. **62**(2): p. 90-95.
245. Badylak, S.F., et al., *Esophageal preservation in five male patients after endoscopic inner-layer circumferential resection in the setting of superficial cancer: a regenerative medicine approach with a biologic scaffold.* Tissue Engineering Part A, 2011. **17**(11-12): p. 1643-1650.
246. Gilbert, T.W., T.L. Sellaro, and S.F. Badylak, *Decellularization of tissues and organs.* Biomaterials, 2006. **27**(19): p. 3675-3683.
247. Freytes, D.O., et al., *Hydrated versus lyophilized forms of porcine extracellular matrix derived from the urinary bladder.* Journal of Biomedical Materials Research Part A, 2008. **87**(4): p. 862-872.
248. Neves, N.M., *Electrospinning for Advanced Biomedical Applications and Therapies*. Smithers Rapra Technology.
249. Haghi, A.K. and G. Zaikov, *Advances in Nanofibre Research, Volume 2*. Smithers Rapra Technology.

250. Jha, B.S., et al., *Electrospun collagen: a tissue engineering scaffold with unique functional properties in a wide variety of applications.* Journal of Nanomaterials, 2011. **2011**: p. 7.
251. Barnes[1], C.P., et al., *Feasibility of electrospinning the globular proteins hemoglobin and myoglobin.* 2006.
252. Buttafoco, L., et al., *Electrospinning of collagen and elastin for tissue engineering applications.* Biomaterials, 2006. **27**(5): p. 724-734.
253. Ma, J., X. He, and E. Jabbari, *Osteogenic differentiation of marrow stromal cells on random and aligned electrospun poly (L-lactide) nanofibers.* Annals of biomedical engineering, 2011. **39**(1): p. 14-25.
254. Boland, E.D., et al., *Electrospinning polydioxanone for biomedical applications.* Acta Biomaterialia, 2005. **1**(1): p. 115-123.
255. Fu, W., et al., *Electrospun gelatin/PCL and collagen/PLCL scaffolds for vascular tissue engineering.* Int J Nanomedicine, 2014. **9**: p. 2335-2344.
256. Lee, S.J., et al., *Development of a composite vascular scaffolding system that withstands physiological vascular conditions.* Biomaterials, 2008. **29**(19): p. 2891-2898.
257. Sarkar, S., et al., *The mechanical properties of infrainguinal vascular bypass grafts: their role in influencing patency.* European journal of vascular and endovascular surgery, 2006. **31**(6): p. 627-636.
258. Yoshimoto, H., et al., *A biodegradable nanofiber scaffold by electrospinning and its potential for bone tissue engineering.* Biomaterials, 2003. **24**(12): p. 2077-2082.
259. Woo, K.M., et al., *Nano-fibrous scaffolding promotes osteoblast differentiation and biomineralization.* Biomaterials, 2007. **28**(2): p. 335-343.
260. Chapekar, M.S., *Tissue engineering: challenges and opportunities.* Journal of biomedical materials research, 2000. **53**(6): p. 617-620.
261. Riboldi, S.A., et al., *Electrospun degradable polyesterurethane membranes: potential scaffolds for skeletal muscle tissue engineering.* Biomaterials, 2005. **26**(22): p. 4606-4615.
262. Ruckh, T.T., et al., *Osteogenic differentiation of bone marrow stromal cells on poly (ε-caprolactone) nanofiber scaffolds.* Acta biomaterialia, 2010. **6**(8): p. 2949-2959.

263. Binulal, N., et al., *Role of nanofibrous poly (caprolactone) scaffolds in human mesenchymal stem cell attachment and spreading for in vitro bone tissue engineering—response to osteogenic regulators.* Tissue Engineering Part A, 2010. **16**(2): p. 393-404.
264. Badami, A.S., et al., *Effect of fiber diameter on spreading, proliferation, and differentiation of osteoblastic cells on electrospun poly (lactic acid) substrates.* Biomaterials, 2006. **27**(4): p. 596-606.
265. Shih, Y.R.V., et al., *Growth of mesenchymal stem cells on electrospun type I collagen nanofibers.* Stem Cells, 2006. **24**(11): p. 2391-2397.
266. Meinel, A.J., et al., *Optimization strategies for electrospun silk fibroin tissue engineering scaffolds.* Biomaterials, 2009. **30**(17): p. 3058-3067.
267. Jin, H.-J., et al., *Human bone marrow stromal cell responses on electrospun silk fibroin mats.* Biomaterials, 2004. **25**(6): p. 1039-1047.
268. Shin, S.-Y., et al., *Biological evaluation of chitosan nanofiber membrane for guided bone regeneration.* Journal of periodontology, 2005. **76**(10): p. 1778-1784.
269. Baiguera, S., et al., *Electrospun gelatin scaffolds incorporating rat decellularized brain extracellular matrix for neural tissue engineering.* Biomaterials, 2014. **35**(4): p. 1205-1214.
270. Gibson, M., et al., *Tissue extracellular matrix nanoparticle presentation in electrospun nanofibers.* BioMed research international, 2014. **2014**.
271. Kuijpers, A.J., et al., *Cross-linking and characterisation of gelatin matrices for biomedical applications.* Journal of Biomaterials Science, Polymer Edition, 2000. **11**(3): p. 225-243.
272. Matthews, J.A., et al., *Electrospinning of collagen nanofibers.* Biomacromolecules, 2002. **3**(2): p. 232-238.
273. Yang, L., et al., *Mechanical properties of single electrospun collagen type I fibers.* Biomaterials, 2008. **29**(8): p. 955-962.
274. Zvibel, I., et al., *Transcriptional profiling identifies genes induced by hepatocyte-derived extracellular matrix in metastatic human colorectal cancer cell lines.* Clinical & experimental metastasis, 2013. **30**(2): p. 189-200.

275. Nguyen, L.L. and P.A. D'Amore, *Cellular interactions in vascular growth and differentiation.* International review of cytology, 2001. **204**: p. 1-48.
276. Nishimura, I., et al., *Precursor tissue analogs as a tissue-engineering strategy.* Tissue engineering, 2003. **9**(4, Supplement 1): p. 77-89.
277. Jang, J.-H., O. Castano, and H.-W. Kim, *Electrospun materials as potential platforms for bone tissue engineering.* Advanced drug delivery reviews, 2009. **61**(12): p. 1065-1083.
278. Chainani, A., et al., *Multilayered electrospun scaffolds for tendon tissue engineering.* Tissue Engineering Part A, 2013. **19**(23-24): p. 2594-2604.
279. Shin, H.J., et al., *Electrospun PLGA nanofiber scaffolds for articular cartilage reconstruction: mechanical stability, degradation and cellular responses under mechanical stimulation in vitro.* Journal of Biomaterials Science, Polymer Edition, 2006. **17**(1-2): p. 103-119.
280. Doshi, J. and D.H. Reneker. *Electrospinning process and applications of electrospun fibers*. in *Industry Applications Society Annual Meeting, 1993., Conference Record of the 1993 IEEE*. 1993. IEEE.
281. Bognitzki, M., et al., *Nanostructured fibers via electrospinning.* Advanced Materials, 2001. **13**(1): p. 70-72.
282. Huang, L., R.P. Apkarian, and E.L. Chaikof, *High-resolution analysis of engineered type I collagen nanofibers by electron microscopy.* Scanning, 2001. **23**(6): p. 372-375.
283. Boland, E.D., et al., *Electrospinning collagen and elastin: preliminary vascular tissue engineering.* Front Biosci, 2004. **9**(1422): p. e32.
284. Xu, C., et al., *Aligned biodegradable nanofibrous structure: a potential scaffold for blood vessel engineering.* Biomaterials, 2004. **25**(5): p. 877-886.
285. Rozario, T. and D.W. DeSimone, *The extracellular matrix in development and morphogenesis: a dynamic view.* Developmental biology, 2010. **341**(1): p. 126-140.
286. Del Gaudio, C., et al., *Induction of angiogenesis using VEGF releasing genipin-crosslinked electrospun gelatin mats.* Biomaterials, 2013. **34**(31): p. 7754-7765.
287. Thomopoulos, S., et al., *Collagen fiber orientation at the tendon to bone insertion and its influence on stress*

*concentrations.* Journal of biomechanics, 2006. **39**(10): p. 1842-1851.
288. Rodeo, S.A., et al., *Tendon-healing in a bone tunnel. A biomechanical and histological study in the dog.* JBJS, 1993. **75**(12): p. 1795-1803.
289. Aurora, A., et al., *Commercially available extracellular matrix materials for rotator cuff repairs: state of the art and future trends.* Journal of Shoulder and Elbow Surgery, 2007. **16**(5): p. S171-S178.
290. Derwin, K.A., et al., *Commercial extracellular matrix scaffolds for rotator cuff tendon repair.* J Bone Joint Surg Am, 2006. **88**(12): p. 2665-2672.
291. Shang, S., et al., *The effect of electrospun fibre alignment on the behaviour of rat periodontal ligament cells.* 2010.